Peak-to-average power ratio of orthogonal frequency division multiplexing

A. D. S. Jayalath and C. Tellambura*

May 14, 2002

Abstract

Orthogonal frequency division multiplexing (OFDM) is successfully used in many wireless digital communication systems over multipath channels. One of the principal disadvantages of OFDM is the occurrence of high peak to average power ratios (PAR). Many PAR reduction techniques have been proposed in the literature. This report describes the PAR problem, PAR reduction methods and related issues. Performances of several PAR reduction techniques are compared. As high peaks are relatively rare, the PAR can be reduced simply by clipping high peaks. However, severe clipping introduces inband distortion and out of band radiation. Multiple signal representation techniques are effective in OFDM system with large number of subcarriers, which reduce the PAR with an increased complexity at the receiver. Although coding techniques limit the PAR 3 dB at most, coding rate is prohibitively low when number of carriers is increased beyond 32.

Key words: OFDM, Peak-to-average power ratio, Clipping, Complementary sequences, interleaving, Partial-transmit sequences, Reed-Muller codes, Rudin-Shapiro, Selected mapping, Tone reservation

1 Introduction

At the start of the new millennium, wireless communication technologies continue to evolve and expand at a phenomenal pace. Third-generation systems involving wide-band code division multiple access (WCDMA), enhanced data rates for global evolution (EDGE), high-speed radio local area networks (LAN), and wireless internet connectivity have been a major focus of recent research and standardization efforts. These broadband networks provide integrated packet-oriented transmission of text, graphics, voice, image, video, and computer data over point-to-point links as well as in broadcast mode. The transmission system adapts to different requirements of individual services in terms of data rate, admissible bit error rate (BER), quality of services (QoS), and maximum delay. Furthermore, bi-directional communication has to be supported.

Performance of these advanced wireless systems heavily depends on the characteristics of the wireless channel such as frequency selective fading, limited bandwidth, rapid changes in propagation conditions and mutual interference of signals. If a conventional single carrier system is used, the channel equalization can be highly complex. Furthermore, channel estimation overhead increases in time-variant channels. Multi-carrier systems such as orthogonal frequency division multiplexing (OFDM) offer an attractive solution.

OFDM has been standardized for many wireless applications. The most desirable advantage of OFDM over single carrier systems is its superior performance in frequency selective fading channels. OFDM systems divide the wide-band signal into several narrow-band signals, so that each of these experiences frequency-non selective fading. Advances in digital signal processing (DSP) have paved the way to simple implementation of OFDM systems. The orthogonality of the OFDM subcarriers is maintained and the channel impact is reduced to multiplication of each subcarrier by a complex transfer factor at the receiver [1]. Thus the signal can be recovered at the receiver without complicated equalization.

OFDM also suffers from some disadvantages. An OFDM symbol consists of large number of independently modulated subcarriers, that can yield a large peak-to-average power ratio (PAR) when the subcarriers add up coherently. A large PAR leads to disadvantages such as increased complexity of the analog-to-digital converter (A/D) and a reduced efficiency of the radio frequency (RF) amplifier. High peaks are clipped by non-linear devices at the transmitter and this causes undesirable effects such as high out of band radiation and inband distortion [2]. Thus PAR reduction techniques are of great importance for OFDM.

*School of Computer Science and Software Engineering, Faculty of Information Technology, Monash University , Clayton Victoria 3800 , Australia , Ph: +61 3 9905 3296 , Fax: +61 3 9905 5146 , Email:jayalath@ieee.org, chintha@csse.monash.edu.au

2 Orthogonal frequency division multiplexing

The concept of using parallel data transmission and frequency division multiplexing was first published in the mid 60's. OFDM was filed for a U.S. patent by Chang [3] at Bell labs in 1966. The idea was to use parallel data transmission and frequency division multiplexing (FDM) with overlapping subcarriers to avoid the high speed equalization. It can also combat impulsive noise, multipath distortion and fully utilize the available bandwidth.

The arrays of sinusoidal generators and coherent demodulators required in parallel systems become unreasonably expensive and complex for large number of subcarriers. Weinstein and Ebert [4] showed that OFDM can be efficiently realized using discrete Fourier transform (DFT) techniques at the transmitter and the receiver. This reduces the amount of hardware both at the transmitter and the receiver. The inverse DFT (IDFT) at the transmitter performs multiplexing and modulation simultaneously, while DFT at the receiver performs demultiplexing and demodulation simultaneously. Both DFT and IDFT are implemented using fast Fourier transform (FFT) algorithms. Advances in very large scale integration (VLSI) and digital signal processing (DSP) technologies have reduced the implementation cost of OFDM systems drastically. Therefore, many OFDM applications are now in the market and many more are waiting to be introduced.

2.1 Advantages and limitations of OFDM

2.1.1 Advantages of using OFDM in wireless communications

These can be summarized as follows.

1. OFDM makes efficient use of the spectrum by allowing subcarriers to overlap [4–6].
2. By dividing the channel into narrow-band flat fading subchannels, OFDM systems are more resistant to frequency selective fading than single carrier systems are [7].
3. OFDM can eliminate inter-symbol interference (ISI) and inter-carrier interference (ICI) by introducing a guard interval [8–11].
4. Using adequate channel coding and interleaving, one can recover symbols lost due to the frequency selectivity of the channel [11–15].
5. Channel equalization becomes simpler than adaptive channel equalization techniques used in single carrier systems [5].
6. DFT modulation and demodulation reduce the complexity of OFDM [4, 7, 16].
7. Differential modulation schemes avoid the need to implement channel estimators [17–22].
8. OFDM is less sensitive to sample timing offsets than single carrier systems are [6].
9. OFDM is robust against cochannel interference and impulsive noise [1, 23].

2.1.2 Limitations of OFDM systems

Major disadvantages of OFDM are:

1. The OFDM signal has a noise like amplitude with a very large dynamic range. Since all practical wireless communication systems are power limited, high PAR is a serious disadvantage of OFDM. Large envelope power fluctuations often require power amplifiers with large back off values. This will also increase the complexity of the analog to digital converters and the digital to analog converters. Clipping of the signal will introduce both in band distortion and out of band radiation [24–32].
2. OFDM is more sensitive to carrier frequency offset and drift than single carrier systems are. Frequency synchronization in OFDM systems is more complicated than that in single carrier systems. Carrier frequency offset disturbs subcarrier orthogonality and resulting inter-channel interference severely degrades the demodulator performance. For high order modulation schemes such as those used for digital video broadcasting (DVB), a frequency offset of a small fraction of the subcarrier symbol rate leads to an intolerable degradation. Therefore, frequency synchronization is one of the most critical tasks performed by an OFDM receiver [33–37].

2.2 Applications of OFDM

OFDM was first used for military high frequency (HF) communication systems, such as the KINEPLEX system [38]. With the introduction of DFT for the modulation process, OFDM received much more attention [1, 4]. Since this early period, OFDM has been considered for many other applications, and became popular with the advancement of VLSI technologies. Some of the early areas of applications were, (a) high-speed voice-band, data communication modems [39, 40] at NEC Corp. (Japan) to alleviate the degradations caused by an impulsive noise environment; (b) digital audio broadcasting (DAB), initially at the CCETT (France) [41–43] but also elsewhere, such as the Institute for Communications Technology (Germany) [44] and the Communications Research Center (Canada). Coded OFDM (COFDM) based DAB systems were initiated by CCETT in France and developed into a new major broadcasting standard by a collaborative project, Eureka 147 [6]. The other major OFDM usage is in digital subscriber line (DSL) technologies [45].

An early multimedia transmit attempt over wireless channels was outside broadcast link (OBL). An OFDM based OBL for broadcasting audio and video signal from a moving vehicle was proposed in [46]. In the experimental OFDM-OBL proposed, the compressed digital video and audio data are distributed among 572 subcarriers in the 9 MHz bandwidth, using differential quadrature phase shift keying (DQPSK) modulation scheme. Digital OFDM-OBL transmits a stable signal under severe multipath fading conditions.

In mobile communication systems, the multipath-fading channel limits system capacity and performance [7]. One of the most common approaches in dealing with fading is diversity. Multi-carrier CDMA (MC-CDMA) techniques have such capability and can be efficiently used for such applications [47, 48]. A multi-user OFDM system in which the data are transmitted for each user continuously over a number of different subcarriers with intervening subcarriers occupied by the other users is described in [49]. The subcarriers assigned to one user have a large separation, to provide frequency diversity and some assistance to frequency selective fading. Different multiple access methods are also proposed for OFDM in [50, 51]. OFDM is also proposed for satellite mobile channels [52, 53].

COFDM in terrestrial digital video broadcasting (DVB-T) enables an end-to-end digital transmission system, which is spectrally efficient and rugged against channel distortions. This can be used for services such as HDTV, offering increased capacity for program broadcasting. Different aspects of digital TV broadcasting are discussed in [54, 55]. DVB systems employing OFDM are being standardized by ETSI [56].

The market trend of mobile computing devices is strongly influencing industry towards the development and the implementation of high-speed wireless local area networks (WLAN). WLAN are primarily affected by interference and multipath fading, as they often use bands where electronic devices radiate RF energy. In this environment direct sequence spread spectrum OFDM (DS-SS-OFDM) is used to combat both interference and multipath fading. OFDM is used for IEEE 802.11a [57] standards and for HIPERLAN/2. OFDM is used in many applications where higher data rates are involved and ruggedness against multipath fading is required. Expected developments of OFDM in future are wideband OFDM (WOFDM), smart antennas, multiple-input-multiple-output systems (MIMO), space-time coding, dynamic packet assignment and dynamic tone/power allocation [58].

OFDM is also expected to play a major role in 4G wireless systems which include peak downlink rates of 2 to 10 Mbps, full macro-cellular/metropolitan coverage, asymmetric with 3G uplinks (EDGE), variable bandwidth - 1 to 5 MHz, adaptive modulation/coding, smart/adaptive antennas supported, internet protocol (IP) packet based, multi inputs/multi outputs (MIMO/BLAST) modes, frame synchronized base stations using geographical positioning systems (GPS), network assisted dynamic packet assignment, general packet radio services (GPRS) networking support [58–61]. OFDM signals are mathematically described next.

2.3 Mathematical representation of OFDM signals

2.3.1 Orthogonality

In OFDM, subcarriers are overlapped but the signal can still be recovered without adjacent subcarrier interference because of the orthogonality between subcarriers [6]. Consider a set of subcarriers $f_n(t), n = 0, 1, \ldots, N-1, t_1 \leq t \leq t_2$. This set is orthogonal if [62]

$$\int_{t_1}^{t_2} f_n(t) f_m^*(t) dt = \begin{cases} 0, & n \neq m \\ \mathrm{K}, & n = m \end{cases} \tag{1}$$

where x^* is the conjugate of x and K is a constant independent of t, n or m. In OFDM the set of transmitted subcarriers can be written as

$$f_n(t) = \exp(j2\pi f_n t) \tag{2}$$

where $j = \sqrt{-1}$ and

$$\begin{aligned} f_n &= f_0 + n\Delta f \\ &= f_0 + n/T \end{aligned} \tag{3}$$

where f_0 is the initial frequency offset. Now we can examine the orthogonality of the subcarriers. If the subcarriers are orthogonal, Eq. (1) should hold. We find

$$\begin{aligned} \int_{t_1}^{t_2} f_n(t) f_m^*(t) dt &= \int_{t_1}^{t_2} \exp(j2\pi(n-m)t/T) dt \\ &= \frac{\exp(j2\pi(n-m)t_2/T) - \exp(j2\pi(n-m)t_1/T)}{j2\pi(n-m)/T} \\ &= \frac{\exp(j2\pi(n-m)t_2/T)\left[1 - \exp(j2\pi(n-m)(t_1-t_2)/T)\right]}{j2\pi(n-m)/T} \\ &= 0 \quad \text{for} \quad (n \neq m) \;\; \& \;\; (n-m)(t_1-t_2)/T \quad \text{is an integer.} \end{aligned} \tag{4}$$

Therefore, if the subcarriers are separated by $1/T$, they are orthogonal to each other provided $t_2 - t_1$ is an integer multiple of T [6].

2.3.2 Baseband representation of OFDM signals

An OFDM symbol consists of N subcarriers spaced by the frequency distance Δf. Thus, the total system bandwidth B is divided into N equidistant subchannels. All subcarriers are mutually orthogonal within a time interval of length $T = 1/\Delta f$. We shall write an ordered N-tuple $\mathbf{X}_m = (X_{m,0}, X_{m,1}, \ldots, X_{m,N-1})$ and let $(\mathcal{Q})^{\mathcal{N}}$ denotes the set of all ordered N-tuples where each $X_{m,n} \in \mathcal{Q}; n = 0, 1, \ldots, N-1$. We shall refer to any member of the set $(\mathcal{Q})^{\mathcal{N}}$ as a *data frame*. Note that each $X_{m,n}$ carries $q = \log_2 M$ data bits. Normal values are $M = 2, 4, 8$ and so on. Each OFDM symbol thus carries $N \log_2 q$ data bits. Each subcarrier can be modulated independently with the complex modulation symbol $X_{m,n}$, where m is a time index and n is a subcarrier index. Thus, within the symbol duration T the following signal of the m-th OFDM block is formed

$$x_m(t) = \frac{1}{\sqrt{N}} \sum_{n=0}^{N-1} X_{m,n} \exp(j2\pi n \Delta f t) g_n(t - mT) \tag{5}$$

where $g_n(t)$ is a rectangular pulse applied to each subcarrier [63]. The total continuous time signal $x(t)$ consisting of all OFDM blocks is

$$x(t) = \frac{1}{\sqrt{N}} \sum_{m=0}^{\infty} \sum_{n=0}^{N-1} X_{m,n} \exp(j2\pi n \Delta f t) g_n(t - mT). \tag{6}$$

As different OFDM symbols do not overlap, we can consider a single OFDM symbol ($m = 0$) without loss of generality. Since only $m = 0$ is sufficient for the problem at hand, $X_{m,n}$ may be replaced by X_n. Now we can write the OFDM signal as

$$x(t) = \frac{1}{\sqrt{N}} \sum_{n=0}^{N-1} X_n e^{j2\pi \Delta f t} \;\; 0 \leq t \leq T. \tag{7}$$

The discrete time representation of the OFDM symbol $x(t)$ can be obtained by appropriate sampling. As the bandwidth of an OFDM signal is $B = N\Delta f$, the signal can be completely determined by its samples if the sampling time $\Delta t = \frac{1}{B} = \frac{1}{N\Delta f}$. The samples of the signal are written as

$$x_k = \frac{1}{\sqrt{N}} \sum_{n=0}^{N-1} X_n e^{j2\pi kn/N}, \quad k = 0, 1, \ldots, N-1. \tag{8}$$

This equation describes exactly the N point inverse discrete Fourier transform (IDFT) of the input data $X_n, n = 0, 1, \ldots, N-1$. This can be easily implemented using inverse fast Fourier transform (IFFT) algorithms. The input symbols X_n represent digitally modulated binary data.

Each modulated symbol X_n is chosen from the set $\mathcal{Q} = \{\lambda_1, \lambda_2, \ldots, \lambda_M\}$ of M distinct elements. The set $\mathcal{Q}$ is called the signal constellation of the M-ary modulation scheme. Common modulation formats, namely binary phase shift keying (BPSK), quadrature phase shift keying (QPSK), M-ary phase shift keying (MPSK)

and M-ary quadrature amplitude modulation (MQAM) can be described as follows:

$$\begin{aligned}
\mathcal{Q}_{\text{BPSK}} &= \{\exp(j\pi x), x = 0, 1\} = \{(-1)^x,\ x = 0, 1\}, \\
\mathcal{Q}_{\text{QPSK}} &= \left\{\exp\left[j\left(\frac{\pi x}{2}\right)\right], x = 0, 1, 2, 3\right\} = \{j^x,\ x = 0, 1, 2, 3\}, \\
\mathcal{Q}_{\text{MPSK}} &= \left\{\exp\left[j\left(\frac{2\pi}{M}x\right)\right], x = 0, 1, \ldots, M-1\right\}, \\
\mathcal{Q}_{\text{MQAM}} &= \{[\pm(2x_1 + 1) \pm j(2x_2 + 1)], x_1 = x_2 = 0, 1, \ldots, \log_2(M) - 2\}.
\end{aligned} \tag{9}$$

Note that for a PSK constellation $\mathcal{Q}$, for any $u \in \mathcal{Q}, |u|^2 = 1$. This condition does not hold for QAM constellations. For an MQAM constellation a normalization factor may be used to make $E[|u|^2] = 1$, where $E[.]$ is the expectation. This normalization factor is $1/\sqrt{10}$ and $1/\sqrt{42}$ for 16QAM and 64QAM respectively. In general, all elements of $\mathcal{Q}$ occur with equal probability $1/q$.

Some higher signal constellations can be realized as a sum of lower order signal constellation points. This leads to the construction of low PAR sequences [64, 65]. These constructions are discussed next.

Reference [64] shows that 16QAM constellation can be obtained by a combination of two 4PSK constellations. The 4PSK constellation can be realized as $\mathcal{Q}_{\text{QPSK}}$ in Eq. (9). Thus one can associate with any 4PSK sequence $\mathbf{X} = (X_0, X_1 \ldots, X_{n-1})$ a unique sequence $x = (x_0, x_1, \ldots, x_{n-1})$ where $x_i \in \mathcal{Z}_4, 0 \leq i \leq N-1$ and $c_i = j^{x_i}$. We can show that the 16QAM constellation is given by

$$\mathcal{Q}_{\text{16QAM}} = \sqrt{2}\exp\left(\frac{\pi j}{4}\right) z_1 + \frac{\sqrt{2}}{2}\exp\left(\frac{\pi j}{4}\right) z_2 \tag{10}$$

where $z_1, z_2 \in \mathcal{Q}_{\text{QPSK}}$. Using Eq. (9), this can be further simplified as

$$\mathcal{Q}_{\text{16QAM}} = \left\{\sqrt{2}\exp\left(\frac{\pi j}{4}\right) j^{x_i} + \frac{\sqrt{2}}{2}\exp\left(\frac{\pi j}{4}\right) j^{y_k}\right\} \tag{11}$$

for some $x_i, y_k \in \mathcal{Z}_4$. Similarly, the QPSK constellation can be written as a summation of two BPSK constellations [65]

$$\mathcal{Q}_{\text{QPSK}} = \frac{\sqrt{2}}{2} z_1 + j\frac{\sqrt{2}}{2} z_2 \tag{12}$$

where $z_1, z_2 \in \mathcal{Q}_{\text{BPSK}}$. Thus QPSK constellation points can be written as

$$\frac{\sqrt{2}}{2}(-1)^{x_i} + j\frac{\sqrt{2}}{2}(-1)^{y_k} \tag{13}$$

for some $x_i, y_k \in \mathcal{Z}_2$. These representations will be used later in the thesis. Next section we derive the bandpass representation of the OFDM signal.

2.3.3 Bandpass representation of signals

This representation can apply to the bandpass OFDM signal. Consider a real valued signal $s(t)$ having a narrow frequency band around f_c. We quickly summarize a mathematical representation of such signals [62]. The positive frequency components of the signal $s(t)$ are given by

$$S_+(f) = 2u(f)S(f) \tag{14}$$

where $S(f)$ is the Fourier transform of $s(t)$ and $u(f)$ is a unit step function. The equivalent time domain signal is given by

$$s_+(t) = s(t) + j\hat{s}(t) \tag{15}$$

where $\hat{s}(t)$ is the Hilbert transform of $s(t)$ [62]. This transform rotates the phases of all frequencies by 90^o. Equivalent low pass signal $S_l(f)$ can be obtained by performing frequency translation of $S_+(f)$ as

$$S_l(f) = S_+(f + f_c). \tag{16}$$

The equivalent time domain signal is

$$\begin{aligned}
s_l(t) &= s_+(t)e^{-j2\pi f_c t} \\
&= \left(s(t) + j\hat{s(t)}\right) e^{-j2\pi f_c t}.
\end{aligned} \tag{17}$$

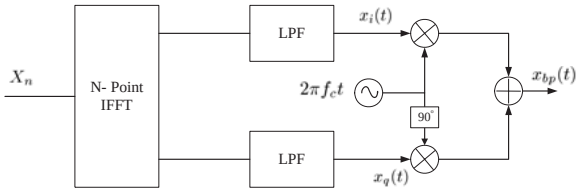

Figure 1: Bandpass OFDM signal generation.

It can be shown that

$$s(t) = a(t)\cos(2\pi f_c t) - jb(t)\sin(2\pi f_c t) \tag{18}$$

$$\hat{s}(t) = a(t)\sin(2\pi f_c t) + jb(t)\cos(2\pi f_c t). \tag{19}$$

Eqn. 18 shows that low frequency signal components of $s(t)$ are modulated on carrier components $\cos(2\pi f_c t)$ and $\sin(2\pi f_c t)$. Since these carrier components are in phase quadrature, $a(t)$ and $b(t)$ are called quadrature components of $s(t)$. The signal in Eq. (18) can also be expressed as

$$\begin{aligned} s(t) &= \Re\left[(a(t) + jb(t))\, e^{2\pi f_c t}\right] \\ &= \Re\left[s_l(t) e^{2\pi f_c t}\right] \end{aligned} \tag{20}$$

where $\Re(x)$ denotes real part of x. The lowpass signal $s_l(t)$ is known as the *complex envelope* of the signal $s(t)$ and is also the equivalent low pass signal. This representation of a bandpass signal can also be used to represent the bandpass OFDM signal, as shown in the next section.

2.3.4 Bandpass representation of an OFDM signal

The baseband OFDM signal is modulated into a high frequency carrier f_c before the transmission. This up converted signal can be expressed as

$$\begin{aligned} x_{bp}(t) &= \Re\{x(t) e^{j2\pi f_c t}\} \\ &= x_i(t)\cos(2\pi f_c t) - x_q(t)\sin(2\pi f_c t) \end{aligned} \tag{21}$$

where $x(t)$ is the complex envelope or the low pass equivalent of the bandpass signal given in Eq. (6). This signal is expressed as

$$x(t) = x_i(t) + jx_q(t) \tag{22}$$

where $x_i(t)$ and $x_q(t)$ are the phase quadrature components of the OFDM symbol given in Eq. (6) and are the real and imaginary outputs of the IDFT process. Figure 1 depicts the bandpass signal generation at the transmitter.

3 Peak-to-average power ratio (PAR)

This section defines PAR and presents oversampling, statistical distribution and various bounds for PAR. It surveys many PAR reduction techniques that have been published in the literature. Root mean square (rms) magnitude of the OFDM signal is defined as the root of the time average of the envelope power $\left(\sqrt{\bar{P}}\right)$, and $\bar{P}$ is defined as

$$\bar{P} = \frac{1}{T}\int_{t=0}^{T} |x(t)|^2 dt = \frac{1}{N}\sum_{n=0}^{N-1} |X_n|^2 \tag{23}$$

where $x(t)$ is OFDM signal defined in Eq. (7). This value $\bar{P}$ corresponds to a single OFDM symbol only and depends on the sequence of information-carrying coefficients $\{X_n\}$. The average power of a set of OFDM symbols can be expressed as $P_{av} = E\{\bar{P}\}$. PAR can be defined as

$$\xi = \frac{\max\limits_{t\in[0,T)} |x(t)|^2}{P_{av}} = \frac{\max\limits_{t\in[0,T)} |x(t)|^2}{E\{|x(t)|^2\}} \tag{24}$$

where $\max|x(t)|^2$ denotes the maximum instantaneous power of the OFDM signal. This is the PAR of the baseband OFDM signal. Throughout this thesis the term **PAR** will refer to the baseband PAR. Several related terms and definitions for PAR are used in the literature. The definition in Eq. (24) is also termed

PAPR [66, 67] and peak-to-average power (**PAP**) ratio as well [68]. PAR and PAPR are the most frequently used terms. Another related term is the **crest factor**, which is the square root of the PAR ($CF = \sqrt{\xi}$) [69–73]. The term peak-to-mean envelope power ratio (**PMEPR**) is also used [65, 74–76]. The definition of PMEPR is also similar to the definition of PAR given in Eq. (24). Strictly speaking, the above definition should be called PMEPR, because $|x(t)|$ is the envelope but not the transmitted signal itself.

A statistical definition of PAR is also useful. An OFDM symbol is said to have a peak at ξ_p at probability P_c if

$$\Pr[\xi < \xi_p] = P_c. \tag{25}$$

The probability that PAR exceeds ξ_p is $(1 - P_c)$. The OFDM signal has a PAR which exceeds ξ_p for less than $100(1 - P_c)\%$ of the OFDM blocks. (i.e $100(1 - P_c)\%$PAR is ξ_p). This definition is used later in the thesis to compare the PAR statistics.

3.1 Maximum PAR of an N subcarrier OFDM signal

The PAR of an OFDM signal is always less than or equal to N, where N is the number of subcarriers. Consider the OFDM signal given in Eq. (7)

$$x(t) = \frac{1}{\sqrt{N}} \sum_{n=0}^{N-1} X_n e^{j2\pi\Delta f t} \tag{26}$$

where the input data is power normalized, without loss of generality, such that $E[|x(t)|^2] = 1$. PAR is bounded as

$$\begin{aligned} \xi &= \max_{t\in[0,T)} |x(t)|^2 \\ &= \max_{t\in[0,T)} \left| \frac{1}{\sqrt{N}} \sum_{n=0}^{N-1} X_n e^{j2\pi\Delta f t} \right|^2 \\ &\leq \frac{1}{N} \left[\sum_{n=0}^{N-1} \left| X_n e^{j2\pi\Delta f t} \right| \right]^2 \\ &\leq N. \end{aligned} \tag{27}$$

This is the maximum of the PAR of a given N subcarrier OFDM system. It is shown in [77] for N subcarrier OFDM system with MPSK modulation that there are only M^2 sequences having maximum PAR of N.

The PAR is a function of the data frame and recall there are q^N distinct data frames for a N subcarrier OFDM signal with q-ary modulation. For any input data frame we have

$$1 < \xi \leq N. \tag{28}$$

For example, for $N = 256$ the PAR can be as high as 24 dB ($10\log_{10}(256)$). Fortunately, very high PAR values are very rare. For example, with BPSK, only four sequences $0000\ldots$, $1111\ldots$, $0101\ldots$ and $1010\ldots$ achieve $\xi = N$. For randomly distributed data, the probability of an occurrence of this is $4/2^N = 2^{2-N}$. This probability is negligible when N is large, as is the case in practice.

3.2 PAR of the bandpass signal

Since $f_c \gg \Delta f$, the peak of the bandpass signal is approximately equal to the peak of the baseband signal

$$\max_{t\in[0,T)} |x(t)|^2 \approx \max_{t\in[0,T)} |x_{bp}(t)|^2 \tag{29}$$

and

$$\begin{aligned} E\left\{|x(t)|^2\right\} &= E\left\{|x_i(t) + jx_q(t)|^2\right\} \\ &= E\left\{|x_i(t)|^2 + |x_q(t)|^2\right\} \\ &= E\left\{|x_i(t)|^2\right\} + E\left\{|x_q(t)|^2\right\}. \end{aligned} \tag{30}$$

For QAM signals

$$|x_i(t)|^2 = |x_q(t)|^2. \tag{31}$$

Therefore

$$E\left\{|x(t)|^2\right\} = 2E\left\{|x_i(t)|^2\right\} = 2E\left\{|x_q(t)|^2\right\}. \tag{32}$$

The average power of the bandpass signal can be found as

$$\begin{aligned} E\left\{|x_{bp}(t)|^2\right\} &= E\left\{|x_i(t)\cos(2\pi f_c t) - jx_q(t)\sin(2\pi f_c t)|^2\right\} \\ &= E\left\{|x_i(t)\cos(2\pi f_c t)|^2\right\} + E\left\{x_q(t)\sin(2\pi f_c t)|^2\right\} \\ &= \frac{1}{2}E\left\{|x_i(t)|^2\right\} + \frac{1}{2}E\left\{|x_q(t)|^2\right\} \\ &= \frac{1}{2}E\left\{|x(t)|^2\right\} \\ &= P_{av}/2. \end{aligned} \tag{33}$$

This yields

$$\begin{aligned} \xi_{bp} &= \frac{\max\limits_{t\in[0,T)}|x(t)_{bp}|^2}{P_{av}} \\ &= 2\frac{\max\limits_{t\in[0,T)}|x(t)|^2}{P_{av}} \\ &= 2\xi. \end{aligned} \tag{34}$$

From Eq. (34) the PAR of the bandpass signal is approximately 3 dB higher than that of the baseband signal.

3.3 Estimating true PAR from discrete time signals

Consider the discrete time representation of the OFDM signal given in Eq. (8)

$$x_k = \frac{1}{\sqrt{N}}\sum_{n=0}^{N-1} X_n e^{j2\pi kn/N}, \quad k = 0, 1, \ldots, N-1. \tag{35}$$

These samples are called Nyquist-rate samples. The continuous time signal is generated from these samples by low pass filtering at the transmitter. In order to obtain the continuous time signal from its samples, N samples are sufficient. Figure 2 shows the continuous time signal and the Nyquist sampled signal. However, the Nyquist rate samples do not necessarily coincide with the peaks of the continuous time signal. Therefore it is essential to oversample the OFDM signal to estimate the true PAR. Figure 2 shows that 4 times oversampling gives more accurate results.

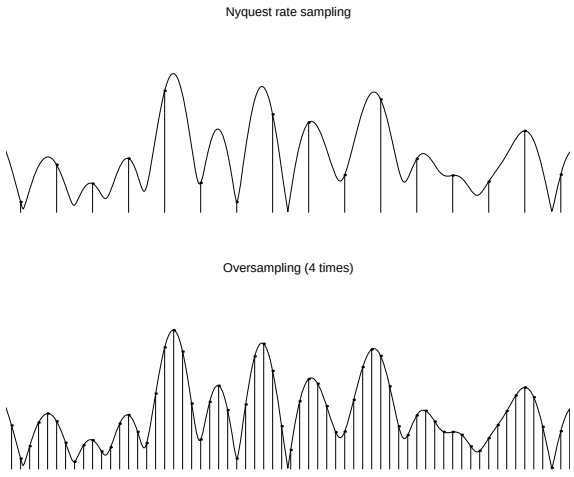

Figure 2: The effect of oversampling.

If the OFDM signal is divided into LN samples, where $L \geq 1$ is an integer referred to as the oversampling factor, the k-th oversampled point of the OFDM signal can be expressed as

$$\begin{aligned} x_k^L &= \frac{1}{\sqrt{N}}\sum_{n=0}^{NL-1} X_n^L e^{j2\pi kn/NL} \\ &= \sqrt{L}\left[\frac{1}{\sqrt{N}L}\sum_{n=0}^{NL-1} X_n^L e^{j2\pi kn/NL}\right] \\ &= \sqrt{L}\,\mathrm{IDFT}(X_n, NL) \end{aligned} \tag{36}$$

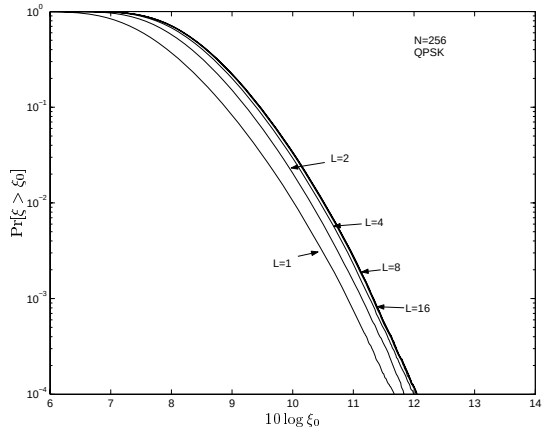

Figure 3: CCDF of PAR with different oversampling ratios.

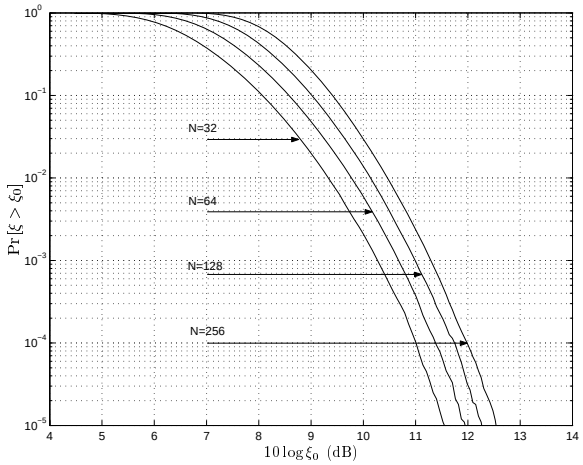

Figure 4: The CCDF for N QPSK subcarriers.

where IDFT(a, b) is the b point IDFT of the signal a and X_n^L is the n-th input signal of the OFDM signal appended with $N(L-1)$ zeros

$$X_n^L = \{X_0, X_1, \ldots, X_{N-1}, 0, 0, \ldots, 0\}. \tag{37}$$

The PAR of oversampled discrete time signal is given by

$$\xi_L = \frac{\max\limits_{k\in[0,NL)} |x_k^L|^2}{E\left\{|x_k^L|^2\right\}}. \tag{38}$$

We have

$$\xi \geq \xi_L > \xi_{Nyq} \tag{39}$$

where ξ_{Nyq} is the PAR estimated using Nyquist samples, defined as

$$\xi_{Nyq} = \frac{\max\limits_{k\in[0,N)} |x_k|^2}{E\left\{|x_k|^2\right\}}. \tag{40}$$

3.4 Statistical distribution of PAR

Dynamic range requirements of the transceiver equipment are determined by the distribution of the peak power of the continuous time signal. Figure 3 depicts the CCDF of PAR estimated using different oversampling rates. Oversampling rate 2 shows higher CCDF values compared to the Nyquist rate sampling case. Over sampling rate 4 improves slightly compared to the oversampling rate 2. The CCDF does not appreciably improve for oversampling rates over 4. Estimation of the true PAR is essential for better performance evaluation of PAR reduction schemes. An oversampling factor of 4 appears sufficient to estimate the actual PAR. Throughout this thesis an oversampling rate of 4 is used unless otherwise specified.

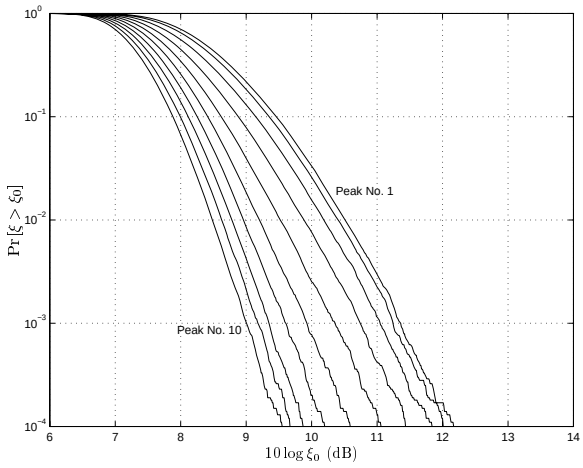

Figure 5: Distribution of 10 peak values of a given OFDM signal.

The CCDF is shown for $N = 32, 64, 128$ and 256 in Figure 4. For 256 subcarriers, the maximum PAR is 24 dB. To reach this however, all the subcarriers need to be in phase at some instant in time, and therefore produce an amplitude peak equal to the sum of the amplitudes of the individual subcarriers. This occurs with extremely low probability for large N. For example, the PAR exceeds 12.5 dB for 1 in 10^5 of all the possible transmitted OFDM symbols.

The distribution of 10 largest peak values of an oversampled ($L = 4$) OFDM signal is depicted in Figure 5. Typically the CCDF of PAR curve for a given OFDM signal is estimated using the maximum peak value. But this figure shows distribution of the highest 10 peaks. While the difference between the distributions of the first two peaks is negligible, there is a difference of 2.5 dB between the first peak and the 10-th peak. The study of multiple peaks in a OFDM signal can lead to a proper understanding about the number of peaks clipped due to insufficient back-off of the transmitter power amplifier.

It is shown in [78], that the amplitude of N point IDFT does not necessarily yield the actual peak power of the signal and oversampling is essential to locate the true peak. Wulich in [79] reported that the continuous wave should be considered in order to reduce the peak factor if the prime reason for peak reduction is to reduce the dynamic range of the power amplifier. He used an illustrative example to show that the continuous time wave of an OFDM signal may be arbitrarily large. But it is reported in [80], that for a band limited periodic signal the amplitude is bounded by the total power and the number of constituent harmonic tones. The signal variation is bounded by the total power and the bandwidth. For a bandlimited non-periodic signal, the amplitude and variation are bounded by the total energy and the bandwidth.

The baseband OFDM signal can be characterized approximately as a band limited complex Gaussian process. Theoretical and empirical expressions derived below use this assumption. The PAR distribution can be estimated using the oversampled OFDM signal. An analytical model for the PAR distribution of OFDM signals with PSK subcarrier modulation is described in [81]. This model is used to derive the achievable information rate for OFDM without channel coding and with a peak power constraint on the transmitted signal. But in this section we will focus only on the empirical approach described in [82] and the theoretical approach presented in [83].

3.4.1 An empirical approach

An empirical expression for the distribution of PAR has been described in [82]. For an OFDM signal with N subcarriers, the samples of the complex baseband signal can be written as Eq. (8). From the central limit theorem it follows that for large values of N, the real and imaginary values of x_k become Gaussian distributed, each with a mean zero and variance 1/2. The amplitude $r_k = |x_k|$ of the OFDM signal is therefore Rayleigh distributed with a probability density function

$$f_{r_k}(r) = 2re^{-r^2}, \quad r \geq 0 \tag{41}$$

while the power ($p_k = r_k^2$) distribution becomes a central chi-square distribution, with a cumulative distribution function (CDF) given by

$$F_{p_n}(p) = \Pr(p_n \leq p) = 1 - e^{-p}. \tag{42}$$

The CDF of the PAR of an OFDM signal can then be derived assuming that the samples are mutually independent and uncorrelated

$$\Pr(\xi \leq \xi_0) \approx (1 - \exp(-\xi_0))^N. \tag{43}$$

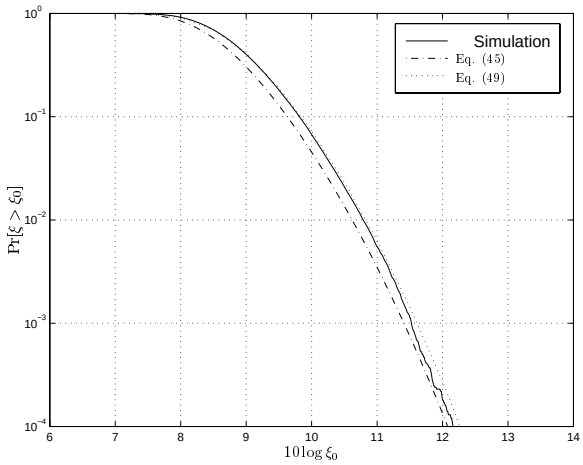

Figure 6: Theoretical and simulated CCDF of PAR of an OFDM signal.

However, by Parseval's relation

$$\sum_{k=0}^{N-1} |x_k|^2 = N. \tag{44}$$

Therefore, the independent assumption in Eq. (43) is not strictly true. As (43) does not also hold for the oversampling case, [82] suggests addition of a certain number of extra independent samples to approximate the effect of oversampling. An empirical expression for the CCDF of PAR can be written as

$$\Pr(\xi > \xi_0) \approx 1 - (1 - \exp(-\xi_0))^{\alpha N} \tag{45}$$

where $\alpha > 1$. Reference [82] shows that $\alpha = 2.8$ is a good approximation for the oversampled OFDM signals in general.

3.4.2 Exact statistical distribution of PAR

Reference [83] derives an expression for the exact distribution of the crest factor of an OFDM signal. The CCDF of PAR is expressed as

$$\Pr(\xi > \xi_0) \approx \left(1 - \frac{\hat{N}_\xi(\overline{\xi})}{0.641N}\right)^{0.641N} \tag{46}$$

where

$$\hat{N}_\xi(\overline{\xi}) = \frac{4N}{\sqrt{15\pi}} \int_{\overline{\xi}}^{\infty} u^2 \int_0^{\infty} e^{-(\phi^2+1)u^2} \left\{ e^{-\psi^2(u,\phi)} - \sqrt{\pi}(u,\phi)\mathrm{erfc}(\psi(u,\phi)) \right\} d\phi du \tag{47}$$

and

$$\psi(u,\phi) \equiv \frac{\sqrt{5}}{2}(\phi^2 - 1)u \tag{48}$$

$\hat{N}_\xi(\overline{\xi})$ is the mean number of peaks above the level $\overline{\xi}$ in one OFDM symbol. As this expression is complicated, an approximation of the peak distribution based on level-crossing rates is also presented. The CCDF of PAR of an OFDM signal is then [83]

$$\begin{aligned} \Pr(\xi > \xi_0) &\approx \Pr(\xi > \overline{\xi} | \xi_0 > \overline{\xi}) \\ &= \begin{cases} 1 - \left(1 - \frac{\xi_0 e^{-{\xi_0}^2}}{\overline{\xi} e^{-\overline{\xi}^2}}\right)^{\sqrt{\frac{\pi}{8}} N \overline{\xi} e^{-\overline{\xi}^2}} & \text{for } \xi_0 > \overline{\xi}, \\ 1 & \text{for } \xi \le \overline{\xi}. \end{cases} \end{aligned} \tag{49}$$

This was derived considering only the peaks exceeding a given threshold $\overline{\xi}$ above zero. A proper $\overline{\xi}$ is selected by making the assumption: *each positive crossing of the level $\overline{\xi}$ has a single positive peak that is above the level $\overline{\xi}$* [83]. It also suggests $\overline{\xi} = \sqrt{\pi}$ for QPSK modulation and slightly lower value for 16QAM.

The CDF for $N = 128, 256$ and 512, are plotted in Figure 7. This Figure also compares the simulation results with Eq. (49) and Eq. (45) for different number of subcarriers. The empirical Eq. (45) result is not very accurate. Figure 6 depicts the CCDF curves of simulation results, the empirical formula Eq. (45) and the

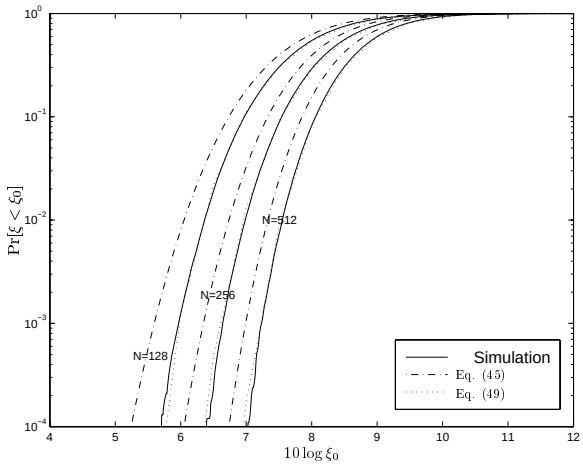

Figure 7: Theoretical and simulated CDF of PAR of an OFDM signal.

theoretical expression Eq. (49). Oversampling factor of 16 with QPSK modulation is used in simulations. Eq. (49) agrees well with the simulation results. There is a slight mismatch between Eq. (45) and the simulation results. Eq. (49) can be used to predict the behavior of OFDM systems. We use this expression in the next chapter to predict PAR when interleaving is used.

Paterson and Tarokh showed [84] that the peak of a continuous signal can be bounded by the maximum of its sampled sequence at Nyquist rate. They proved that

$$\begin{aligned}\max_{0\le\theta\le 2\pi} x(\theta) &\le \left(\frac{2}{\pi}\log(2N)+2\right)\max_{0\le k\le N} x\left(\frac{2\pi k}{N}\right)\\ &\le \left(\frac{2}{\pi}\log(2N)+2\right)\max_{0\le k\le N} x_k.\end{aligned} \tag{50}$$

However this bound is not based on the oversampled sequence. A tight bound for the continuous time OFDM signal based on oversampled sequence is derived in [75]. According to Theorem 2 in [75], if $h(z)$ is a complex polynomial of degree $N-1$, then the maximum of $|h\left(e^{j\theta}\right)|$ is bounded by the maximum of its samples on the unit circle as

$$\max_{\theta}\left|\sum_{n=0}^{N-1} X_n e^{jn\theta}\right| \le \frac{k}{k-\pi}\max_{0\le k\le LN}\left|\sum_{n=0}^{N-1} X_n e^{j\frac{2\pi nk}{LN}}\right| \tag{51}$$

where L is the oversampling factor and $L > \pi$. An upper bound for the CCDF of PAR is derived using the above relationship

$$\Pr(\xi > \xi_0) \le L_{opt} N e^{-\xi_0(1-\pi/L_{opt})^2} \tag{52}$$

for $\forall\xi > 0$, L_{opt} is the optimum oversampling factor given by

$$L_{opt} = \pi\xi_0\left(1+\sqrt{1-\frac{1}{\xi_0}}\right) \tag{53}$$

Eq. (53) is obtained considering the fact that $L_{opt} > \pi$ [75].

3.4.3 Asymptotic results

The statistical behavior of PAR($\mathbf{a}$) for large N is important, as in some practical applications, N can be as large as 2048 or more. A bound for probability that the PAR of an OFDM signal will exceed a given level is derived in [85]. In this study special attention has been given to the case in which the number of subcarriers grows to infinity. It is claimed that this bound can be applied to OFDM systems with a moderate number of subcarriers with good accuracy. We can show that PAR($\mathbf{a}$) grows as $\ln N$; that is, for a randomly picked data sequence, PAR($\mathbf{a}$) is unlikely to be significantly less than $\ln N$. From Eq. (43), we get

$$\begin{aligned}\Pr\{\xi \le \alpha\ln N + h\} &= (1-e^{-(\alpha\ln N+h)})^N\\ &\simeq e^{-N^{(1-\alpha)}e^{-h}} \quad \text{for} \quad N\to\infty\end{aligned} \tag{54}$$

where $\alpha \geq 1$. This follows readily from fact that $\lim_{n\to\infty}(1-\theta/n)^n = e^{-\theta}$. If $\alpha = 1$ and $h = -h$ in Eq. (54), we see that

$$\Pr\{\xi \leq \ln N - h\} \simeq e^{-e^h}. \tag{55}$$

This is the formal mathematical equivalent of our above statement. This also elicits information about clipping and coding for PAR reduction. Clipping is a method to deal with high peak amplitude excursions at the transmitter output (Chapter 6). This is necessary because the D/A converter has a limited resolution (ie the number of bits) and the power amplifier cannot be linear over an amplitude range that includes the peak amplitudes. A clip occurs when the signal amplitude exceeds a predefined threshold and hence clipping is described as follows:

$$x_c(t) = \begin{cases} x(t) & \text{if } |x(t)| \leq x_{clip} \\ x_{clip}e^{j\angle x(t)} & \text{if } |x(t)| > x_{clip} \end{cases} \tag{56}$$

where $x_{clip} > 0$ is the clipping threshold. The probability of clipping is the number of clips per unit time. Of course, each clipping device introduces data symbol errors and out-of-band noise. Eq. (55) shows that for a normal OFDM system, if the clipping threshold is set below $\ln N$, then the clipping probability will be unity for large N. Likewise, Eq. (54) suggests if the clipping threshold is set above $\alpha \ln N$, then the clipping probability can be arbitrarily reduced. Here the right hand side of Eq. (54) explicitly shows that the decay rate depends on both α and h.

Additionally, coding seems unnecessary for PAR reduction of $\alpha \ln N$ or higher as clipping will not occur very often. In contrast, clipping will introduce significant distortion if it is used to keep the PAR at a level significantly below $\ln N$. At this point coding becomes interesting. Consider coding to reduce the PAR to h below $\ln N$, where $|h|$ is small compared to $\ln N$. Lets assume a binary modulation (i.e. $x_k \in (+1, -1)$). From Eq. (55), the achievable coding rate is

$$R(h) = \frac{\log_2(2^N e^{-e^h})}{N} = 1 - \frac{e^h}{N \log_2 e}. \tag{57}$$

As h increases, the achievable coding rate tends to zero. Similarly if h is negative, the achievable coding rate tends to one, suggesting that the PAR can be limited to a level above $\ln N$ with very little redundancy. Moreover, the required amount of redundancy decays exponentially with the difference between the target PAR and $\ln N$. It appears that any family of good codes (i.e., of non-vanishing coding rate) must have a PAR bound of around $\ln N$.

3.4.4 Code rate

Consider MPSK modulated N subcarriers, which can accommodate $N \log_2(M)$ information bits at most. Suppose that we need a code rate $R = 1 - K/(N \log_2(M))$ to limit the PAR to ξ_0. Thus we have

$$\Pr(\xi < \xi_0) = \frac{M^{N\log_2(M)-K}}{M^N} \tag{58}$$

which can be rearranged as

$$R = 1 + \frac{1}{N \log_2(M)} \log_2 \Pr(\xi < \xi_0). \tag{59}$$

This probability term can be estimated by simulation. Figure 8 shows the required code rate to limit the PAR. For $N = 128$, to reduce PAR to 7 dB from 21 dB for the uncoded case, the required code rate is 0.98. This suggests that the PAR can be much reduced by a small amount of redundancy. Unfortunately, it has so far not been possible to discover such a code.

When multiple symbol representation is used (eg. PTS, SLM) to reduce the PAR, several OFDM symbols are generated from the same information sequence and the one with the minimum PAR is chosen for the transmission. Let K be the number of different OFDM symbols generated. The redundancy (χ) required in this case can be expressed as

$$\chi = \log_2(K) \text{ bits.} \tag{60}$$

Code rate for multiple symbol representation can be written as

$$R_c = \frac{N \log_2(M) - \log_2(K)}{N \log_2(M)}. \tag{61}$$

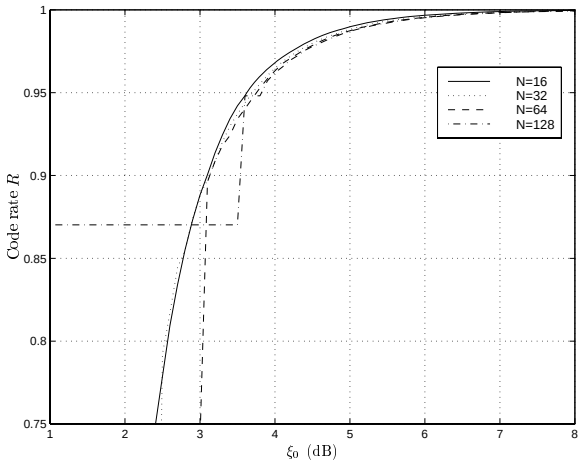

Figure 8: Code rate for limiting the PAR.

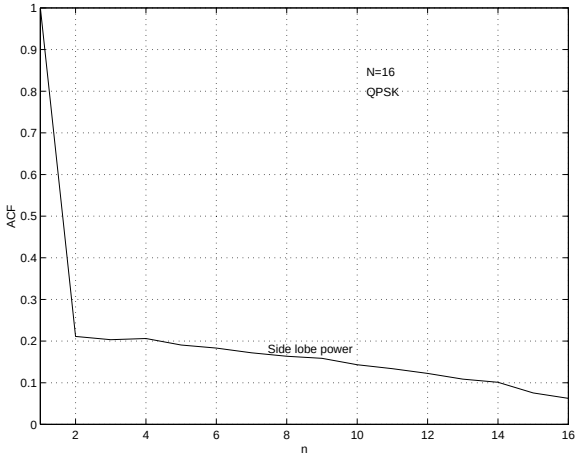

Figure 9: APA of the input signal.

3.5 Aperiodic auto-correlation and PAR

The CCDF of PAR is often used to observe the PAR statistics. The aperiodic auto-correlation (APA) of the input sequence also gives a measure of the output PAR. Peak value of the APA is the average power of the signal. Sidelobes of the ACF indicate the correlation of the input sequence [86]. If the sidelobes of ACF have higher values, then the input sequence is highly correlated and its PAR is large. The high correlation in the input to the IDFT causes the subcarriers to align in phase. After summing these in-phase functions, the output might have large amplitudes, resulting in higher PAR. The APA of the input sequence $\mathbf{X}$ can be given by

$$\rho(k) = \sum_{n=1}^{N-k} X_{n+k} X_n, k = 0, 1, ..., N-1. \tag{62}$$

The maximum PAR is bounded as shown in [86]

$$\xi \leq 1 + \frac{2}{N} \sum_{k=1}^{N-1} |\rho(k)|. \tag{63}$$

Therefore, a measure of PAR of OFDM signals can be obtained by observing the APA. Figure 9 shows a ACF of an OFDM signal with 16 subcarriers. Sidelobe power can be clearly observed in the figure. If a PAR reduction scheme is applied, a reduction in the sidelobe power can be observed.

3.6 Using the infinity-norm

This method was suggested by Van-Eetvelt [87]. The L_p-norm of continuous function $s(t)$ is defined as

$$L_p(s(t)) = \left[\frac{1}{T}\int_0^T |s(t)|^p\, dt\right]^{1/p}. \tag{64}$$

To compute the PAR using the infinity norm L_∞ we can use the fact that for increasing p the L_p norm is non-decreasing. So in practice, taking a sufficiently large power (p) allows the peak value to be approximated as closely as required. However, computing this integral is not so easy. The use of the discrete-time PAR is much more convenient.

In the next section, the procedure of [88] for computing the continuous-time PAR of an OFDM signal with BPSK subcarriers will be generalized. The new method can handle higher-order complex signalling constellations. An upper bound and a lower bound on the PAR will be derived. The upper bound can be shown to be applicable to high PAR sequences, and also shown to be related to Merit Factor.

3.7 Computation of continuous-time PAR

To compute the continuous-time PAR, the roots of the derivative of the envelope power function (EPF) are required. At first, finding the required roots appears tedious, since this derivative consists of sinusoidal functions. The problem suggests a general root finding algorithm for non-linear functions. Fortunately, this difficulty can be avoided for the BPSK case [88]. In this section we present the computation of continuous time PAR for M-ary constellations.

For MPSK, the data symbol for n-th subcarrier $X_n \in \{1, \zeta, \ldots \zeta^{M-1}\}$ where $\zeta^M = 1$ and $M = 2, 4, 8, \ldots$, and $|X_n|^2 = 1$. For MQAM, X_n is complex but not necessarily of unit amplitude. The following development holds for MPSK constellations and for MQAM, the average constellation power must be normalized to unity (details omitted). The continuous-time PAR is defined as the maximum of the baseband EPF. We can show that the EPF [88, 89]

$$P_X(t) = \sum_{k=0}^{N-1} \Re(\beta_k)\cos(2\pi k t) + \Im(\beta_k)\sin(2\pi k t) \tag{65}$$

where

$$\beta_k = \begin{cases} 1 & k = 0 \\ \dfrac{2}{N}\displaystyle\sum_{n=0}^{N-1-k} X_n^* X_{n+k} & k = 1, 2, \ldots, N-1 \end{cases} \tag{66}$$

and $\Re(z)$ and $\Im(z)$ are real and imaginary parts of z. The technique [88] is limited to BPSK subcarriers, for which the β_k's are real. With complex signalling constellations, the EPF Eq. (65) would consist of both $\cos(2\pi k t)$ and $\sin(2\pi k t)$ terms. This EPF hence cannot be transformed into a linear combination of Chebysev polynomials of the first kind. In the sequel, we show that this EPF can be transformed into a sum of Chebysev polynomials of the first kind and second kind. We define the maximum norm as $\|P_X(t)\|_\infty = \max_t P_X(t)$. In passing, we note that

$$\int_0^1 (P_X(t) - 1)\, dt = 0. \tag{67}$$

This means $\|P_X(t)\|_\infty$ is greater than unity. To compute $\|P_X(t)\|_\infty$ exactly, the roots of $\frac{dP_X(t)}{dt} = 0$ are needed. Let us define

$$Q_X(t) = P_X\left[\frac{\cos^{-1} t}{2\pi}\right] = \sum_{k=0}^{N-1} \Re(\beta_k) T_k(t) + \Im(\beta_k) U_{k-1}(t)\sqrt{1-t^2} \tag{68}$$

where $T_k(t) = \cos(k\cos^{-1} t)$ is the k-th order Chebysev polynomial of the first kind and

$$U_{k-1}(t) = \sin(k\cos^{-1} t)/\sqrt{1-t^2}$$

is the Chebysev polynomials of the second kind [90, p. 1054]. Note that $T_0(t) = 1$, $T_1(t) = t$, $T_2(t) = 2t^2 - 1$ and so on (explicit expressions for the coefficients of $T_n(t)$ and $U_n(t)$ for any n are available). Both $T_n(t)$ and $U_n(t)$ satisfy the recursion $f_{n+1}(t) = 2t f_n(t) - f_{n-1}(t)$ for $n \geq 1$.

Since $Q_X(t)$ has a factor of $\sqrt{1-t^2}$, we need a squaring operation to eliminate this factor. Differentiating $Q_X(t)$ with respect to t and performing some manipulations, we obtain the polynomial equation

$$(1-t^2)\left(\sum_{k=0}^{N-1} \Re(\beta_k)\dot{T}_k(t)\right)^2 = \left(\sum_{k=0}^{N-1} \Im(\beta_k)\left[\dot{U}_{k-1}(t)(1-t^2) - U_{k-1}(t)\right]\right)^2. \tag{69}$$

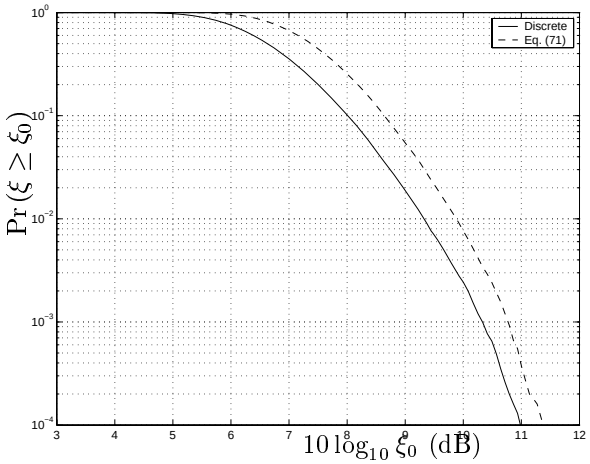

Figure 10: The CCDF for 64, QPSK subcarriers.

This equation has up to $2N-2$ real roots (a polynomial of degree n will have n real or complex roots). We need the real roots that lie between -1 and $+1$. Let those roots be $\xi_1, \xi_2, \ldots, \xi_M$ where $M \leq 2N-2$. Let us define the set

$$\Lambda = \left\{0, \frac{1}{2}, \frac{\cos^{-1}\xi_1}{2\pi}, \ldots, \frac{\cos^{-1}\xi_M}{2\pi}\right\}. \tag{70}$$

The continuous-time PAR is obtained by

$$\|P_X(t)\|_\infty = \max_{t\in\Lambda} P_X(t). \tag{71}$$

This method has been implemented using Maple and Matlab for $N = 64$ and QPSK modulated subcarriers. The CCDF results are shown in Figure 10 in which the discrete-PAR is calculated using only N samples. The difference between the exact PAR and the discrete PAR is about 0.5 dB. The use of an oversampling factor of 4 is sufficient to close this gap.

3.7.1 New bounds on the PAR

Applying the Cauchy-Schwarz bound $|\sum a_k b_k|^2 \leq \sum |a_k|^2 \sum |b_k|^2$ to Eq. (65), we obtain

$$\begin{aligned} P_X(t) &= \sum_{k=0}^{N-1} |\beta_k| \cos(2\pi k t - \phi_k) \\ &\leq \left(\sum_{k=0}^{N-1} |\beta_k|^2\right)^{\frac{1}{2}} \left(\sum_{k=0}^{N-1} |\cos(2\pi k t - \phi_k)|^2\right)^{\frac{1}{2}} \\ &\leq \left(N \sum_{k=0}^{N-1} |\beta_k|^2\right)^{\frac{1}{2}}. \end{aligned} \tag{72}$$

Finally, we obtain the two bounds

$$1 + \sum_{k=1}^{N-1} \Re(\beta_k) \leq \|P_X(t)\|_\infty \leq \left(N + N \sum_{k=1}^{N-1} |\beta_k|^2\right)^{\frac{1}{2}}. \tag{73}$$

The lower bound is simply $P_X(0)$. The lower bound shows that the larger the sum of $\Re(\beta_k)$ for $k > 1$, the larger the PAR will be. Recall that the PAR of a length N sequence lies in the range 1 to N. The minimum value of this upper bound is $\sqrt{N}$, which occurs when $\beta_k \approx 0$ for $k = 1, \ldots, N-1$. So the upper bound will be tight only for sequences with PAR above $\sqrt{N}$. For sequences with very low PAR (such as complementary sequences), this upper bound will be a poor bound. Figure 11 shows the CCDF for both the upper bound and the PAR. Note that these QPSK sequences are generated via a pseudo-random generation algorithm that is biased so that only sequences with high PAR are generated. The upper bound is within 0.5 dB of the exact value in such cases.

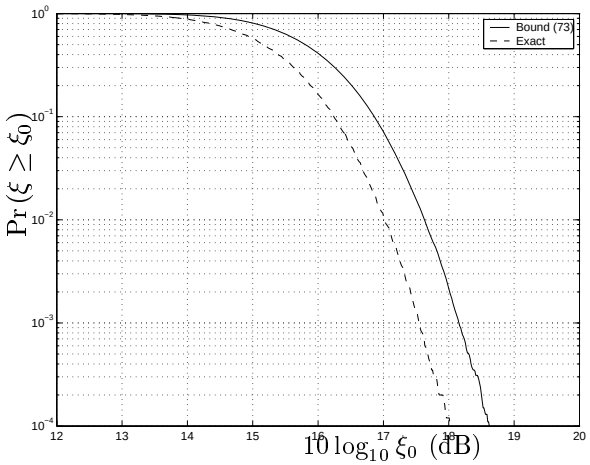

Figure 11: The biased CCDF for 128 QPSK subcarriers.

3.7.2 Comparison with other bounds

A parameter closely related to PAR is the Merit Factor (MF). For a length N sequence, the MF is defined as [91]

$$M = \frac{2}{\sum_{k=1}^{N-1} |\beta_k|^2}. \tag{74}$$

Combining this with Eq. (73), we have

$$\|P_X(t)\|_\infty \leq \left[N\left(1+\frac{2}{M}\right)\right]^{\frac{1}{2}}. \tag{75}$$

Although a length 13 binary sequence exists with MF as high as 14.08, infinite binary sequence constructions appear to have MF no higher than 6.0, (e.g. for shifted-Legendre sequences) as $N \to \infty$. m-sequences and Rudin-Shapiro sequences both have MF asymptotes of 3.0, and a 'random' sequence will have an MF close to 1.0 as $N \to \infty$. If we substitute these values for M into Eq. (75) then we observe the following (rather loose) asymptotes on the upper bound on PAR.

$$\begin{aligned}
M \to 1, &\quad \|P_X(t)\|_\infty \leq \sqrt{3N} &&\text{random binary sequence}\\
M \to 3, &\quad \|P_X(t)\|_\infty \leq \sqrt{\tfrac{5N}{3}} &&m\text{-sequence, Rudin-Shapiro sequence}\\
M \to 6, &\quad \|P_X(t)\|_\infty \leq \sqrt{\tfrac{4N}{3}} &&\text{shifted-Legendre sequence}
\end{aligned}$$

We stress that the upper bound of Eq. (73) is very weak for low PAR sequences. It remains an open problem to find a tighter bound for low PAR sequences. But the bound of Eq. (73) becomes useful for upper-bounding high-PAR sequences, as shown in Figure 8. Table 1 illustrates the 'looseness' of the bound for some sample low PAR sequences, making a comparison with the upper-bound of [89], which is given by

$$\|P_X(t)\|_\infty \leq 1 + \sum_{k=1}^{N-1} |\beta_k|. \tag{76}$$

We also compare with the upper-bound of [84], which is given, for length $2^m - 1$ m-sequences, by

$$\|P_X(t)\|_\infty \leq \frac{2^m}{2^m-1}\left(\frac{2\log 2}{\pi}(m+1)+2\right)^2. \tag{77}$$

For m-sequences, the bound of [84] is asymptotically tighter than Eq. (73) and Eq. (76), but looser than the bound in [89], for m-sequences of length less than $2^{11}-1$ (resp. $2^{14}-1$). However, the bound of [84] requires virtually no computation. It is evident from Table 1 that all three upper bounds are loose in comparison to the actual PAR but the upper bounds of both [89] and Eq. (73) become tight for high PAR sequences.

Table 1: A comparison of bounds for m-sequences, shifted-Legendre and Rudin-Shapiro sequences.

$m-$ sequences

N	$\|P_X(t)\|_\infty$	$Eq.(73)$	$Eq.(76)$	$Eq.(77)$	M
31	3.04	7.60	22.30	5.06	2.32
63	2.75	10.40	26.31	5.92	2.79
127	3.03	14.47	30.82	8.42	3.08
255	3.60	20.95	35.80	11.55	2.77
511	5.35	29.10	41.20	16.35	3.04
1023	4.99	40.97	47.02	22.00	3.12

Shifted-Legendre Sequences

N	$\|P_X(t)\|_\infty$	$Eq.(73)$	$Eq.(76)$	M
11	1.31	3.58	1.91	12.1
31	1.84	6.38	3.26	6.41
61	2.14	9.05	4.61	5.85
127	2.34	13.01	6.09	6.00
251	2.73	18.27	8.24	6.06
503	3.26	25.94	11.72	5.92
1019	2.83	36.86	15.58	6.01

Rudin-Shapiro Sequences

N	$\|P_X(t)\|_\infty$	$Eq.(73)$	$Eq.(76)$	M
32	2.00	7.35	3.75	2.91
64	2.00	10.30	4.56	3.05
128	2.00	14.63	6.03	2.98
256	2.00	20.64	7.59	3.01
512	2.00	29.22	10.06	2.99
1024	2.00	41.30	13.40	3.00

3.8 Low PAR sequences and non data applications

In many practical applications waveforms with low PAR are needed [92]. A single sequence having low PAR is the requirement in non-data applications, while data applications (eg. OFDM) needs many such low PAR sequences such that data can be mapped to these. Additionally, encoding and decoding should be simple. Radar and sonar are some of the examples of non-data applications where only a single low PAR sequence is required. A phase sequence can be denoted by $p = \{e^{j\varphi_0}, e^{j\varphi_1}, \ldots, e^{j\varphi_{N-1}}\}$. The problem is to find suitable phase sequences with low PAR. Several such waveform generations are described in [92].

Two choices for such sequences with low PAR are presented in [69]. The first choice is the multitone signal with Shapiro-Rudin phases. Rudin-Shapiro sequences has a PAR under 3 dB, if the number of tones is a power of two. The second choice is the Newman phases. The Newman phases yield smaller crest factor than the Rudin-Shapiro phases. The Newman phases are generated as follows [69]:

$$\varphi_k = \frac{\pi(k-1)^2}{N}. \tag{78}$$

Reference [93] studies the Newman phase sequences in detail and shows that the 2.6 dB PAR always prevails for large N. A numerical technique for finding the phases that minimize the PAR, when sinusoids are not necessarily equally spaced is developed in [94]. Another two approaches to realize sequences with low PAR are presented in [95] and [96]. The latter showed that generally any binary or polyphase sequence, belonging to a pair of complementary sequences, can be used to construct the initial phases of tones forming the multitone signal with the crest factor less or equal to 3 dB. It also shows that the proposed Shapiro-Rudin sequences are only the representatives of the much larger family of binary Golay complementary sequences. Recently Golay complementary sequences have been used to reduce PAR of OFDM signals. We will discuss these in the section on PAR reduction techniques.

A phasing scheme with low PAR based on analysis of the instantaneous envelope power of a multitone signal is presented in [97]. It uses the variance in the instantaneous envelope power as a parameter for determining better combination of the initial phases of all tones. A relationship between the initial phase (θ_k) and the variance (σ^2) of the instantaneous envelope power is derived as

$$\sigma^2 = 2A^2 \sum_{k=1}^{N-1} \sum_{l=k+1}^{N} \sum_{m=l}^{N+k-l} \cos(\theta_l - \theta_k - \theta_{m+l-k} + \theta_m) \tag{79}$$

where A is a constant. An iterative numerical approach is presented to calculate the initial phases based on the above relationship. PAR as small as 2.4 dB can be obtained for $N \geq 3$. For some special cases, where $N = 9, 11, 16$ and 23, PAR is 1.2 dB.

3.8.1 Constructing Single Sequences with Low PAR

Sequences with low APA are often parameterized by their MF (74). Finding sequences with highest MF is closely related to the APA problem, and has been studied by a few authors [91, 98]. The BPSK sequence with highest known MF is of length 13 and has an MF of 14.08. Although BPSK sequences have been found with MF $\simeq$ 9.0 up to length 117, these sequences are the result of optimized computer search. Very few infinite constructions for high MF sequences are known. The best-known are the Offset-Legendre, Twin-Prime, and (Modified)-Jacobi constructions. These constructions generate sequences with optimally low APA and with MF $\to$ 6.0 as $N \to \infty$, and this is the highest asymptote known for BPSK. A recent Legendre-type infinite construction has generated sequences with moderately low APA, and again with MF $\to$ 6.0 as $N \to \infty$. In contrast, both the m-sequence and length 2^m complementary sequence have an asymptotic MF of 3.0 [98]. Next, we survey various PAR reduction techniques that have been published in the literature.

4 PAR reduction schemes for OFDM

PAR reduction in OFDM is a challenging task. Schemes proposed for this purpose can be divided into following categories:

1. **Signal distortion techniques**: Clipping, Pre-distortion,
2. **Coding techniques**: Block codes, Convolutional codes, Golay complementary sequence, Reed Muller codes,
3. **Multiple signal representation**: Partial transmit sequences(PTS), Selected mapping (SLM), Selective scrambling, Interleaving,

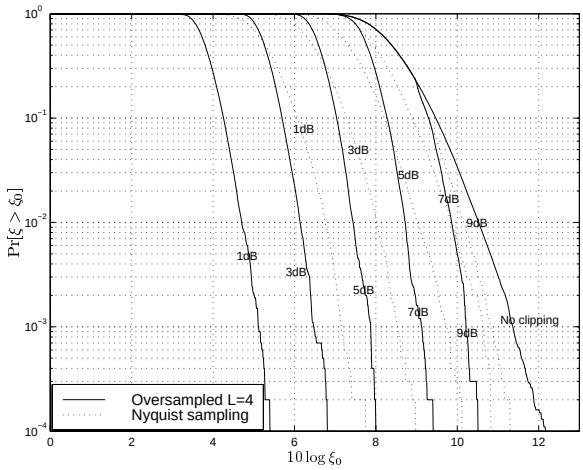

Figure 12: CCDF of PAR after clipping.

4. **Modified signal constellations**,
5. **Pilot tone methods**,
6. **Other methods**.

4.1 Signal distortion techniques

PAR can be reduced by distorting the OFDM signal. Unfortunately, these distortion techniques introduce out of band radiation (OBR) and degrade the BER.

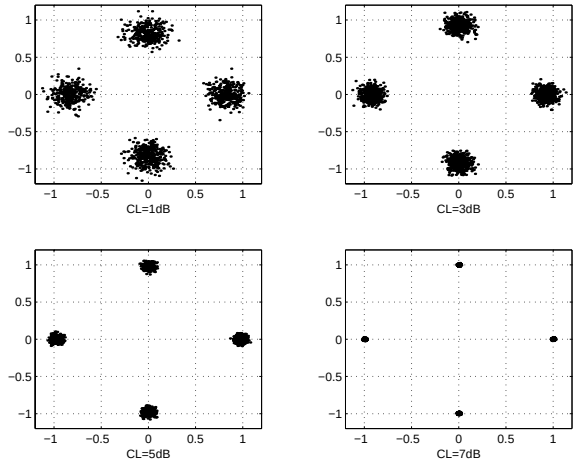

Figure 13: Distortion of the signal after clipping.

4.1.1 Deliberate clipping to reduce PAR

The simplest way to reduce the PAR is to clip the high peak values. As high peaks occur with very low probability, a small amount of clipping will not increase the BER significantly. However, clipping will cause undesirable OBR, in band distortion and inter-modulation products if severe clipping is performed. Several PAR reduction proposals based on clipping techniques and the analysis of effects of clipping can be found in the literature. Figure 12 depicts the CCDF of PAR of an OFDM signal after various levels of clipping. An OFDM system with 256 subcarriers and QPSK modulation is simulated. The clipping level is defined as

$$CL = 20\log_{10} x_{clip} \tag{80}$$

where x_{clip} is the clipping threshold. Clipping of the k-th output sample $x_k = r_k e^{j\phi_k}$ is performed according to the rule given in Eq. (56), which can be expressed in oversampled form as follows:

$$|\hat{r}_k| = \begin{cases} r_k & r_k \leq x_{clip}, \\ x_{clip} & r_k > x_{clip} \end{cases} \qquad 0 \leq k \leq LN-1 \tag{81}$$

where L is the oversampling factor.

A PAR reduction of 6 dB is observed with 1 dB clipping, while it is about 4 dB for 3 dB clipping. But severe signal distortion occurs with high level of clippings. The OFDM signal must be oversampled before the clipping to overcome the peak regrowth at the low-pass filter output. Figure 12 depicts the effect of oversampling in the performance of clipping. Oversampling causes an improvement in PAR reduction. The effect of oversampling before digital clipping on the PAR is reported in [99]. A theoretical analysis is also presented to justify the simulation results obtained. Figure 13 shows the received signal points after clipping. Severe distortion is observed for the 1 dB clipping, while the distortion is negligible for 7 dB clipping. Therefore, PAR reduction can be tradedoff against BER performance. Chapter 6 provides further results.

Clipping process reduces the output power. Let P_{co} denotes the output power of the clipped OFDM signal. If the amplitude of the OFDM signal is Rayleigh distributed, which is the case with OFDM when N is large, the average output power is given by [100]

$$P_{co} = \left(1 - e^{-\gamma^2}\right) P_{in} \tag{82}$$

where P_{in} is the input power to the soft limiter and γ is the clipping ratio given by $\gamma = x_{clip}/\sqrt{P_{in}}$. $\gamma = 0$ corresponds to the hard envelope limiter while $\gamma = \infty$ refers to a system without clipping.

Clipping in OFDM will increase OBR and degrade the BER performance. OBR caused by clipping can be reduced by using a suitable filter followed by the clipping device. Such a filter causes peak regrowth [2, 101]. If the OFDM signal is clipped at the Nyquist rate, the clipping noise will fall in-band, which cannot be reduced by filtering. This can be avoided by oversampling the signal. In reference [101] simulations are performed to find the peak regrowth due to filtering and the BER performance is also evaluated for clipped and filtered OFDM signals. BER can be improved by using a suitable forward error correction code. Reference [102] shows that appropriate clipping together with small oversampling factor followed by a mild filter can greatly increase the performance. The effect of clipping of both baseband and bandpass multicarrier signals is investigated in [103]. The effect of filtering on the performance of OFDM systems is also reported in [104]. A relationship between guard band and the cyclic prefix is obtained. There is an optimum guard band which incurs minimum capacity loss.

The distortion caused by clipping is analyzed in [25, 26]. Several modulation schemes are examined to find the effects of clipping. Results show that a controlled amount of clipping is permissible in many cases, due to low probability of high peaks.

Decision aided reconstruction (DAR) is proposed in [105] for mitigating the clipping noise. The receiver is assumed to know the clipping level. DAR is an iterative reconstruction technique, which increases the receiver complexity. Several DFT operations are performed at the receiver before reconstructing the original signal.

Performance of amplitude clipped high order OFDM is presented in [106] while the asymptotic behavior of level clipped OFDM signal, when its order N approaches infinity is analyzed in [107]. An expression for the probability of clipping is found and the upper bound of the probability of error is derived. An approximation for the resulting increase in BER in baseband transmission is given in [108]. In [109] spectral spreading of the distortion is considered, but only for real-valued baseband DMT signals.

An iterative maximum likelihood (ML) algorithm is presented in [110] to recover the signal distorted by the nonlinear devices. The loss in mutual information caused by the non-ideal properties of the transmitter is quantified. The optimal ML derived has an exponential complexity. To reduce complexity a simple algorithm that iteratively estimates the nonlinear distortion is introduced. In parallel with this algorithm the technique proposed in [111] is used to reduce the OBR cased by the clipping of the signal.

Clipping with frequency domain filtering is proposed in [112] to reduce the PAR. Frequency domain filtering is used to reduce the OBR of the clipped signal. Frequency domain filtering is simple and has superior performance compared to the time domain filtering after clipping. Although the BER performance would not be affected by this new scheme out-of-band power is reduced significantly.

Another area of research related to clipping of OFDM signals is to find the effect of different nonlinearities. Extensive research has been undertaken to understand the effect of high power amplifier (HPA) nonlinear distortion in OFDM systems in [113–115].

4.1.2 Pre-distortion

Pre-distortion techniques based on companding, phase and amplitude correction and clipping are discussed in this section. The use of companding techniques to reduce the PAR has been proposed by several authors

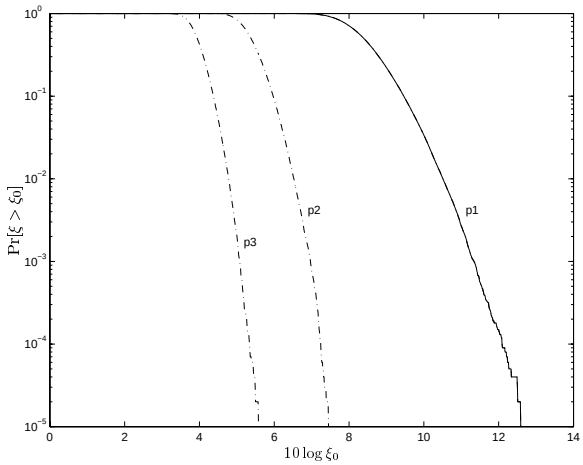

Figure 14: CCDF of PAR with companding transform.

[116–123]. An OFDM signal is considered similar to a speech signal in the sense that large signals only occur infrequently, and hence the same companding technique (μ law) has been used to improve the PAR [118]. The samples of OFDM signal are companded before being converted into analog waveform. The amplitude of small samples is increased while the peaks remain unchanged after the companding. Therefore, the average power is increased and the PAR is reduced. Further results and comments on this technique are reported in [124, 125]. Companded and uncompanded signals with equal power are compared in [125]. An expression for the PSD of the companded signal is also derived.

A method that combines the advantages of clipping and companding is proposed in [126]. Small samples are enhanced and large samples are compressed while keeping the average power unchanged. With appropriate selection of companding form and its corresponding inflexion point, PAR can be reduced significantly. The average power of the transmitted signals will be unchanged after the companding transform if the average power is set to the transform inflexion point and the companding form is odd symmetrical with reference to the inflexion point. The sample $\hat{x}_k$ after companding transform can be expressed as

$$\hat{x}_k = \frac{V x_k}{\ln(1+\mu)|x_k|} \ln\left[1 + \frac{\mu}{V} x_k\right] \tag{83}$$

where V is the inflexion point when $\mu \leq 5$. Accordingly V is the average power of the signal. The received sample $\hat{r}_k$ after inverse-companding can be expressed as

$$\hat{r}_k = \frac{V' r_k}{\mu |r_k|} \left\{ \exp\left[\frac{|r_k| \ln(1+\mu)}{V'} \right] - 1 \right\} \tag{84}$$

where V' is the average power of the received signal, r_k is the sampled received signal. The BER performance with companding in an AWGN channel is better compared to that with the clipping and filtering. Figure 14 shows the CCDF of PAR after the companding transform is taken. A PAR reduction of 7 dB is observed for $\mu = 3$ while a 5 dB reduction is observed for $\mu = 1$ at 0.01%PAR. The distortion of the signal increases with the value of μ.

A predistortion technique employing minimum mean squared distance (MMSE) criterion is reported in [122, 123]. The MMSE predistortion strategy is set forth by modelling the phase distortion (PD) as a third order polynomial device, with complex valued coefficients

$$y = x(p + q|x|^2) \tag{85}$$

where x and y denote the input and the output of the PD. Optimal values for p and q are found by minimizing the mean squared distance between the actual PD output and the output corresponding to the ideal linearizing PD. An amplitude and phase predistortion technique for a OFDM transmission system employing multilevel QAM is reported in [127] and its performance is compared with that of the MMSE technique above. The general technique presented in [128] is applied to OFDM in [127]. The proposed amplitude and phase distortion technique can be described as follows.

Figure 15 depicts the functional block diagram of the amplitude and phase distortion. The output $y(t)$ is obtained as the product of the input $x(t)$ and the output of a nonlinear memoryless device consisting of the parallel two branches. The upper branch compensates for the nonlinear AM/AM conversion of the power amplifier, while the lower branch compensates for the AM/PM conversion. These AM/AM and AM/PM terms

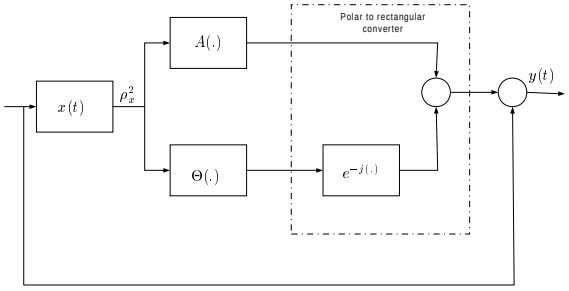

Figure 15: Functional block diagram of the amplitude and phase distortion.

are described in detail in Chapter 2. The ideal linearizing function $A(\rho^2)$ and $\Theta(\rho^2)$ are in practice approximated as polynomials in ρ^2 of orders N_A and N_Θ respectively as follows [128]:

$$\hat{A}(\rho^2) = \sum_{i=0}^{N_A} \beta_i \rho^{2i}, \quad \hat{\Theta}(\rho^2) = \sum_{i=0}^{N_\Theta} \gamma_i \rho^{2i} \tag{86}$$

where β_i and γ_i denoting appropriate real valued coefficients that are to be calculated through joint minimization of the mean squared distances between polynomials and the ideal responses of $A(\rho^2)$ and $\Theta(\rho^2)$. In addition the mapping law $\exp\{-j\Theta(\rho^2)\}$ is implemented as a truncated Taylor series expansion of order N_e.

4.2 PAR reduction codes

In principle block coding schemes to reduce the PAR have many advantages. First, the transmission of side information to the receiver is unnecessary. Second, codes can include error control capability, which can reduce the BER. Good coding schemes, which reduce PAR and provide good error correction capabilities having higher code rates have been elusive to date.

4.2.1 PAR, Hamming distance and complementary sequences

A M-ary code $\mathcal{C}$ is a given set of N-tuples $\mathbf{X} = (X_0, X_1, \ldots, X_{N-1})$, where each $X_n \in \mathcal{Q}$. The Hamming distance between two sequences $(\mathbf{X}, \mathbf{Y})$ or codewords is defined as

$$d_H(\mathbf{X}, \mathbf{Y}) = \sum_{n=0}^{N-1} \delta(X_n - Y_n) \tag{87}$$

where $\delta(\cdot)$ is the Kronecker delta function. A critical parameter of a code $\mathcal{C}$ is the minimum Hamming distance, or just minimum distance, which measures how good it is at error-correcting. This is defined to be the smallest of the distances between any two distinct codewords. That is

$$d_{\min} = \min\{d_H(\mathbf{X}, \mathbf{Y}) \mid \mathbf{X}, \mathbf{Y} \in \mathcal{C}, \mathbf{X} \neq \mathbf{Y}\}. \tag{88}$$

The PAR of a code $\mathcal{C}$ is defined as

$$\mathrm{PAR}_{\max} = \max\{\mathrm{PAR}(\mathbf{X}) \mid \forall \mathbf{X} \in \mathcal{C}\}. \tag{89}$$

Finally, the code rate of a code $\mathcal{C}$ is defined as

$$R = \frac{\log_2 \sharp(\mathcal{C})}{N \log_2 M} \tag{90}$$

where $\sharp((\mathcal{C}))$ denotes the number of elements of set $(\mathcal{C})$. The following notation will be used where necessary. An $[n, k, d_{\min}, \eta]$-code is a code of length n, containing k information symbols, with minimum distance $d_{\min}$ and $\mathrm{PAR}_{\max}$ η.

One of the earliest low PAR code constructions was that proposed by Jones et al. [24], with parameters $[4, 3, 2, 1.75]$. Input data is mapped only to the OFDM symbols with low PAR. To do this high PAR OFDM

symbols are excluded thus reducing the efficiency of the transmission. PAR of all possible data sequences are computed and a code book is generated consisting of only the sequences having low PAR. This code book is prohibitively large if the number of subcarriers are large, making it highly complex to implement. Efficient realization of low PAR codes for OFDM systems with large number of subcarriers needs algebraic coding rules and decoding algorithms.

Several authors noted that low PAR codes can be constructed using complementary sequences. A pair of sequences $\mathbf{X}$ and $\mathbf{Y}$ is complementary if

$$\rho_{\mathbf{X}}(k) + \rho_{\mathbf{Y}}(k) = 2\delta(k) \quad k = 0, 1, \ldots, N-1$$

where $\rho_x(y)$ is the aperiodic auto-correlation function of x with a displacement of y. Taking the Fourier transform of this, we have

$$P_{\mathbf{X}}(t) + P_{\mathbf{Y}}(t) = 2.$$

Hence it is clear the PAR of $\mathbf{X}$ and $\mathbf{Y}$ must be less than or equal to 2. Recently, Davis and Jedwab made a significant breakthrough by identifying the relationship between complementary sequences and Reed-Muller codes [129]. We next describe several other contributions before elaborating on Davis and Jedwab's codes.

Reference [130] reported a work similar to [24], where the redundant bit is chosen as the inverse of the one of the information bits in the same data frame. This coding scheme [130] eliminates codewords with maximum PAR, but not the second maximum (next highest peak) and ones below that. Unfortunately, when N increases the difference between maximum PAR and peak below that reduces rapidly giving negligible PAR reduction. A modified version of the simple block coded presented in [130] is reported in [131].

It is shown in [132] that the use of systematic odd parity checking coding (SOPC) proposed in [130] is not effective in terms of PAR reduction when N is large. Therefore, PAR can not be reduced by eliminating codewords with maximum peaks. However, it is found [133] that, when N is large, high PAR reduction still can be obtained if the long information sequence is divided into several sub-blocks, and each sub-block is encoded with SOPC. An extended version of sub-block coding termed redundant bit location optimized sub-block coding, in which position of the odd parity bit is optimized to get low PAR is also presented. Another scheme combining two codes to represent the same information in a sub-block is presented. Each of the latter schemes requires sending of side information to the receiver. Therefore it further reduces the bandwidth efficiency.

In [24] coding was performed using a code book, which contains all the codes with low PAR. Suitable codes were identified and potential gains are explored in [134]. A method of manipulating standard block codes to provide the additional benefit of envelope limitation with additional redundancy was introduced in [135]. While [135] was an acceptable engineering solution to the problem, the envelope fluctuation achieved were still not ideal and there is no way of bounding the degree of envelope limitation for a particular type of code.

A polynomial time algorithm for determining optimal phase shift for the codes reported in [134], is presented in [136]. This algorithm computes the phases that minimize the maximum PAR taken over all possible transmitted signals. It further claims that the new algorithm enables the use of method reported in [134] to various medium length as well as long codes of practical interest.

A block coded modulation technique to reduce PAR, based on [24] is presented in [27,137]. Binary sequence with fixed length are mapped to M-ary sequences with fixed length. Then M-ary sequences of small sizes with PAR less than a threshold are searched. The searched small size M-ary sequences are then partitioned according to the maximal minimum distance between the M-ary sequences. Finally, M-ary sequence of large sizes are constructed by concatenating the searched M-ary sequences of small size, where the PAR of the long M-ary sequences is also ensured less than or equal to the threshold used in the search of the small length M-ary sequences. QPSK and 8PSK sequences are studied. Optimal QPSK sequences of length 4 are listed. Desirable PAR properties can be obtained by selecting a suitable threshold PAR and mapping the input sequences into QPSK sequences having PAR less than the selected threshold PAR and maximum free distance of mapped sequences. In [24] the symbols for which peak factor is higher than some given *a priori* threshold value are not transmitted. In [138] a similar method is proposed.

Another coding scheme termed as redundant bit position rotation sub-block coding (RBPR-SBC) is reported in [139]. In this new scheme redundant bit positions are changed and the sequence with the minimum PAR is chosen for the transmission. An early termination threshold for PAR is proposed to reduce the complexity of the system. The PAR of an OFDM signal can be reduced substantially by coding to select only those messages with low peak factor as valid code-words in the scheme [140]. It is also shown that the asymptotic limit of the PAR lies between 2 dB and 3 dB when such a code is employed.

A system based on amplitude limiting and forward error correcting coding (AL-FEC) is proposed in [141]. A bandpass filter is used to suppress the OBR and FEC is used to correct the bit errors caused by the amplitude limiting. A BCH code is used as the FEC. The AL-FEC method is compared to two methods namely [24] and [142]. It shows that AL-FEC reduces PAR more than that described in [24]. For $N = 8$ and the code rate of 3/4 [24] reduces the PAR to 3 dB, while this method can reduce it to 1 dB for the same BER. In [142], the code

length is always equal to the number of subcarriers N. Consequently, the error correcting capability is uniquely determined by N. In AL-FEC a code with a different length can be employed thereby achieving desirable error correcting capability, theoretically without limit. On the other hand it can be used with an OFDM system with any number of subcarriers. But it further states that for the same N Reed Muller codes [142] perform better.

The use of m-sequences to reduce the PAR is reported in [143]. In this approach a block of m input bits are mapped an m-sequence of length $2^m - 1$. This results in a code rate of $\frac{m}{2^m-1}$. In the original contribution [143], it is claimed that the PAR can be limited to 0.58, 0.28, 0.14, 0.07 and 0.03 dB for m=3,4,5,6 and 7, respectively. The PAR reduction shown in [143] is incorrect [144, 145]. According to [144] the m-sequences for $3 \leq m \leq 10$ can only yield PAR values of 5.4 to 7.3 dB. Both [144] and [145] show that the PAR can not be established solely on the basis of N samples of the OFDM signal and oversampling is necessary, thus the inaccuracy of the results of [143]. The main disadvantage of using m-sequences is the extremely low code rates when N increases.

Let $\mathcal{C}$ be a code defined over an equal energy constellation. Let R denotes the rate and N denotes the length of $\mathcal{C}$, then $\mathcal{C}$ has 2^{RN} codewords. One way to compute the codewords with large PAR is by examining all codewords of $\mathcal{C}$ and computing the peaks of the corresponding signals at some selected time points. Thus, there is little hope for computing the PAR of an arbitrary code for large values of N using existing methods, since the computation is difficult. The computation of the code $\mathcal{C}$ having large PAR at a given instance of time is intimately related to minimum-distance decoding of $\mathcal{C}$ [146]. As any code $\mathcal{C}$ used in communications must have an efficient minimum-distance decoding algorithm. This can be exploited to compute the PAR of practical codes. An algorithm to determine the PAR of a code that has a polynomial complexity as a function of the length and linear complexity as a function of minimum-distance decoding complexity of the code, is presented in [146]. A PAR reduction scheme based on this algorithm is also reported.

Representation of QPSK sequences in terms of addition of two BPSK sequences is used in [65] to construct QPSK sequences having a PAR less than 4 dB. If $\mathcal{C}_1$ and $\mathcal{C}_2$ denote two BPSK codes having $\mathrm{PAR}(c_1) < \xi_1$ and $\mathrm{PAR}(c_2) < \xi_1$ for all $c_1 \in \mathcal{C}_1$ and $c_2 \in \mathcal{C}_2$. Then the $\mathrm{PAR}(c) \leq \frac{1}{2}(\sqrt{\xi+1} + \sqrt{\xi+1})^2$ for all $c \in \mathcal{C}$ where $\mathcal{C}$ is the QPSK code given by Eq. (13). A similar approach using Eq. (11) is used in [64] to construct 16QAM sequences having low PAR using two QPSK sequences. The PAR of the constructed 16QAM sequences are bounded by 5.56 dB.

The use of analog codes to reduce the PAR is presented in [147]. Analog codes are constructed using Reed-Solomon codes over complex numbers. These codes are used to correct the errors caused by clipping the high peaks of the signal. Such clipping errors which may be regarded as impulse noise are the type of noise analog codes are suited for. It is shown that the analog codes are best suited for cable transmission.

4.2.2 Golay complementary sequences and Reed-Muller codes

Many of the early code proposals were comprehensively generalized by Davis and Jedwab when they proposed an infinite family of binary Golay complementary sequences with parameters $[2^m, \log_2(m!) + m, 2^{m-2}, 2.0]$, and defined them as certain Reed-Muller (RM) $\mathrm{RM}(2, m)$ cosets of $\mathrm{RM}(1, m)$ [28, 148]. This gave a set of codes that had predictable and guaranteed error control and envelope limitation properties. These codes might not have optimal error correcting capability when compared with standard alternatives, but a reduction in coding gain could be quite easily outweighed by a greater reduction in envelope fluctuation.

We call this family DJ, where DJ comprises codewords, $c(\mathbf{x})$, which is defined in corollary 4 in [129]. For any permutations π of the symbols $\{1, 2, \ldots, m\}$ and for any c, $c_k \in \mathcal{Z}_{2^h}$

$$X_i = 2^{h-1} \sum_{k=1}^{m-1} x_{\pi(k)} x_{\pi(k+1)} + \sum_{k=1}^{m} c_k x_k + c \tag{91}$$

gives the i-th symbol of a Golay sequence over $\mathcal{Z}_{2^h}$ of length 2^m, where $(x_1, x_2, \ldots, x_m)$ is the binary representation of symbol position $i, i \in 2^m$ $(i = \sum_{j=1}^{m} x_j 2^{m-j})$. Here $\mathcal{Z}_{2^h} = \{0, 1, \ldots, 2^h - 1\}]$ and each subcarrier contains exactly $h, (h > 1)$ code bits. This explicitly determines $2^{h(m+1)}.m!/2$ Golay sequences over $\mathcal{Z}_{2^h}$ of length 2^m. This is the DJ construction generalized to higher alphabets and to PARs which are a multiple of 2. The construction is optimal for low N. For instance, for $m = 3$ and binary sequences we can construct an optimal $[8, \log_2(48), 2, 2.0]$ DJ code. There are only 16 more sequences with PAR ≤ 2.0 which are not included in the DJ set, and the inclusion of any of these sequences would reduce d from 2 to 1. Unfortunately the rate, k/N, of the DJ construction vanishes rapidly for $N > 32$. Therefore the DJ construction is only practically useful in the context of OFDM for systems requiring no more than 32 subcarriers. It remains an open problem to discover low PAR error-correcting code constructions for $N > 32$ with an acceptable rate. Unfortunately, many OFDM systems require anything from 8 to 8192 subcarriers.

Reference [149] presents the associated encoding procedure for these codes and a maximum likelihood decoding algorithm that uses a distance-preserving map between the codewords of the quaternary $RM_4(1, m)$ and the codewords of the binary code $RM(1, m + 1)$. Performance results are presented for adjacent channel

interference (ACI) and average BER in a time dispersive fading channel. A detailed description of these codes is presented next.

4.2.3 Rudin-Shapiro Recursion

Rudin-Shapiro (RS) polynomials are defined recursively by the formulas [150]

$$\begin{aligned} P_{n+1}(z) &= P_n(z) + z^{2n} Q_n(z) \\ Q_{n+1}(z) &= P_n(z) - z^{2n} Q_n(z), \quad n \geq 0, \end{aligned} \tag{92}$$

where $P_0(z) = Q_0(z) = 1$. RS sequences belong to a larger family of Golay sequences of length 2^k [96]. Construction of RS sequences is equivalent to the recursive construction of Golay complementary pairs [69]. However, in Golay complementary pairs the number of tones is not restricted to power of two as in the case of RS sequences. Binary and multi-phase Golay complementary sequences can be used to construct multitone signals with flat envelopes rendering a PAR of at most 3 dB [96,151]. Based on this results a code was proposed by van Nee [152] to build a special class of block codes that guarantee a PAR of 3 dB at most. Such codes can be constructed for any number of subcarriers N, provided N is a power of two. When employing MPSK to modulate the subcarriers, M-ary source vectors X_m of length $(\log_2 N + 1)$ are encoded into M-ary codewords C_m of dimension N. These codes can be regarded as linear block codes with the generator matrix G_N for the first-order Reed-Muller code $\mathrm{RM}(1, \log_2 N)$, translated by a constant offset D_N, called the kernel, is a row vector of length N with elements representing the phases of Golay complementary sequences, while G_N has dimension $N(\log_2 N + 1)$. These are complementary codes of length N. These codes are a special case of DJ codes described earlier.

The complementary code has a rate of $(\log_2 N + 1)/N$ which decreases with the length of the code. This is due to the higher amount of redundancy needed to limit the PAR to 3 dB as the number of subcarriers increases. The amount of information encoded into an OFDM symbol with a code of length N and using MPSK is $I_{block} = (\log_2 N + 1) \log_2 M$ bit. This gives a data rate of

$$R = \frac{1}{T_S} I_{block} = \frac{(\log_2 N + 1) \log_2 M}{T_S} \text{bps}. \tag{93}$$

With a total bandwidth of $W = N/T_P$ required for the N subcarriers and taking into account the guard time, a bandwidth efficiency of

$$\frac{R}{W} = \frac{T_P}{T_S} \frac{(\log_2 N + 1) \log_2 M}{N} (\text{bps})/\text{Hz} \tag{94}$$

can be achieved for the OFDM signal. The code rate and the bandwidth efficiency decay when the number of subcarriers is increased.

4.2.4 Decoding of complementary codes

The error rate performance of OFDM transmission using complementary codes shall now be investigated for coherent detection. It is assumed that the receiver can perfectly synchronize to the transmitted signal.

First, an AWGN channel with a two-sided noise PSD N_0 is used. The minimum distance, defined as the minimum number of elements in which two codewords differ, is equal to $N/2$ for the complementary code of length N [152]. Consequently, the minimum Euclidean distance d^e_{min} between two codewords in the N-dimensional complex vector space spawned by the encoder output vectors is given by a phase shift of $2\pi/M$ for $N/2$ subcarriers, i.e.

$$d^e_{min} = \sqrt{N/2}.2 \sin\left(\frac{\pi}{M}\right) \tag{95}$$

for MPSK. If soft-decision maximum likelihood (ML) decoding is employed at the receiver, the probability that a neighboring codeword at a distance d^e_{min} from the transmitted word be detected equals [153]

$$P_2 = Q\left(\sqrt{2 \frac{T_P}{T_S} \gamma_b \frac{I_{block}}{N} \left(\frac{d^e_{min}}{2}\right)^2}\right) \tag{96}$$

where $\gamma_b = E_b/N_0$ defines the SNR per bit and Q denotes the complementary Gaussian cumulative distribution function.

In order to get a tight approximation for the codeword error probability, the weight distribution of the code must be considered, i.e., P_2 is multiplied by the number of neighboring codewords. Additionally, the codeword error probability is translated into the symbol error rate. These two conversions are jointly accomplished by

introducing a factor B which depends on the transmission scheme. When assuming Gray encoding for the M-ary symbols, the expectation of the number of bit errors per symbol error tends towards one if the SNR increases. The approximate BER P_{bit} in the AWGN channel then becomes

$$P_{bit} = \frac{B}{\log_2 M} Q\left(\sqrt{2\frac{T_P}{T_S}\gamma_b I_{block}\left(\sin\frac{\pi}{M}\right)^2}\right). \tag{97}$$

Different transmission techniques can very easily be compared with this formula. It is clear that a long code provides a lower BER than short codes when employing an identical modulation scheme. Using a higher-level modulation scheme with the same code on the other hand renders a higher error rate as a result of the smaller d^e_{min}.

4.3 Multiple signal representation

Several statistically independent OFDM symbols are generated using the same data sequence and the one with minimum PAR is selected for transmission. This approach is also known as adaptive symbol selection [154]. Here, mostly the phases of the mapped signals are changed. Two promising techniques to improve the statistics of PAR in this way are selective mapping (SLM) [155] and partial transmit sequences (PTS) [29].

4.3.1 Data permutation (interleaving) approach

It is observed that highly correlated data frames have large PARs, which could thus be reduced, if the long correlation patterns are broken down. A set of fixed permutations (interleaving) is used to break these correlation patterns. In this approach $K-1$ interleavers are used at the transmitter. These interleavers produce $K-1$ permuted frames of the input data. The four times oversampled IDFT of each frame (including the uncoded frame) is used to compute its PAR. The minimum PAR frame of all the K frames is selected for transmission. The identity of the corresponding interleaver is also sent to the receiver as side information. Interleaving can be done either in bit level or symbol level (Figure 16). Bit level interleaving requires extra $K-1$ symbol mapping blocks and serial to parallel converter blocks compared with the symbol level interleaving. Thus, symbol level interleaving is less complex than bit level interleaving [156–162]. Mathematical explanation of the interleaving idea is presented next.

Symbol interleaving

Let $\mathbf{X} = (X_0, X_1, \ldots, X_{N-1})$ be the input data sequences mapped to a suitable constellation $\mathcal{Q}$. Then the permuted sequences are given by

$$\mathbf{X}_{\pi_i} = (X_{\pi_i(0)}, X_{\pi_i(1)}, \ldots, X_{\pi_i(N-1)}) \text{ for } i = 1, 2, \ldots K$$

where $\{n\} \leftrightarrow \{\pi_i(n)\}$ is a one-to-one mapping and $\pi_i(n) \in \{0, 1, ..., N-1\}$ for all n. Both the transmitter and the receiver store the permutation indices $\{\pi_i(n)\}$ in memory, thus interleaving and de-interleaving are simple. The PAR of the sequence having minimum PAR $\xi_{\min}$ is given by

$$\xi_{\min} = \min_{0\le i\le K}\left[\max_{0\le k\le LN} |\mathrm{IDFT}(\mathbf{X}_{\pi_i}, LN)|^2\right] \tag{98}$$

where $\mathrm{IDFT}(x, LN)$ is the LN point IDFT of the sequence x giving out $y_k, k = 0, 1, \ldots, LN-1$ and L is the oversampling factor. Finally, the permuted sequence giving out the $\xi_{\min}$ is selected for the transmission.

Bit interleaving

Let $\mathbf{d} = (d_0, d_1, \ldots, d_{qN-1})$ be the input data sequences which will be mapped to a 2^q-ary signal constellation. Then the permuted bit sequences are given by

$$\mathbf{d}_{\pi_i} = (d_{\pi_i(0)}, d_{\pi_i(1)}, \ldots, d_{\pi_i(qN-1)}) \text{ for } i = 1, 2, \ldots K.$$

Data of these permuted sequences are grouped into N blocks each containing q bits. Each of these q bits block is then mapped to a 2^q-ary constellation point X_n. Again the minimum PAR sequence for the transmission is found using Eq. (98).

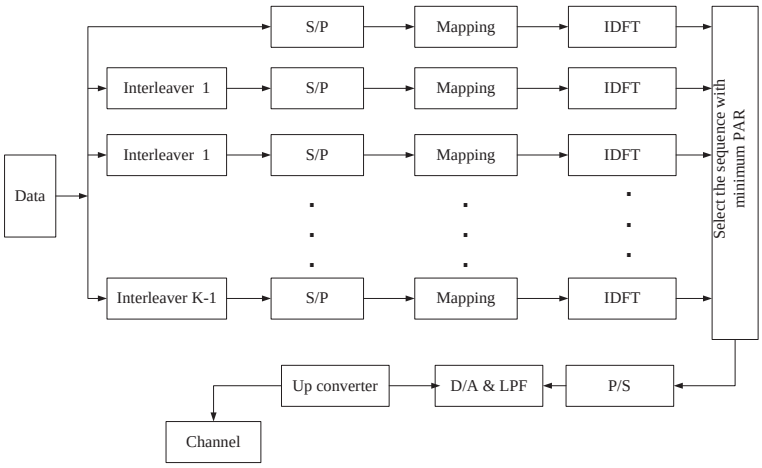

Figure 16: Bit interleaving.

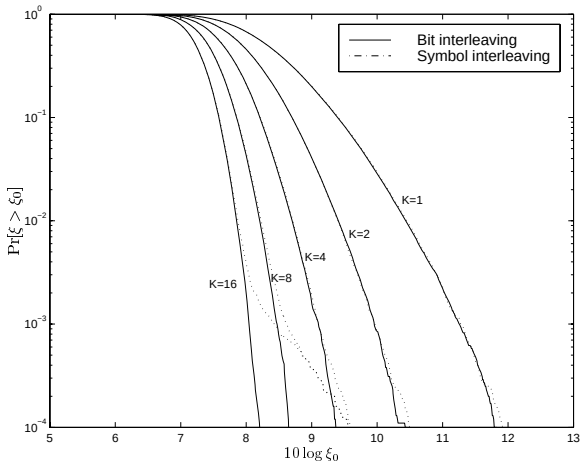

Figure 17: CCDF of PAR after interleaving.

Statistical distribution of PAR of interleaved OFDM signals

Figure 17 depicts the simulation results of CCDF of PAR with symbol level and bit level interleaving. Simulation results are obtained for 256 subcarrier OFDM system with QPSK modulation and pseudo random interleaving. PAR statistics improve significantly with the number of permutations performed. PAR reduction of about 3.75 dB is observed at 0.01% PAR when $K = 16$ (15 permutations are performed). Both schemes show similar performances until $K = 4$. Symbol interleaving does not improve the PAR statistics after 0.1%PAR when $K = 8$ and no improvement is observed after 0.5%PAR when $K = 16$. These results indicate that the number of statistically independent permutations is limited when symbol interleaving is performed.

4.3.2 Selected mapping (SLM)

In SLM one favorable signal is selected from a set of different signals which all represent the same information at the transmitter [155]. For that, U distinct vectors $\mathbf{P}^u = [P_0^u, P_2^u, \ldots, P_{N-1}^u]$, with $P_n^u = e^{j\varphi_n^u}, \varphi_n^u \in [0, 2\pi)$. Modulated symbols (X_n) are multiplied with U vectors $\mathbf{P}^u$ resulting U different sequences. The IDFT of each of these frames are taken and the one with the minimum PAR is chosen for transmission. Identity of the vector used to generate the low PAR sequence is also transmitted with the date. This approach can be used with arbitrary number of subcarriers with moderate complexity. A theoretical expression is derived considering different sequences are statistically independent. A method to generate U distinct vectors is also presented [155].

The use of SLM without explicit side information is reported in [163]. Here, the binary data vectors are scrambled before mapping them to complex signals. To generate U different transmit sequences $\mathbf{x}_u, 0 \leq u \leq U$, representing the same binary word q, labels b^u are inserted as prefix to q. The labels are U different binary vectors of length $\lceil \log_2 U \rceil$, and $b^0 = 0$ is assumed. The concatenated binary vector is then fed into a scrambler consisting of a shift-register with feedback branch, which is reset to zero-state before the scrambling takes

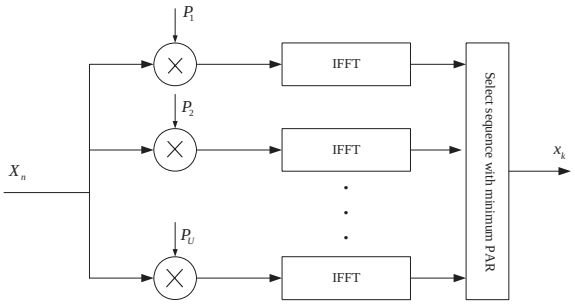

Figure 18: SLM encoder.

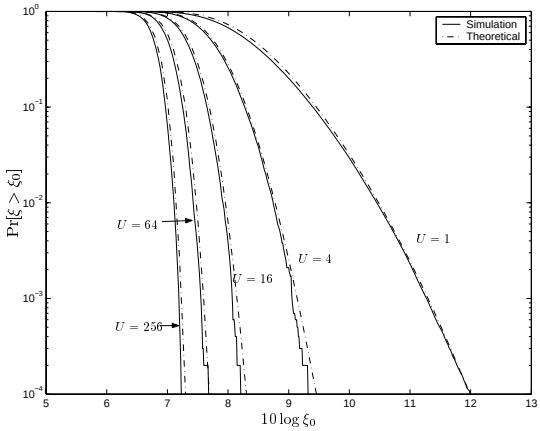

Figure 19: CCDF of PAR of an SLM-OFDM signal.

place. The scrambled sequence is then processed as usual. At the receiver the descrambler performs the inverse operation to the scrambler in the transmitter. Side information is not essential to recover the data. When errors occur during the transmission, the descrambler causes a moderate multiplication of these errors.

Let pseudo noise vectors $P_u = \left[e^{j\phi_0^u}, e^{j\phi_1^u}, \ldots, e^{j\phi_{N-1}^u}\right]$, $\phi_n^u \in (0, 2\pi]$, $u \in \{0, 1, \ldots, U-1\}$. Also let $a \otimes b$ represent the vector product of a and b. For a given input frame X, the lowest PAR sequence $X \otimes P_{\tilde{u}}$, $\tilde{u} \in \{0, 1, \ldots, U-1\}$ is selected for transmission. Receiver has to know the corresponding vector to decode the signal without errors. Corresponding system block diagram is shown in Figure 18.

4.3.3 Blind SLM receiver

It appears that the SLM receiver needs to know $\tilde{u}$. Clearly, $\log_2(U)$ bits are required to represent this information, which is of critical importance to the receiver. One solution is to reserve several subcarriers (i.e. pilot tones) for side information. In a frequency selective fading channel, such pilot tones may be lost and an irrevocable decoding error can occur. Extra protection bits may need to be sent and the total redundancy can thus exceed $\log_2(U)$ bits. A scheme without explicit side information is reported in [164]. Labels representing the side information are inserted as a prefix of the binary input data and passed through a scrambler. However, this scheme needs to send the labels together with the data for the descrambling operations although they are not explicitly used at the receiver.

Here, we present a novel blind decoding algorithm (ie. without the knowledge of the generation process at the transmitter) to recover SLM-OFDM. The blind SLM receiver utilizes (1) X_n's are restricted to a given signal constellation, (2) The set of P_u's is fixed and known a prior, (3) $X \otimes P_u$ and $X \otimes P_v$ are sufficiently different for $u \neq v$. The Hamming distance is N between any two P_u and P_v. The necessary condition for this method to work is $X_n e^{j\phi_n^u} \notin \mathcal{Q}$ for all n and u. The set of P_u can be chosen readily to ensure this.

More generally, let $f_j(c), j = 1, 2, \ldots, U$ are a set of U mappings of vector c. For a given c, let $f_{\tilde{u}}(c)$ have the minimum PAR. A blind receiver does not need to know $\tilde{u}$. For simplicity, let us assume a distortionless and noiseless channel. Now the receiver gets $f_{\tilde{u}}(c)$ and computes $f_j^{-1}\left(f_{\tilde{u}}(c)\right)$ for $j = 1, 2, \ldots, U$. Note that $f_j^{-1}\left(f_{\tilde{u}}(c)\right)$ will not be a vector of symbols from the constellation $\mathcal{Q}$ unless $j = \tilde{u}$. This is the basis of the blind receiver.

For coded OFDM, the blind algorithm can use minimum-distance decoding via the Viterbi algorithm. As linear block codes, convolutional codes and trellis codes have well-defined trellises our blind algorithm can be

integrated into the channel decoder itself. For uncoded OFDM it is prohibitive to search all possible sequences and we thus derive a suboptimal metric. We compare our blind algorithm against an idealized receiver which has perfect side information. We show that the performance degradation is negligible for two particularly important cases (1) A non-linear amplifier is applied to OFDM signals with SLM (2) Subcarriers experience Rayleigh fading.

Blind SLM demodulation

Consider the received signal r_n after the DFT demodulation at the receiver

$$R_n = H_n X_n e^{j\phi_n^u} + \eta_n \tag{99}$$

where $j = \sqrt{-1}$, H_n is the frequency response of the fading channel at the n-th subcarrier and η_n is a complex AWGN sample. Let $r = [r_0, r_1, \ldots, r_{N-1}]$ and $H = [H_0, H_1, \ldots, H_{N-1}]$. The optimal blind SLM receiver uses the decision metric

$$\mathcal{D} = \min_{\substack{[\hat{X}_0, \hat{X}_1, \ldots, \hat{X}_{N-1}] \in C \\ P_{\hat{u}}, \hat{u} \in \{0,1,\ldots,U-1\}}} \sum_{n=0}^{N-1} \left| R_n e^{-j\phi_n^{\hat{u}}} - H_n \hat{X}_n \right|^2. \tag{100}$$

This minimization can be performed as follows. The minimum-distance $H \otimes \hat{X}$ to $r \otimes P_0^*$ is determined, where P_0^* is the conjugate of P_0. This can be done by the Viterbi algorithm for coded systems or by searching all q^N data sequences for uncoded q-ary modulation. This process is repeated for $P_1, P_2, \ldots, P_{U-1}$. The global minimum-distance solution yields the best estimates for X and $\tilde{u}$. The overall complexity is U times that of COFDM without SLM.

Consider the QPSK constellation given by

$$\mathcal{Q}_{\text{QPSK}} = \left\{ e^{j\pi m/2}, m = 0, 1, \ldots, 3 \right\}. \tag{101}$$

For the uncoded case, there are $UN4^N$, $|.|^2$ operations to solve Eq. (100). This is not of very high complexity and can be performed only for small N. We next propose a suboptimal decoding metric with low complexity.

Suboptimal metric

Now $H_n^{-1} R_n e^{-j\phi_n^{\hat{u}}}$ is detected (ie. hard decision) into its nearest constellation point. That is, a hard decision is made for each subcarrier. This whole process is repeated for $0 \leq \hat{u} \leq U-1$. The minimum Euclidean distance solution yields the data sequence. The suboptimal metric can thus be written as

$$\mathcal{D}_{\text{so}} = \min_{P_{\hat{u}}, \hat{u} \in \{0,1,\ldots,U-1\}} \sum_{n=0}^{N-1} \min_{\hat{X}_n \in \mathcal{Q}_{\text{QPSK}}} \left| H_n^{-1} R_n e^{-j\phi_n^{\hat{u}}} - \hat{X}_n \right|^2. \tag{102}$$

Now there are only $4UN$, $|.|^2$ operations to be performed. Performance analysis of the blind SLM receiver is presented in Appendix A.

An OFDM system with 256 quadrature amplitude modulation (QPSK) modulated subcarriers is used in all the simulations. For uncoded OFDM the suboptimal decoding algorithm Eq. (102) is used at the receiver. Performance of the blind detection algorithm (BSLM) is compared with a SLM scheme with perfect side information (PSI-SLM). Figure 20 compares the performance in an AWGN channel. As expected, received data can be perfectly decoded using the blind detection algorithm. Figure 21 compares the BER of BSLM receiver and PSI-SLM in an AWGN channel and a soft-limiter (non-linearity) with back-off values 2 dB, 5 dB and 7 dB. BER is not degraded when using BSLM for these levels of back-offs at the soft-limiter.

Having established the validity of our blind algorithm for an AWGN channel and non-linear channels, we next investigate its performance in fading channels. Trellis coded modulation (TCM) and Rayleigh fading are considered. TCM schemes employ redundant non-binary modulation and a finite-state encoder, which governs the selection of modulation signals to generate coded signals [165]. In the receiver, a soft-decision Viterbi decoder recovers the noisy signals. Non systematic, eight-state encoder with 8PSK mapping is used in the simulations. Note that 8PSK COFDM has the same spectral efficiency as uncoded QPSK-OFDM. Figure 22 shows BER in a Rayleigh fading channel. Perfect channel estimation (CSI) and ideal interleaving are assumed. Once again BER does not degrade for COFDM with our blind algorithm. However, BER is slightly degraded for BSLM if channel coding is not used. Figure 23 compares the BER of coded and uncoded OFDM signals in AWGN and Rayleigh fading channels. TCM-OFDM has about 13 dB gain in a Rayleigh fading channel and a 3 dB gain in an AWGN channel at a BER of 10^{-4}. The proposed BSLM algorithm can decode coded OFDM symbols completely in both AWGN and fading channels even in the presence of a non-linear amplifier.

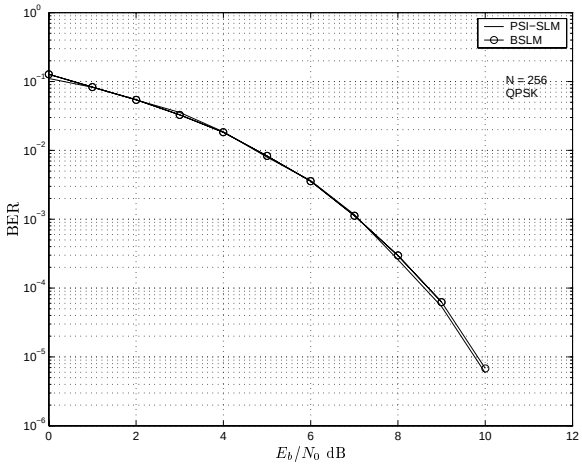

Figure 20: BER performance in an AWGN channel.

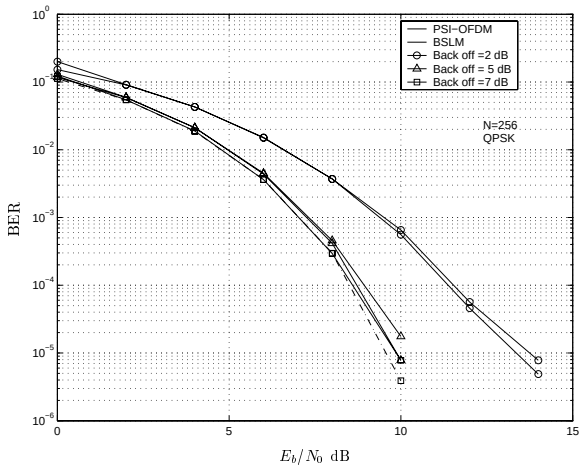

Figure 21: BER performance in a soft limiter and an AWGN channel.

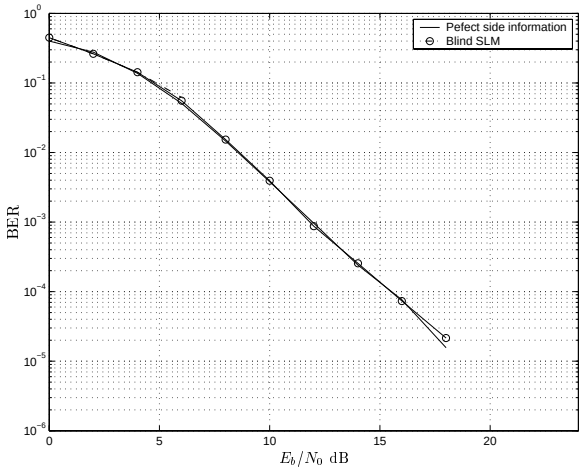

Figure 22: BER performance in a Rayleigh fading channel with perfect CSI (8 states- 8PSK TCM coded OFDM).

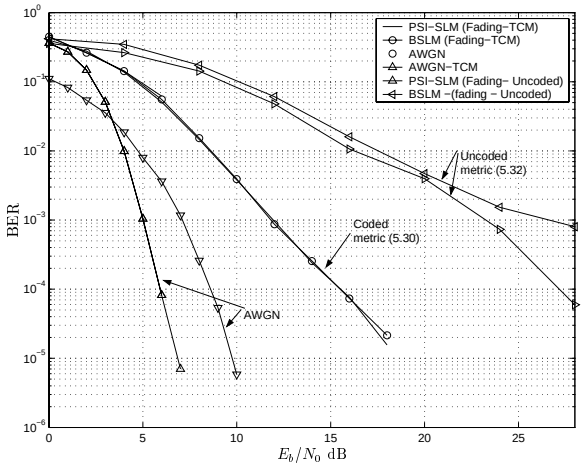

Figure 23: Comparison of BER of PSI-SLM and BSLM in different channels with and without coding.

4.3.4 Partial transmit sequences

In PTS, low PAR is achieved by optimally combining signal sub-blocks [29–32]. PTS introduces additional complexity but improves PAR statistics. Many improvements to this technique have been reported. Several phase factor optimization criteria for PTS are presented [78, 166, 167].

Subblock design

The first step of PTS is to identify a suitable set of subblocks. The data frame is defined as a vector, $\mathbf{X} = [X_0, X_1, \ldots, X_{N-1}]^T$, where X_n is the data symbol for subcarrier $n, n = 0, 1, \ldots, N-1$. The problem is to partition $\mathbf{X}$ into M subblocks. Let I_m be the subcarrier indices for the m-th subblock, $\mathbf{X}_m$. We now have the following relationships

$$I_n \cap I_l \qquad n \neq l \tag{103}$$

and

$$\bigcup_{m=1}^{M} I_n = \{0, 1, \ldots, N-1\}. \tag{104}$$

Subblock partitioning can be classified into three categories: adjacent, interleaved and pseudo random subblock partitioning [30]. In the adjacent scheme, $\frac{N}{M}$ successive subcarriers are sequentially assigned into the same subblock. That is

$$I_1 = 1, 2, \ldots, \frac{N}{M} - 1, \tag{105}$$

$$I_2 = \frac{N}{M}, \frac{N}{M} + 1, \ldots, \frac{2N}{M} - 1 \tag{106}$$

and so on. For the interleaved subblock partitioning, every carrier spaced M apart is allocated at the same subblock. That is

$$I_1 = 0, M, 2M, \ldots, \left(\frac{N}{M} - 1\right) M, \tag{107}$$

$$I_1 = 1, M+1, 2M+1, \ldots, \left(\frac{N}{M} - 1\right) M + 1 \tag{108}$$

and so on. Finally, each subcarrier is assigned into any one of the subblocks randomly in the pseudo-random scheme. That is, $\frac{M}{N}$ entries in each I_n are selected randomly. In each case, disjoint subblocks are generated and optimally combined to reduce the PAR. These three schemes are graphically illustrated in [168]. A general PTS scheme is depicted in Figure 24.

Optimal combining

The IDFT of $\mathbf{X}_m$ s are called partial transmit sequences. Let $y_{k,m}$ for $k = 0, 1, \ldots, 4N-1$, $m = 1, 2, \ldots, M$, be the $4N$ point IDFT of $\mathbf{X}_m$ appropriately zero-padded

$$y_{k,m} = \sum_{n \epsilon I_m} X_n e^{\frac{j 2\pi n k}{4N}}. \tag{109}$$

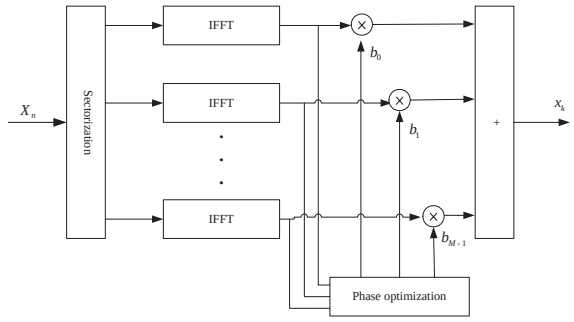

Figure 24: Block diagram of an PTS scheme.

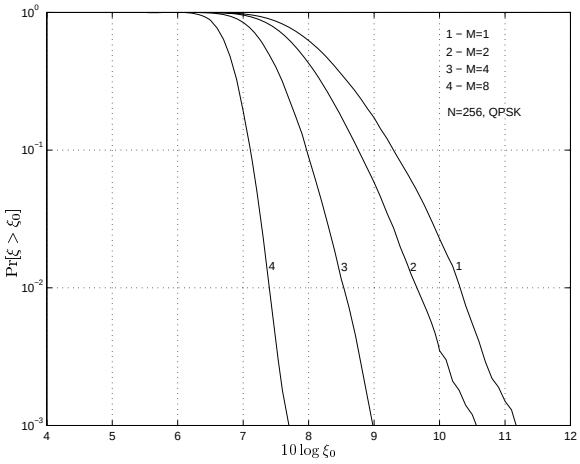

Figure 25: Performance of PTS OFDM.

Oversampling rate 4 (4N) is used for accurate PAR estimation. Using the linearity property of IDFT, the time domain samples can be represented as

$$s_k = \sum_{m=1}^{M} b_m y_{k,m} \qquad k = 0, 1, \ldots, 4N-1 \tag{110}$$

where $\{b_m, m = 1, 2, \ldots, M\}$ are weighting factors. They are further assumed to have pure rotations (i.e., $b_m = e^{j\phi_m}$). The weighting factors are chosen to minimize the PAR of $\mathbf{X}$.

To reduce the complexity of this minimization, a suboptimal choice is used by limiting all to +1 or -1. Without any loss of performance we can set $b_1 = 1$ and observe that there are $M-1$ binary variables to be optimized. Finally the optimal PAR (ξ_{optimal}) can be found using

$$\xi_{\text{optimal}} = \min_{b_1,\ldots,b_M} \left(\max_{0 \le k \le 4N} \left| \sum_{m=1}^{M} b_m y_{k,m} \right|^2 \right). \tag{111}$$

In PTS, PAR in Eq. (111) is computed for all the binary combinations and hence requires 2^{M-1} iterations. Note that the above development is similar to [30] except for the use of oversampling. The performance of PTS schemes with adjacent partitions is shown in Figure 25. An OFDM system with 256 carriers and QPSK modulations is used for the simulations. Results are presented for $M = 2, 4$ and 8 with weighting factors $b_m = \pm 1$. It improves the statistics of PAR by 0.75 dB, 2.2 dB and 3.5 dB at 0.1% of PAR. PTS with $M = 16$ is highly complex even with binary weighting factors (± 1). It needs 2^{15} iterations for each OFDM symbol.

The number of phase rotations can be increased in order to increase the number of alternative transmit signals. In a cyclically shifted sequence (CCS) system [169] more alternative transmit signals are produced by cyclically shifting the data after or before they are phase shifted. The complexity of PTS can be reduced by using CCS-PTS. But additional side information about the shifts is a disadvantage.

In a sub-block partitioning scheme [168], modulated symbols are assigned into partial sub-blocks randomly. Active subcarrier in each partial sub-block is duplicated and concatenated repetitively to generate a complete sub-block. Thus, the active subcarriers of each sub-block appear as if they have been interleaved. Therefore, this

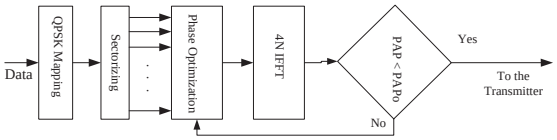

Figure 26: Adaptive PTS approach.

method concatenates of pseudo random and interleaved sub-block partitioning [29]. The same PAR reduction can be achieved with reduced complexity.

In the sub-optimal combining algorithm [68, 170], binary weighting factors are considered. An, input data block is divided into M sub-blocks and M partial transmit sequences are formed. Initially, all weighting factors are assumed to be 1 ($b_m = 1$). The first weighting factor is inverted ($b_1 = -1$) and PAR is computed. If the new PAR is less than the earlier one b_1 is retained as part of the final weighting factors, otherwise b_1 is reverted to its previous value. The algorithm continues in this fashion until all M possibilities have been explored. This is known as the flipping algorithm. Computer simulations show that the great reduction in complexity can be achieved with the little degradation in performance. For $M = 16$, this degradation is about 1 dB at 0.1 % PAR..

A method to increase number of permutations of PTS for a given number of subblocks and phase factors is presented in [171]. These are obtained by cyclically shifting the data after its phase is rotated. These alternate sequences can be generated with trivial operations at the transmitter.

Reliable side information is essential in PTS approach to recover data. This can be sent as explicit side information at the expense of some loss in efficiency. An alternative approach to send side information with no loss in efficiency is reported in [172]. A marker that uniquely identifies the inversion sequence is embedded into the transmitted data. The Weighting factors are assumed to be ± 1. If the inversion sequence rotate the cluster every other tone in that cluster is rotated by $\pi/4$. This information is detected at the receiver to recover that data. Several detection schemes are also reported. The performances in fading channels using forward error correction codes are presented and showed only a minimal degradation compared to the ideal side information.

Adaptive PTS

In this section we describe an adaptive algorithm for combining the PTSs. As above, we only consider binary (i.e., 1 and -1) weighting factors and we divide the input data block into M subblocks. As a first step, assume that $b - m = 1$ for all m and compute the PAR of the combined signal Eq. (111). If it is less than a set threshold PAR_T, then stop optimization immediately. If not, invert the first weighting factor ($b_1 = -1$) and recompute the resulting PAR. If it is less than L, retain b_1 as part of the final phase sequence and stop optimization. The algorithm continues in this fashion until PAR is less than PAR_T or all or part (K) of the 2^{M-1} combinations are searched. The corresponding block diagram is shown in Figure 26.

Let $b = [b_1, b_2, \ldots, b_M]$. The adaptive algorithm can now be written as follows:

step 1 Set $b = [1, 1, \ldots, 1]$,

step 2 Set IterCount = 1,

step 3 While PAR(**X'**) $>$ PAR_T or IterCount $< K$,

step 4 Change b by one bit,

step 5 IterCount ++

Here, K can be set to 2^{M-1} or a lesser value. The maximum number of iterations of this technique is K, and the minimum is 1. The actual number of iterations varies from one input frame to another. We characterize the complexity of this scheme by the average number of iterations per input frame.

In the following results, 10^5 random OFDM symbols were generated to obtain CCDFs. We assume 256 subcarriers throughout and use QPSK data symbols with the energy normalized to unity. Figure 27 shows the CCDF for $M = 8$. The 0.01% PAR of the original OFDM signal is about 11.8 dB. The ordinary PTS technique improves it by 3.75 dB. Curve 2 shows results for APTS with a threshold value PAR_T of 7.5 dB. In the region CCDF$< 10^{-2}$, both the techniques provide identical performance. Ordinary PTS requires 128 iterations per OFDM symbol while APTS requires only 16 (on average) iterations per OFDM symbol. This amounts to an 87% reduction in complexity.

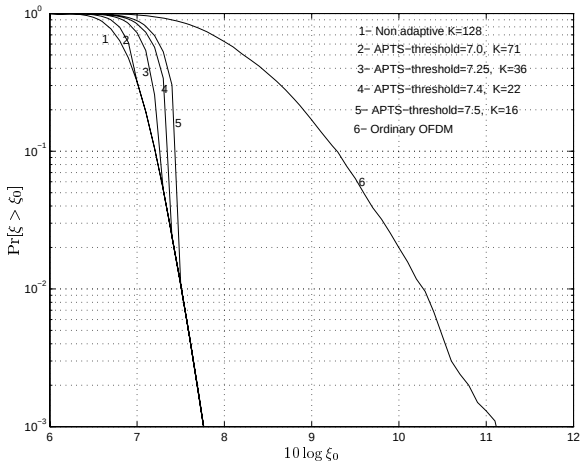

Figure 27: CCDF of an OFDM signal with APTS ($M = 8$).

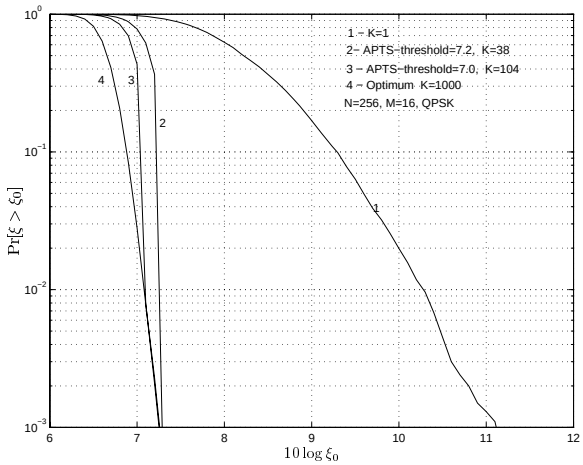

Figure 28: Comparison of performance of optimum PTS with APTS for $M = 16$.

Results are also shown for APTS with PAR_T of 7.4 dB, 7.25 dB and 7.0 dB. These require 22, 36 and 71 iterations (on average) and reduce complexity up to 83%, 72% and 44% respectively. Therefore, it is evident that the complexity of APTS can be reduced greatly by limiting the number of iterations by selecting a suitable threshold value. Lower threshold values yield better performance but result in higher complexity.

Figure 28 shows results for 16 subblocks (M=16). Strictly speaking, the optimal PTS curve requires 32768 iterations per OFDM symbol, which cannot be implemented at all. We therefore use randomly-generated 2000 binary weighting patterns, compute the PAR of each and subsequently take the minimum PAR as the optimal PAR. Curve 2 and 3 show the performance of APTS with K=1000 and threshold limits of 7.2 dB and 7.0 dB respectively. Curve 2 and 3 correspond to an average of 38 and 104 iterations, yielding complexity reduction of 98% and 94.8% respectively, when compared with the optimum result. The performance loss is only about 0.1 dB at 0.1% PAR. By contrast, the flipping algorithm [170] requires only 16 iterations in this case, but results in a performance loss of 1 dB. It is evident that the adaptive approach is a promising solution for considerably reducing the complexity of PTS.

A new algorithm to improve the weighting factor computation

A new algorithm for computing the weighting factors that achieves *better* performance than the exhaustive *binary* search approach is presented in [173,174]. The effects of non-linear amplifiers on the performance of the new algorithm, including the power spectral density and in-band distortion are investigated in this section.

The new algorithm can be explained as follows [173]. For the PTS approach, the input data vector $\mathbf{X}$ is partitioned into disjoint subblocks, as $\{\mathbf{X}_m | m = 1, 2, \ldots, M\}$, and these are combined to minimize the PAR. While several subblock partitioning schemes do exist, the simplest scheme for which the subblocks consist of a contiguous set of subcarriers and are of equal size is assumed. Now, suppose that for $m = 1, \ldots, M$, $\mathbf{A}_m = [A_{m1}, A_{m2}, \ldots, A_{m,LN}]^T$ is the zero-padded IDFT of $\mathbf{X}_m$. These are the partial transmit sequences. The objective is thus to combine these in such a way that the PAR is minimized. The signal samples at the output

of the PTS combiner can be written as

$$\mathbf{S} = \begin{bmatrix} A_{11} & A_{21} & \dots & A_{M1} \\ A_{12} & A_{22} & \dots & A_{M2} \\ \dots & \dots & \dots & \dots \\ A_{1LN} & A_{2LN} & \dots & A_{MLN} \end{bmatrix} \begin{bmatrix} e^{j\phi_1} \\ e^{j\phi_2} \\ \vdots \\ e^{j\phi_M} \end{bmatrix} \tag{112}$$

where $\mathbf{S} = [S_1(\Phi), \dots, S_{LN}(\Phi)]^T$ contains the optimized signal samples. We shall write the weighting factors as a vector, $\Phi = [\phi_1, \phi_2, \dots, \phi_M]^T$. The weighting factors $\{\phi_k\}$ are chosen to minimize the peak of the signal samples $|S_k(\Phi)|$. So the minimum PAR is related to the problem

$$\begin{aligned} &\text{minimize} \quad \max_{0<k\leq LN} |S_k(\Phi)| \\ &\text{subject to} \quad 0 \leq \phi_m < 2\pi, \quad m = 1, \dots, M. \end{aligned} \tag{113}$$

Suppose $\hat{\phi}_m$ to be the global optimal solution to this problem. Unfortunately, there appears to be no simple way to obtain $\hat{\phi}_m$ analytically.

Suboptimal exhaustive search (SES) algorithms

The weighting factors are restricted to a finite set of values and hence Eq. (113) is approximated by the problem

$$\begin{aligned} &\text{minimize} \quad \max_{0<k\leq LN} |S_k(\Phi)| \\ &\text{subject to} \quad \phi_m \in \left\{ \frac{2\pi l}{W} | l = 0, \dots, W-1 \right\}. \end{aligned} \tag{114}$$

If the number of rotation angles W is "sufficiently" large, the solution of Eq. (114) will approach that of Eq. (113). Furthermore, ϕ_1 can be fixed without any performance loss. Now, there are only $M-1$ free variables to be optimized and hence W^{M-1} distinct phase vectors, Φ_i, need to be tested. As such, Eq. (114) is solved using W^{M-1} iterations; the i-th iteration involves computing LN signal samples, each of which is denoted by $S_k(\Phi_i)$, using Eq. (112) and choosing the maximum $|S_k(\Phi_i)|$ value. At the end of each iteration, the phase vector is retained if the current value of $\max|S_k(\Phi_i)|$ is less than the previous maximum. The phase vector that is retained after all the iterations are completed will be an approximation to the global optimal solution of Eq. (113).

In most reported studies, $W = 2$ and one is able to obtain the OBPS. In some cases, the use of more rotation angles ($W > 2$) has been found to yield diminishing returns.

In SES, the computational load consists of M IDFTs, MLN complex multiplications per iteration, and LN operations of $|\cdot|$. If $W = 2$ or 4, the multiplications can be replaced by additions. It might also be possible to use DFT algorithms that are suitable for handling data sets with a large number of zeros in order to reduce complexity. Such issues are not pursued in this letter. As the computational cost of M IDFTs is fixed for any algorithm, for comparative purposes, we ignore the fixed cost component and define the measure of complexity as

$$N_c = W^{M-1}LN. \tag{115}$$

This measure indicates the total number of operations of $|\cdot|$ and multiplications required. Given that its value increases exponentially with M, SES may not be feasible for $M > 8$.

New algorithm

The motivation for a new algorithm arises from the following observation. For given Φ, we have the i-th row of Eq. (112) as

$$S_i(\Phi) = A_{1i}e^{j\phi_1} + A_{2i}e^{j\phi_2} + \dots + A_{Mi}e^{j\phi_M} \tag{116}$$

where A_{ri}, $r = 1, 2, \dots, M$, are fixed complex numbers dependent only on the input data frame. What choice of Φ will minimize the amplitude of this sum? If we sort $|A_{ri}|$ as

$$|A_{r_1 i}| > |A_{r_2 i}| > \dots > |A_{r_M i}|,$$

where $\{r_1, \dots, r_M\}$ is a permutation of $\{1, \dots, M\}$, and choose

$$\phi_{r_l} = \begin{cases} -\angle A_{r_l i} & l = 1, 3, \dots \\ \pi - \angle A_{r_l i} & l = 2, 4, \dots \end{cases} \tag{117}$$

where $\angle$ denotes the phase angle of a complex number, then the minimum amplitude sample is given by

$$S_i(\Phi) = |A_{r_1 i}| - |A_{r_2 i}| + |A_{r_3 i}| - \dots \tag{118}$$

The phase selection Eq. (117) yields nearly always the maximum amount of amplitude cancellation for the i-th signal sample. As a result, it is very easy to find Φ that will nearly always minimize the amplitude of a single signal sample. Let $\hat{\Phi}_i$ be the solution Eq. (117) that nearly always minimizes $|S_i|$. Each $\hat{\Phi}_i$ can be viewed as a reasonable - but not necessarily the optimal solution for Eq. (113). Our next step is therefore to compute all LN such solutions and choose the one that minimizes the maximum signal samples.

Similar to the SES algorithms for Eq. (114), the new algorithm can be applied in LN iterations to obtain a solution for Eq. (114); the i-th iteration involves computing LN signal samples $S_k(\hat{\Phi}_i)$ using Eq. (112) and choosing the maximum of $|S_k(\hat{\Phi}_i)|$. At the end of each iteration, the phase vector is retained if the current value of $\max|S_k(\hat{\Phi}_i)|$ is less than the previous maximum. There are two main differences between the SES algorithms and the new algorithm. First, the number of iterations changes from W^{M-1} to LN. Second, the phase vectors are computed differently. The weighting factors from Eq. (117) are not restricted to 0 and π, which is the case for SES with $W = 2$. Rather, they are continuous variables between 0 and 2π.

As with Eq. (115), we define the measure of complexity as

$$N_c = LN \times LN. \tag{119}$$

The first LN denotes the number of iterations and the second denotes the number of operations per iterations. As well, for $W = 2$, comparison of Eq. (115) and Eq. (119) reveals that the new algorithm is more complex than SES for small M but less complex for large M (> 8).

To justify the new algorithm vis-a-vis the SES approach, it is necessary to demonstrate two things. First, we must demonstrate that the PAR reduction achieved with the new algorithm is better and its complexity is less than or similar to that of SES. Second, we must also demonstrate that, if the weighting factors used in the new algorithm are quantized, the resulting performance loss will be small. This is particularly relevant if coherent demodulation is to be employed. These two issues are studied by simulation. In the results which follow, 10^5 OFDM signals are generated in each case. The transmitted signal is oversampled by a factor of 4 ($L = 4$). All results are for 256-subcarrier and QPSK-modulated systems.

Figure 29 compares the performance of the two algorithms as function of M, the number of subblocks. For $M = 2, 4$, the new algorithm performs more than 1 dB better than the OBPS solution. For $M = 8$, the performance gain is about 0.5 dB. For $M = 16$, both the algorithms perform nearly equal. However, in this case, the OBPS search requires 2^{15} operations per iteration. As this would take up an enormous amount of computer time, the results for the $M = 16$, OBPS curve are shown for a limited, random search of the weighting factor space. We performed only 500 trials and in [175] it was observed that 2000 trials would result in performance which was essentially equivalent to the OBPS. If the entire 2^{15} combinations were tested at each iteration, we would expect the $M = 16$, OBPS curve to improve somewhat (i.e., it should be better than the new algorithm). Note that on the basis of Eq. (115) and Eq. (119), the OBPS search is 32 times more complex than the new algorithm for $M = 16$. We also tested the execution speed ratio for the two algorithms executed by Matlab on a 900 MHz Pentium machine. For $M = 16$, the OBPS algorithm was 20 times slower than the new algorithm. Thus, in this particular case and for a similar level of performance, the new algorithm is less complex. Based on this figure and other simulations not shown here, we can conclude the following: as M increases, the performance of both algorithms will converge while the complexity of the OBPS approach continues to increase exponentially.

Next, we consider quantization of the weighting factors in the new algorithm to Q bits. That is, the weighting factors are rounded off to the nearest element in the set $\{k\pi/2^{Q-1} | k = 0, 1, \dots, 2^{Q-1}\}$. The minimum overhead required to transmit all the weighting factors to the receiver is then $(M-1)Q$ bits. Figure 30 shows results for $Q = 1, 2$ and ∞. Even $Q = 1$ achieves a performance level within 0.4 dB of the unquantized case ($Q = \infty$). Performance degradation for the $Q = 2$ case is negligible.

The effect of the oversampling factor L on the performance of the new algorithm is presented next. If L is increased, improved performance can be expected for the new algorithm. This occurs at an increasing level of complexity. Figure 31 evaluates the performance of the new algorithm as a function of the oversampling factor, L. Increasing L beyond 4 seems to bring very little improvement in performance.

The conventional OFDM and PTS-OFDM signals are passed through SL and SAPA non-linear devices and the PSDs are estimated. Figure 32 shows the PSD for a soft limiter with different back-off values. At 5 dB back off the out-of-band noise of the two signals is nearly the same. When the back off is increased to 7 dB, the out-of-band noise of PTS-OFDM is 20 dB below at $B_n = 2$ to that of OFDM. This difference increases to 60 dB, when the back off is increased to 9 dB.

Somewhat similar performance is observed for a SSPA non-linear device, as depicted in Figure 33. Again, no significant difference is observed for 5 dB back off, while out of band radiation is reduced by 10 dB and 50

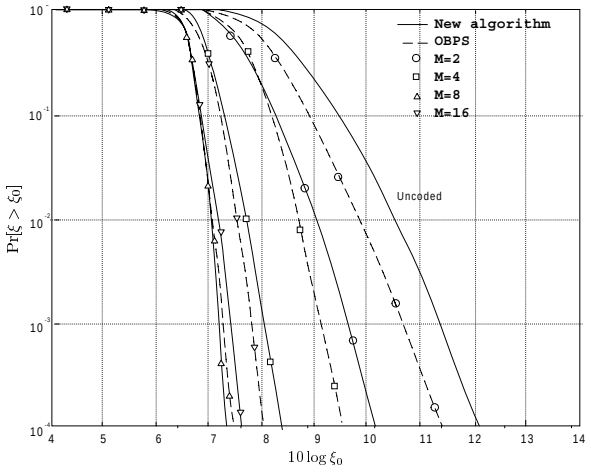

Figure 29: Comparison of the new algorithm and the OBPS algorithm.

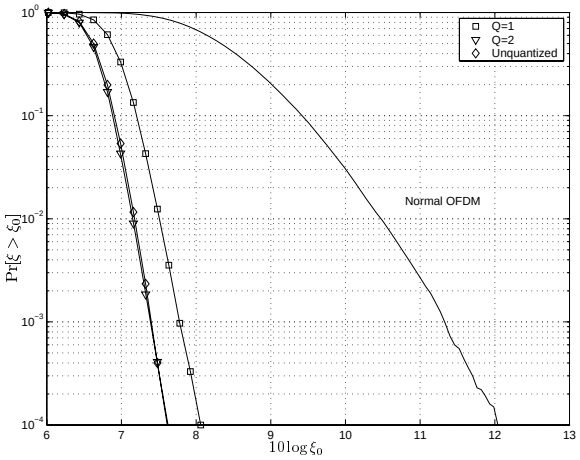

Figure 30: The effect of quantization on the new algorithm, for $M = 8$.

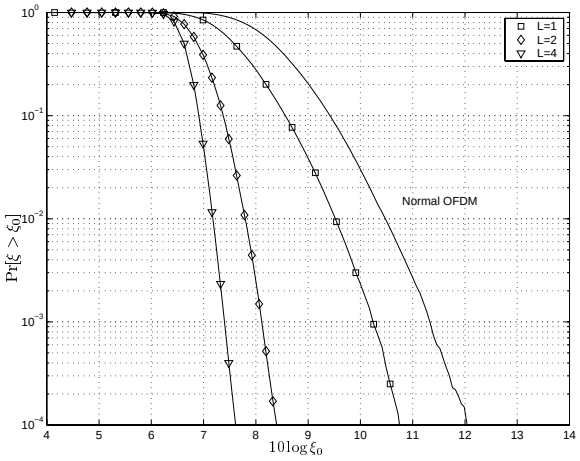

Figure 31: The effect of oversampling on the new algorithm, for $M = 8$.

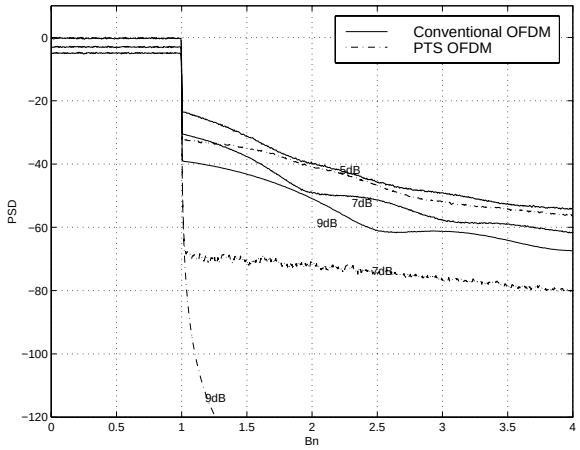

Figure 32: PSD of conventional OFDM and PTS-OFDM after a soft limiting non-linear device.

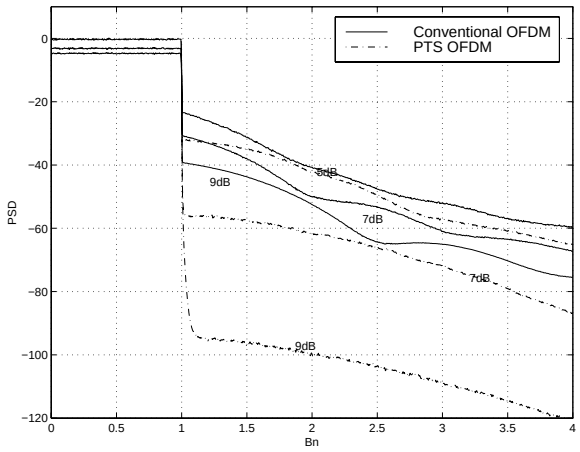

Figure 33: PSD of conventional OFDM and PTS-OFDM after an SSPA non-linear device.

dB at $B_n = 2$ for 7 dB and 9 dB back offs. Therefore, it is evident that PTS with the new algorithm reduces the out-of-band noise of an OFDM signal significantly.

Figure 34 and Figure 35 show the constellation diagrams of the received signal of conventional OFDM and PTS-OFDM. A high level of in-band distortion occurs for conventional OFDM for a 5 dB back off. The severity of distortion reduces with the increasing back off. Even for an 11 dB back off some in-band signal distortion occurs. In contrast, in-band distortion occurs only for a 5 dB back off for PTS-OFDM. Clearly, the in-band signal distortion can be reduced significantly by using PTS-OFDM.

Side information

To recover the data, the receiver must know the exact weighting factors used to reduce the PAR. Reliable side information is an important factor for PTS to work properly. If side information is added into the OFDM symbol after the PAR optimization, a peak regrowth might occur. An alternative way to send side information is proposed in [172]. The basic idea is to insert a marker onto the transmitted data that can uniquely identify the inversion sequence at the receiver.

Marking algorithm [172]

Phase rotation of ± 1 is assumed. If the phase rotation does not occur ($b_m = 1$), do nothing. Otherwise, if $b_m = -1$, then rotate every other tone in the cluster by $\pi/4$. This is equivalent to the use of two constellations for data; one standard constellation and the other rotated by $\pi/4$. This algorithm puts an embedded marker on those clusters that have been rotated.

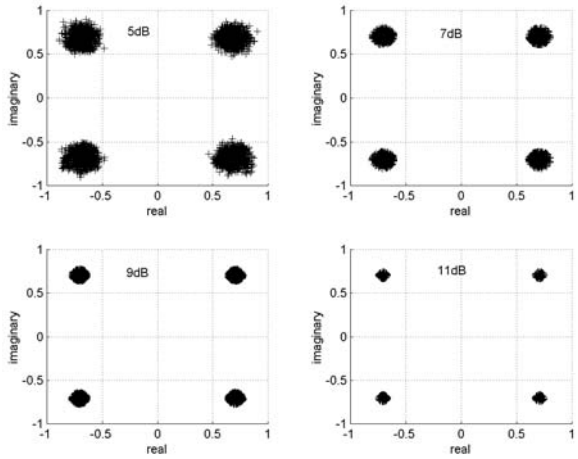

Figure 34: Signal constellation at the receiver of conventional OFDM after a soft limiting non-linear device.

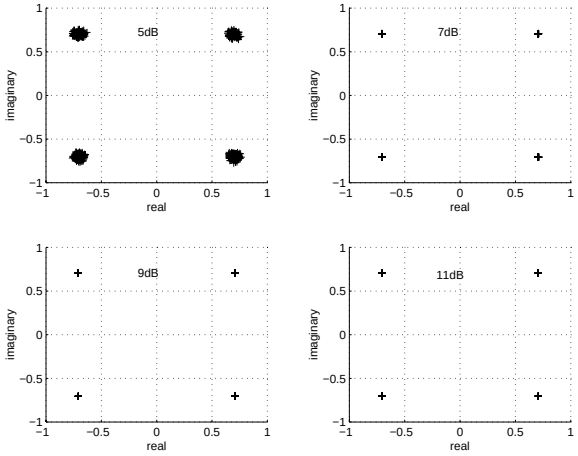

Figure 35: Signal constellation at the receiver of PTS OFDM after SL non-linear device.

Detection scheme

With the modulation removed, the data symbols are differentially detected by computing the following test statistics for each cluster

$$Z_m = \sum_{j=1}^{N/M-1} (Y_{j,m} Y^*_{j+1,m})^4 \tag{120}$$

where $Y_{j,m}$ represents the j-th tone in the m-th subblock. If the cluster has not been rotated $Z_m = N/M - 1$, where as $Z_m = -(N/M - 1)$ if the cluster has been rotated. Therefore, the optimized binary weighting factors can be easily recovered. In the next section we introduce a new scheme to send side information which will not effect the optimum PAR.

Novel scheme to send side information

We can set $b_1 = 1$ without loss of generality. In our approach side information is placed in the first subblock such that it will not be changed during the optimization. The idea is to put the side information of the current OFDM symbol in the first subblock of the next OFDM symbol. The current symbol is optimized with the embedded side information of the previous OFDM symbol. Optimum conditions can be preserved in this manner. The algorithm can be explained as follows.

- μ-th OFDM symbol is partitioned into M-subblocks and optimum weighting factors are obtained by performing the required number of iterations, while keeping the first weighting factor unity.
- Identity of the optimal weighting factors are embedded onto the 1-st subblock of the $\mu + 1$-th OFDM symbol.

- $(\mu+1)$ OFDM symbol is optimized and optimal weighting factors are inserted onto the 1-st subblock of the $\mu+2$ OFDM symbol.
- This procedure is followed for all the OFDM blocks and very first OFDM symbol is transmitted without any side information, while extra dummy OFDM symbol needs to be transmitted to carry the side information of the last OFDM block.

At the receiver, current OFDM symbol is recovered using the side information received through the next OFDM symbol. This is the only disadvantage of the proposed scheme. There is an additional delay of one OFDM symbol at the receiver to recover the data completely. The phase of the first subblock is not changed during the optimization process. Therefore, side information corresponding to the previous OFDM symbol can be recovered without decoding the OFDM symbol completely.

The process can be explained mathematically as follows. Let the complete OFDM symbol is given by $[S_{\mu-1,0},\ldots,S_{\mu-1,c-1},X_{\mu,c},\ldots,X_{\mu,N-1}]$, where μ refers to the OFDM symbol number and $S_{\mu,n}$ is the n-th carrier reserved for the side information of $(\mu-1)$-th OFDM symbol. c is the total number of carriers reserved for side information. Then the PAR optimization algorithm can be expressed using the linearity property of DFT as before

$$\xi_{\text{optimal}} = \min_{b_1,\ldots,b_M}\left[\max_k\left(|s_{\mu-1,k}|^2+|y^1_{\mu,k}|^2+\left|\sum_{m=2}^{M}b_m y^m_{\mu,k}\right|^2\right)\right] \tag{121}$$

where

$$s_{\mu-1,k} = \sum_{n=0}^{c-1} S_{\mu-1,n}e^{j2\pi nk/N},$$

$$y^1_{\mu-1,k} = \sum_{n=c}^{N/M-1} X_{\mu,n}e^{j2\pi nk/N},$$

and

$$y^m_{\mu,k} = \sum_{n=N/M}^{N-1} X^m_{\mu,n}e^{j2\pi nk/N}$$

where $X^m_{\mu,n}$ is the n-th subcarrier of the m-th subblock of μ-th OFDM symbol. It is evident from Eq. (121) side information of $\mu-1$-th OFDM symbol can be recovered easily at the receiver which can be described as follows. The transmitted signal is given by,

$$y^{optimal}_{\mu,k} = s_{\mu-1,k}+y^1_{\mu,k}+\sum_{m=2}^{M} b^{optimal}_m y^m_{\mu,k}, \quad k=0,1,\ldots,N-1. \tag{122}$$

At the receiver an DFT operation is performed first

$$R_n = \sum_{k=0}^{N-1} y^{optimal}_{\mu,k}e^{-j2\pi nk/N} \tag{123}$$

giving out

$$R_n = [S_{\mu-1,0},\ldots,S_{\mu-1,c-1},X_{\mu,c},\ldots X_{\mu,N/M-1},b^{optimal}_{\mu,2}X_{\mu,N/M},\ldots,b^{optimal}_{\mu,M}X_{N-1}]. \tag{124}$$

Thus, side information of the $\mu-1$-th OFDM symbol $\mathbf{S}_{\mu-1}$ is recovered. It is suggested to use a simple forward error correcting code to protect the side information against errors.

4.3.5 Selective scrambling

A technique called selective scrambling is reported in [176]. Four codewords in which the first two bits are 00, 01, 10, 11 are formed by concatenating each of these bit pairs with four fixed cyclically inequivalent m-sequences. The sequences are then mapped to QPSK symbols and the sequence with the minimum PAR is chosen for the transmission. A specific function for selecting the QPSK sequence with minimum PAR is also presented.

4.4 Modified signal constellation

In single carrier systems adjacent channel interference specifications require the use of tightly band limited signaling formats. To meet these requirements, pulse shapes that span many symbols are used. Typically, a Nyquist pulse shape such as a raised cosine is used. These pulse shapes can cause a substantial increase in the peak power of traditional linear modulation formats such as MPSK and MQAM.

The PAR of an OFDM system with MPSK modulation and N subcarriers may be high as $10\log_{10}(N)$. If some of these N subcarriers (N_n) are made to zero, the theoretical maximum PAR reduces to $10\log_{10}(N-N_n)$. This fact has been exploited by several authors to reduce the PAR. Parallel combinatory OFDM (PC-OFDM) is proposed in [177,178]. In the transmitter first, which subcarriers to be zero and nonzero are chosen. Then $N-N_n$ nonzero subcarriers are modulated by MPSK. Now another set of bits called parallel combinatory bits are mapped to the zero positions of the OFDM symbol. There are $\begin{pmatrix} N \\ N_n \end{pmatrix}$ different ways to choose N_n zeros out of N subcarriers. Therefore, the total number of bits carried by a PC-OFDM signal can be expressed as

$$m_{tot} = (N-N_n)\log_2(M) + \left\lfloor \log_2 \begin{pmatrix} N \\ N_n \end{pmatrix} \right\rfloor \tag{125}$$

where $\lfloor x \rfloor$ is the largest integer smaller than or equal to x.

PC-OFDM uses an MPSK signal constellation extended with an additional zero amplitude point. From an MPSK signal constellation an $(M+1)$-ary amplitude and phase shift keying (APSK) constellation is constructed. The bandwidth efficiency of PC-OFDM may be higher compared to conventional OFDM depending on N_n. The complexity of the PC-OFDM system increases when N and N_n increase. The difficult part is to select the zero positions of the OFDM signal for given parallel combinatory bits. Introduction of zero amplitude signal point further reduces the Euclidian distances between signal points. However, simulation results show that PC-OFDM performs better than OFDM in an AWGN channel but not in fading channels.

A similar approach called expansion of the signal space for PAR reduction (ESPAR) is presented in [179]. Here, N_c out of N subcarriers are selected and modulated by BPSK and the rest of the subcarriers are set to zero. This can be regarded as a special case of PC-OFDM.

Another approach is known as Tone Injection (TI) [180]. This approach expands the constellation to a bigger one, where one of several values that carry the same information can be selected. This extra degree of freedom is used to generate multicarrier signals with lower PAR. The process of constellation expansion can be explained as follows. If X_n carries b_k bits, then it could take one of 2^{b_k} discrete values. If a QAM constellation with minimum distance between points d_k is assumed, the real and imaginary parts of X_n can take values $\pm d_k/2, \pm 3d_k/2, \ldots, \pm(M_k-1)d_k/2$, where $M_k = 2^{b_k/2}$ is the number of levels per dimension. Real and imaginary parts of constellation points are modified such that PAR is reduced. Note that no side information is needed. If we assume the constellation point is A then the modified point is expressed as $\hat{A} = A + pD + jqD$, where p and q are any integer value and D is a positive real number known at the receiver. An iterative approach is presented to find proper values for p and q. A 6 dB reduction in PAR is observed with moderate complexity.

A method which enlarges the constellation size of the QAM modulation at tones so that several signal represent the same information in presented in [181]. Several constellation shaping techniques to reduce the PAR is reported in the literature [182–184].

4.5 Pilot tone methods

PAR can also be reduced by reserving some of the subcarriers for peak reduction purpose and optimizing their values. Although this approach reduces the efficiency of the OFDM it does not need side information. The general idea follows from [110,185–189].

The OFDM symbol expressed in Eq. (8) can be written as $\mathbf{x} = Q\mathbf{X}$, where Q is the IDFT matrix with elements $q_{n,k} = \frac{1}{\sqrt{N}} e^{j2\pi kn/N}$.

Now by adding a vector $C = [C_0, C_1, \ldots, C_{N-1}]^T$ to $\mathbf{X}$ we get

$$\mathbf{x} + \mathbf{c} = Q(\mathbf{X} + \mathbf{C}) \tag{126}$$

where $\mathbf{c} = Q\mathbf{C}$. Then $\mathbf{C}$ is selected to meet the following targets:

1. $\mathbf{X}$ can be decoded efficiently from $\mathbf{X} + \mathbf{C}$ without degrading the performance,
2. PAR can be reduced by optimizing $\mathbf{c}$,
3. $\mathbf{c}$ can be computed efficiently.

First $\mathbf{C}$ is constrained to nonzero values over a subset $\{i_1, i_2, \ldots, i_L\}$, where $L << N$, i.e.

$$C_k = \begin{cases} C_k, & k \in \{i_1, i_2, \ldots, i_L\} \\ 0, & else. \end{cases} \tag{127}$$

The, values of $X_k, k \in \{i_1, i_2, \ldots, i_L\}$, are set to zero, such that the sets of nonzero values for $\mathbf{X}$ and $\mathbf{C}$ are mutually exclusive. Setting of some values of $\mathbf{X}$ to zero causes a data rate loss. Data rate loss (R_{DL}) can be expressed as

$$R_{DL} = \frac{L}{N}. \tag{128}$$

To reduce the data loss, L should be minimized. Demodulation is very simple at the receiver. No side information is needed as the receiver knows the PAR reduction subcarrier positions beforehand. At the receiver simply these subcarriers are disregarded and other subcarriers are demodulated.

The problem of finding the optimum values for $\mathbf{C}$ is presented in [180]. If the nonzero values of $\mathbf{C}$ is expressed as $\hat{\mathbf{C}} = [C_{i_1}, C_{i_2}, \ldots, C_{i_L}]$, and $\hat{Q} = [q_{i_1} \ldots q_{i_L}]$ the sub matrix of Q constructed by choosing its columns $\{i_1, i_2, \ldots, i_L\}$ then $\mathbf{c} = Q\mathbf{C} = \hat{Q}\hat{\mathbf{C}}$. Finally the optimum values of c can be calculated by solving

$$\min \|\mathbf{x} + \mathbf{c}\|_\infty = \min \|x + \hat{Q}\hat{\mathbf{C}}\|_\infty \tag{129}$$

where $\|x\|_\infty$ denotes the $\infty - norm$[1] of the vector x. This optimization problem is convex in the variable C_{i_k} and can be easily cast as a linear program (LP), having $2L+1$ unknowns and $2N$ inequalities. As this problem has a structured LP as Q is the IDFT matrix [180] presented an algorithm having a complexity of order $O(N)$. A PAR reduction of 6 dB was observed with $\frac{L}{N} = 5\%$ at CCDF less than 10^{-5}. A 10 dB reduction of PAR has been observed for $\frac{L}{N} = 20\%$. This approach is termed as Tone Reservation (TR).

Selective mapping and cyclic coding is combined to reduce PAR in [190]. The optimum amplitude and phase of additional peak reduction subcarriers (PRC) are obtained using a code book, which is obtained using a search for all possible combinations. The phase of PRCs is set to 0° or 180° and the PRC subcarriers are turn on and off. There are therefore $3^{N_{PRC}}$ combinations for the PRCs for each information codeword, where N_{PRC} is the number of PRCs. For each information codeword $3^{N_{PRC}}$ combinations need to be searched in order to minimizing PAR. This approach is again highly complex for systems with more than 16 subcarriers or more than 10 PRCs. Therefore may suitable only for OFDM systems with small number of subcarriers, but bears the advantage of not sending side information.

Adaptive subcarrier selection is presented in [191]. Subcarriers with low SNR are excluded at the transmitter, which improves the BER of the signal. Here these excluded subcarriers are used to reduce the PAR of the signal, thereby achieving low BER and PAR. An iterative technique to find a suitable reduction function corresponding to excluded subcarriers is also presented.

The use of parity subcarriers to reduce the PAR is reported in [189]. A PAR suppressing signal is generated at parity subcarriers when ever the PAR is above a threshold level. These parity subcarriers are based on the coding scheme prosed in [135]. The process of generating suppressing signal is iterated till peak power reduce to the given threshold. A PAR reduction of 5 dB is observed for 8 subcarrier OFDM signals. This method may not be suitable for OFDM systems with large number of subcarriers.

4.6 Other methods

Hadamard transform is used in [67] to lower the correlation relationship of the input sequence such that the PAR of the OFDM signal is reduced. This is a simple technique of taking Hadamard transform of the input sequence before the IDFT. At the receiver an inverse Hadamard transform is performed after the DFT. Here, the reduction of PAR is not significant although no side information to the receiver is an advantage.

Two new subcarrier phasing algorithms that reduce the PAR of an OFDM signal is presented in [192]. The PAR reduction is achieved using the lowpass equivalent representation of the bandpass waveform. The original system of N bandpass subcarriers is then converted to a system of $\frac{N(N-1)}{2}$ lowpass carriers, typically with multiple lowpass carriers at each lowpass frequency. PAR reduction is then accomplished by setting the phase angles of the original bandpass carriers such that groups of lowpass carriers with the same lowpass frequency are eliminated.

A method applicable to multicarrier systems employing FEC is presented in [193]. This reduces the PAR having minimal effect on the coding gain. The motivation behind this approach is that in the presence of FEC mechanism small number of deliberate changes in the encoded data made infrequently would have negligible effect on the final error rate at the receiver. Here, Reed Solomon (RS) encoded multicarrier systems with multi-level encoding is considered. Interestingly an algorithm to find a input symbol, which is mostly effecting the particular peak is presented. This algorithm can be explained as follows:

[1] The $\infty - norm$ of the vector is the maximum of the absolute values of its components

1. Determine the location of the largest peak occurring (L),
2. Determine the sub-channel (input symbol) which will result in the maximum minimization of the given peak. For a complex input $X_i + jY_i$ this is computed as

$$E_i = X_i \cos(2\pi Li/N) - Y_i \sin(2\pi Li/N) + \sqrt{(X_i^2 + Y_i^2)} \tag{130}$$

3. Apply a phase correction to the chosen symbol as follows:

$$P_i = -(2\pi Li)/N \arctan(Y_i/X_i) \tag{131}$$

4. Remodulate the changed symbols and transmit the modified sequence.

Discrete samples of the OFDM signal exhibit much greater peak amplitudes, which result in high PARs. There are some proposals to achieve constant envelope OFDM signals. An attempt to get a constant discrete OFDM samples using a modified constellation is reported in [194]. For N subcarriers constant envelope is obtained if MPSK is used and $M \leq \sqrt{N}; N = 2^m$, where m is a positive integer. New codes providing constant envelope discrete time signals are also proposed. But due to signal generation and low pass filtering at the final stage of the transmitter variations of the signal envelope occurs. The use of discrete cosine transform (DCT) instead of DFT to achieve constant envelope is proposed in [195]. It is shown that there exists some sequences which leads to constant envelope in DCT based multicarrier systems.

Peak power suppression of multicarrier systems by band-limiting the subchannels by filtering before multiplexing is proposed in [196, 197]. In this scheme the transmit pulse power is decreased whenever the PAR is above a given threshold level. Simulations results show that a significant reduction in PAR is observed without noticeable increase in BER. A technique based on selection of time limited waveforms of the different subcarriers is reported in [198]. In this method the time waveforms of subcarriers are used to create the appropriate correlation that reduces the PAR of the OFDM signal. Trellis shaping is also considered for PAR reduction [199].

A scheme called clustered OFDM is proposed in [200,201] to obtained and OFDM transmission scheme with low PAR. In clustered OFDM subcarriers are clustered into several smaller blocks and transmit over separate transmitter antennas. A single receiver antenna is used. Apart from low PAR due to reduction in number of carriers in each cluster there are few other advantages of using clustered OFDM:

- Short packets can be accommodated efficiently since minimal training is required,
- By dividing the transmitted bandwidth into many narrow subchannels, the effect of delay spread can be minimized,
- The PAR is reduced since there are fewer tones per transmitter,
- Under some conditions coding across frequency is more effective since the fading on each cluster is independent.

PAR reduction achieved by reducing number of subcarriers in an OFDM system is very small. Therefore PAR reduction codes are used in each clusters.

A model to analyze the effect of clipping of discrete multitone signal is presented in [202]. This model provides information on the reduction of the signal level, the total noise power due to clipping and spectral properties of the noise. Filtering after clipping can reduce the spectral splatter but may cause some peak re-growth causing higher PAR.

An approach called carrier interferometry coding (CI) to reduce the PAR is discussed in [203, 204]. In CI-OFDM each bit is modulated onto all of the N subcarriers, and the separability of the bits is maintained through the use of carefully selected phase offsets. The carrier interferometry coded OFDM signal can be expressed as

$$x(t) = \frac{1}{\sqrt{N}} \sum_{n=0}^{N-1} \sum_{i=0}^{N-1} e^{j2\pi i \Delta f t} e^{i\theta_n} \tag{132}$$

where θ_n is the phase offset, which is given by

$$\theta_n = \frac{2\pi}{N} n, \quad n = 0, 1, \ldots, N-1 \tag{133}$$

A PAR reduction scheme utilizing the shift property of DFT is proposed in [205].

4.7 Comparison of PAR reduction techniques

A comparison of PAR reduction performance of some of the above mentioned techniques is presented in Table (2) [206]. The PAR is probabilistically measured at 0.1%PAR. Overhead required is measured as the number of extra bits required by the PAR reduction scheme divided by the actual number of information bits in an OFDM symbol. According to this table coding techniques achieve lowest PAR. However the overhead is unacceptable. Adaptive symbol selection techniques are suitable for systems with large number of carriers, but PAR reduction is moderate. Although clipping and windowing can reduce PAR, severe clipping or windowing increases the BER. Use of peak reduction carriers is one of the best solutions to reduce the PAR. High reduction in PAR is achieved by increasing the number of PAR reduction carriers. PAR reduced by about 7 dB when 20 % PAR reduction carriers are used. This scheme become inefficient when the number of peak reduction subcarriers are increased.

Table 2: Comparison of PAR reduction performances.

Scheme	N	Modulation	PAR (dB)[a]	Reduced PAR (dB)[a]	overhead
Block coding [24]	8	BPSK	9.0	4.45	14%
			9.0	3.0	33%
Complementary codes [152]	8	8PSK	11.0	3.0	100%
	32	8PSK		3.0	433%
Low-crest factor [207]	32	BPSK	11.0	6.5	33 %
				3.3	100%
SLM $U = 4$ [208]	128	16QAM	11.4	8.6	0.4%
	128	QPSK	11.4	8.6	0.8%
	512	QPSK	11.8	9.3	0.2%
PTS $M = 4$ [29]	128	16QAM	11.4	9.0	1.2%
	128	QPSK	11.4	9.0	2.4 %
	512	QPSK	11.8	9.3	0.6%
Clipping/filtering [101]	128	QPSK	11.2	9.1	0%, (2.0 dB) [b]
Peak windowing [152]	48	16QAM	11.0	6.0	0%, (0.6 dB) [b]
Peak reduction carriers [209]	512	QPSK	12.0	8.0	5.0%
		QPSK	12.0	5.0	20%

[a] PAR at 0.1%PAR
[b] BER degradation due to inband distortion

4.8 PAR reduction in multicarrier CDMA - (MC-CDMA)

Recently much attention has been given for combining OFDM and code division multiple access (CDMA) techniques, resulting multi-carrier CDMA (MC-CDMA). MC-CDMA sends a single data symbol in multiple narrow-band subcarriers. Each subcarrier is encoded with a phase offset of 0 or π based on an orthogonal spreading code. For a spreading code of length N there are N subcarriers. This is also a multiple access scheme since different users use the same set of subcarriers but with a different spreading codes that are orthogonal to each other. OFDM structure reduces the intra-cell interference and increases the capacity within a cell in a cellular environment using many parallel subcarriers. In contrast, direct sequence CDMA (DS-CDMA) is specially robust against inter-cell interference by spreading each user's signal across the system bandwidth using a unique high chip rate spreading code. MC-CDMA combines both both techniques, thereby reducing both inter and intra cell interferences by spreading every data bit across a set of orthogonal subcarriers. By doing this MC-CDMA provides an efficient method of frequency diversity, especially suitable for fading channels. The lowpass equivalent transmitted signal $x_{mc}(t)$ of an MC-CDMA system can be expressed as [210]

$$x_{mc}(t) = \sqrt{\frac{eE_b}{NT_b}} \sum_{m=0}^{M-1} a_m[k] \sum_{n=0}^{N-1} c_m[n] e^{\frac{j2\pi n}{T_b}} P_{T_b}(t - kT_b),\ kT_b \leq t < kT_b + T_b \tag{134}$$

where N is the number of subcarriers, $a_m[k]$ is the m-th user's binary antipodal input data symbol in k-th bit interval and $c_m[n], n = 0, 1, \ldots, N-1$ is the n-th chip of the spreading code assigned to the i-th user. E_b and T_b are the bit energy and the bit duration of the considered system respectively. The shaping pulse $P_{T_b}(t) = 1$ for $0 \leq t < T_b$ and zero otherwise. The subcarriers are spaced by $1/T_b$. MC-CDMA also suffers from high PAR problem. Several techniques for PAR reduction are reported to date [66, 70, 71, 211–213].

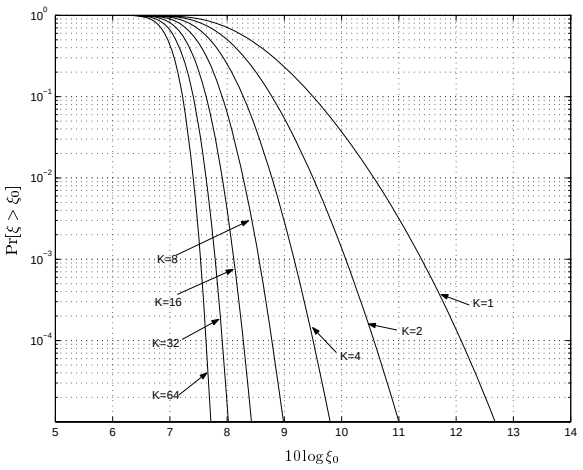

Figure 36: CCDF of PAR of an OFDM signal.

4.9 PAR reduction for Multicode CDMA

Multicode CDMA [214] is one of the techniques that has been proposed to support multirate operation in a packetized CDMA network. It provides easy integration of data streams having variable rates into a common unified architecture, with all the transmissions modulating the same carrier, occupying the same bandwidth and having the same processing gain. In a multicode CDMA system if a user needs K times the basic source rate, K spreading codes are assigned to it. The user converts its packet stream into K basic-rate parallel packet streams which are spread using the K different codes, respectively. Intuitively, with multicode CDMA, the different data rate requirements of the users can be easily catered for by assigning enough number of codes to each user. In multicode CDMA, a Walsh-Hadamard transform of input data is taken before spreading. The output of the operation is not binary, rather multilevel. Thus multicode signal can have a large variation in the envelope power giving out high PAR. PAR reduction in multicode CDMA can be seen in recent reach efforts [215–219]. The PAR of milti-code CDMA can be defined as

$$\xi = \frac{1}{N} \max_{0 \le n \le N} |S_n|^2 \tag{135}$$

where N is the block length and S_n's are multilevel output signals of the Hadamard transform.

5 Effect of PAR reduction on system performance

An OFDM system with 256 carriers, 16QAM and a guard interval of 12.5% is simulated. The OFDM signal is passed through nonlinear devices. Figure 36 depicts the CCDF of PAR of an OFDM signal. It also shows the PAR reduction using adaptive symbol selection (SLM). When $K = 2$, two OFDM symbols are generated from the same information sequence and one with the minimum PAR is chosen for the transmission. Similarly, when $K = 16$, 16 different OFDM symbols using the same information sequence is generated. These different sequences can be generated in different ways as shown in References [29,155,157]. When $K = 16$, PAR reduction on the order of 4 dB at 0.01% PAR is obtained. This PAR reduction is obtained with the increase in the system complexity. An OFDM system with 256 carriers needs highly complex systems at the transmitter to reduce the PAR below 7 dB. PAR reduction codes are capable of achieving low PAR when N is small. But these schemes reduce the system throughput significantly as N gets large.

5.0.1 Inband distortion

The effect of inband distortion can be observed by the BER performance. Figure 37 depicts the BER performance of an OFDM signal passing through a soft limiter nonlinear device described in section IV. This figure shows BER performance of both ordinary OFDM and PAR reduced OFDM signals for different back-off values of the nonlinear device. P-OFDM refers to the PAR reduced OFDM. PAR of the signal is reduced by adaptive symbol selection (SLM). We can observe a significant improvement in BER even in an AWGN channel depending on the back-off value of the non-linear device. No significant improvement in BER is observed when the back-off is very low, 0 dB for example. In this case both OFDM and PAR reduced OFDM experience severe signal

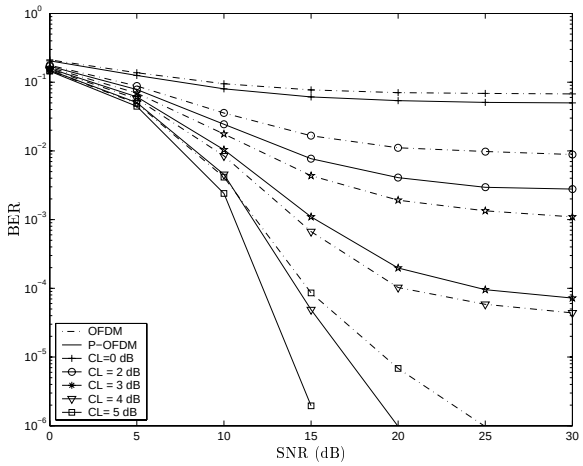

Figure 37: Bit error rate in an AWGN channel, 16QAM with adaptive symbol selection (K=16).

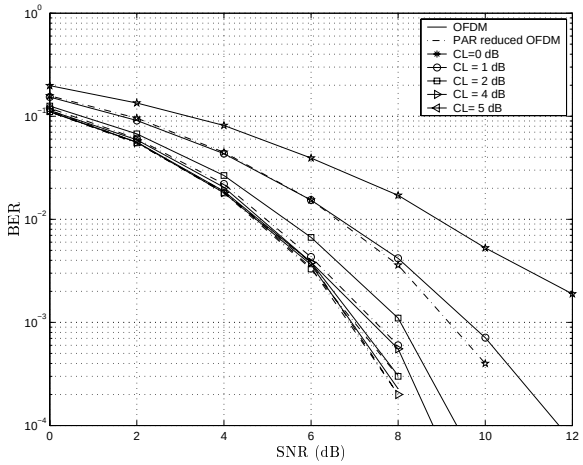

Figure 38: Bit error rate in an AWGN channel (PAR reduced to 3 dB).

distortions. When the back off greater than 2 dB a clear improvement in BER is observed. In these cases distortion in OFDM is high while the distortion in PAR reduced OFDM is low. When the back-off is increased to 5 dB an improvement of about 10 dB is observed at 10^{-6} BER. If the back-off is increased further both scheme does not experience signal distortion thus would not show any BER degradation. Results shown in Figure 37 are obtained without using any forward error correction (FEC) codes. Typically wireless systems needs FEC to combat channel impairments. These FEC codes can also be used to improve the BER caused by peak limiting. Figure 38 shows the BER of an OFDM signal coded with Golay complementary sequences and QPSK modulation. Number of carriers in the coded system is 32 and PAR 3 dB at most. A significant improvement in BER is observed even for a clipping level of 0 dB.

5.0.2 Out of band radiation

OFDM in general has sharp signal transitions at the signal boundaries, giving out high OBR even without nonlinearity effect. This can be alleviated by using extended guard intervals at both ends of the OFDM signal and a smoothing window function (raised cosine window) [22]. Figure 39 depicts the spectrum of an OFDM signal when passed through a SSPA nonlinear device. Curves 1 to 7 represent the different back-off values of the amplifier. For example, for a back-off of 9 dB, to provide -80 dB adjacent channel separation requires a channel spacing of about three times the symbol rate for normal OFDM, with the PAR reduced OFDM the channel spacing is nearly the symbol rate. Thus, PAR reduced OFDM provides a spectrally-efficient solution for the adjacent channel interference problem, which can arise in portable cellular applications. This performance also reveals that depending on the permissible OBR level, the amplifier back-off can be reduced by 2 to 3 dB when the PAR of an OFDM is reduced considerably. When the back-off of the amplifier is increased, OBR level is reduced.

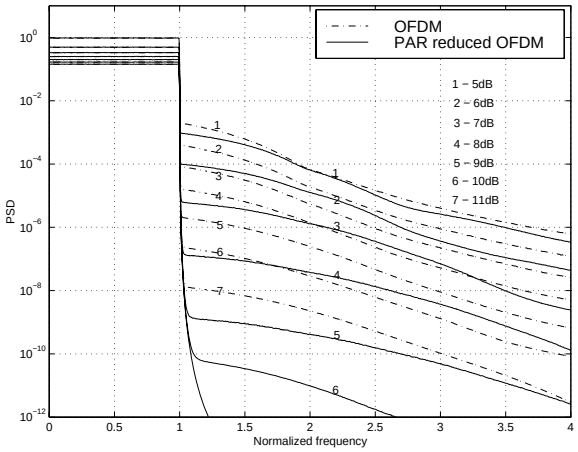

Figure 39: Spectrum of an OFDM signal after passing through a SSPA.

6 Conclusion

PAR of an OFDM signal can be substantially high. This report has presented the statistical distribution of PAR, computational methods and PAR reduction techniques. As high peaks are relatively rare, the PAR can be reduced by either clipping these peaks or using a predistortion scheme and filtering. These techniques introduce inband distortion depending on the degree of clipping. Multiple signal representation is also being used in many PAR reduction techniques, such as PTS, SLM and interleaving. These techniques reduce the PAR with an increased complexity at the receiver. Coding techniques based on Golay complementary sequences are capable of limiting the PAR 3 dB at most. But coding rate is prohibitively low for OFDM systems with large number of carriers ($N > 32$). A significant amount of PAR reduction at the transmitter allows lower dynamic ranges for the transceiver equipment. This reduces the inband distortion and out band noise to a large extend. However, finding a better PAR reduction technique is still an ongoing problem.

References

[1] J. A. C. Bingham, "Multicarrier modulation for data transmission: An idea whose time has come," *IEEE Commun. Mag.*, vol. 28, pp. 5–14, May 1990.

[2] X. Li and L. J. Cimini, "Effects of clipping and filtering on the performance of OFDM," in *IEEE Vehicular Technology Conference*, vol. 2, (New York, NY,USA), pp. 1634–1638, IEEE, 1997.

[3] R. W. Chang, *Orthogonal frequency division multiplexing.* U. S. Patent 3 488 445, filed Nov. 14, 1966, issued, Jan. 6, 1970.

[4] S. B. Weinstein and P. M. Ebert, "Data transmission by frequency-division multiplexing using the discrete Fourier transform," *IEEE Trans. Commun. Technol.*, vol. Com-19, pp. 628–634, Oct. 1971.

[5] W. Y. Zou and Y. Wu, "COFDM: An overview," *IEEE Trans. Broadcast.*, vol. 41, pp. 1–8, March 1995.

[6] P. Shelswell, "The COFDM modulation system: The heart of digital audio broadcasting," *Electronic and Communication Engineering Journal*, vol. 7, pp. 127–135, June 1995.

[7] L. J. Cimini, "Analysis and simulation of a digital mobile channel using orthogonal frequency division multiplexing," *IEEE Trans. Commun.*, vol. COM-33, pp. 665–675, July 1985.

[8] A. Vahlin, H. N., and R. L. Frank, "Use of a guard interval in OFDM on multipath channels," *IEE Elect. Lett.*, vol. 30, pp. 2015–2016, Nov. 1994.

[9] R. F. Ormondroyd and J. J. Maxey, "Comparision of time guard-band and coding startegies for OFDM digital cellular radio in multipath fading," in *IEEE Vehicular Technology Conference*, (New York, NY, USA), pp. 850–854, IEEE, 1997.

[10] R. Morrison, L. J. Cimini, and S. K. Wilson, "On the use of a cyclic extension in OFDM," in *IEEE Vehicular Technology Conference*, vol. 2, (Atlantic City, NJ, USA), pp. 664–668, IEEE, 2001.

[11] H. Kang, H. Kim and K. Hwang, W.and Kim, "OFDM system with the guard interval and the one-tap equalizer bank for the wireless-LAN," in *International Conference on Consumer Electronics*, pp. 20–21, IEEE, 2000.

[12] P. de Bot and P. Baggen, "Error correcting coding for OFDM broadcasting over frequency selective channels," in *IEE Colloquium on Digital Terrestrial Television*, pp. 3/1–3/4, IEE, 1993.

[13] A. Jones and T. Wilkinson, "Combined coding for error control and increased robustness to system nonlinearities in OFDM," in *IEEE Vehicular Technology Conference*, pp. 904–908, IEEE, 1996.

[14] K. Witrisal, Y. H. Kim, and R. Prasad, "A novel approach for performance evaluation of OFDM with error correction coding and interleaving," in *IEEE Vehicular Technology Conference*, pp. 294–299, IEEE, 1999.

[15] A. D. S. Jayalath, *Application of Orthogonal Frequency Division Multiplexing with concatenated coding in Wireless ATM.* Master thesis, Asian Institute of Technology, 1998.

[16] R. Nee and R. Prasad, *OFDM for wireless multimedia communications.* Artech House Publishers, Mar. 2000.

[17] H. Rohling and V. Engels, "Differential amplitude phase shift keying (DAPSK)-a new modulation method for DTVB," in *International Broadcasting Convention*, pp. 102 –108, IBC, 1995.

[18] K. Baum and N. Nadgauda, "A comparison of differential and coherent reception for a coded OFDM system in a low C/I environment," in *IEEE GLOBECOM*, pp. 300 –304, IEEE, 1997.

[19] M. Lott, "Comparision of frequency and time domain differential modulation in an OFDM system for wireless ATM," in *IEEE Vehicular Technology Conference*, pp. 877 –883, IEEE, 1999.

[20] H. Rohling and T. May, "OFDM systems with differential modulation schemes and turbo decoding techniques," in *International Zurich Seminar on Broadband Communications*, pp. 251 –255, IEEE, 2000.

[21] E. Haas and S. Kaiser, "Analysis of two-dimensional differential demodulation for OFDM," in *IEEE GLOBECOM*, pp. 751–755, 2000.

[22] G. A. Awater and R. van Nee, "Implementation of the magic WAND wireless ATM modem," in *IEEE GLOBECOM*, pp. 1–6, IEEE, 1999.

[23] M. Budsabathon and S. Hara, "Robustness of OFDM signal against temporally localized impulsive noise," in *IEEE Vehicular Technology Conference*, pp. 1672–1676, IEEE, 2001.

[24] E. A. Jones, T. Wilkinson, and S. Barton, "Block coding scheme for reduction of peak-to-mean envelope power ratio of multicarrier transmission schemes," *IEE Elect. Lett.*, vol. 30, pp. 2098–2099, Dec. 1994.

[25] D. W. Bennett, P. B. Kenington, and R. J. Wilkinson, "Distortion effects of multicarrier envelope limiting," *IEE Proc. Commun.*, vol. 144, pp. 349–356, Oct. 1997.

[26] M. Friese, "On the degradation of OFDM-signals due to peak-clipping in optimally predistorted power amplifiers," in *IEEE GLOBECOM*, (Sydney, Australia), pp. 936–944, IEEE, 1998.

[27] P. Fan and X.-G. Xia, "Block coded modulation for the reduction of the peak to average power ratio in OFDM systems," in *Wireless and Networks*, pp. 1095–1099, IEEE, 1999.

[28] J. A. Davis and J. Jedwab, "Peak-to-mean power control in OFDM Golay complementary sequences and Reed-Muller codes," Technical Report, HPL-97-158, HP Laboratories, 1997.

[29] S. H. Müller, R. W. Bäuml, R. F. H. Fisher and J. B. Huber, "OFDM with reduced peak-to-average power ratio by multiple signal representation," *Annals of Telecommunications*, vol. 52, pp. 58–67, Feb. 1997.

[30] S. H. Müller and J. B. Huber, "OFDM with reduced peak-to-average power ratio by optimum combination of partial transmit sequences," *IEE Elect. Lett.*, vol. 33, pp. 368–369, Feb. 1997.

[31] S. H. Müller and J. B. Huber, "A novel peak power reduction scheme for OFDM," in *IEEE PIMRC*, pp. 1090–1094, IEEE, 1997.

[32] S. H. Müller and J. B. Huber, "A comparison of peak power reduction schemes for OFDM," in *IEEE GLOBECOM*, vol. 1, pp. 1–5, IEEE, Nov. 1997.

[33] P. Moose, "A technique for orthogonal frequency division multiplexing frequency offset correction," *IEEE Trans. Commun.*, vol. 42, pp. 2908–2914, Oct. 1994.

[34] F. Classen and M. Meyr, "Frequency synchronization alogorithms for OFDM systems suitable for communications over frequency selective fading channels," in *IEEE Vehicular Technology Conference*, pp. 1655–1659, IEEE, 1994.

[35] H. Nogami and T. Nagashima, "A frequency and timing period acquisition technique for OFDM systems," in *IEEE PIMRC*, pp. 1010–1015, IEEE, Sept. 1995.

[36] Y. H. Kim, H. G. Kim, I. Song, M. J. Lee, and S. H. Yoon, "A coded OFDM system for time-varying multipath Rayleigh fading environment," in *IEEE MILCOM*, pp. 867–871, IEEE, 1997.

[37] N. Mochizuki, Y. Matsumoto, M. Mizoguchi, T. Onizawa, and M. Umehira, "A high performance frequency and timing synchronization," *IEEE GLOBECOM*, pp. 3443–3448, 1998.

[38] B. R. Saltzberg, "Performance of an efficient parrallel data transmission system," *IEEE Trans. Commun. Technol.*, vol. COM-15, pp. 805–811, Dec. 1967.

[39] B. Hirosaki, "An orthogonally multiplexed QAM system using the discrete Fourier transforms," *IEEE Trans. Commun.*, vol. COM-29, pp. 982–989, July 1981.

[40] B. Hirosaki, "A 19.2 Kbps voice-band data modem based on orthogonally multiplexed QAM techniques," in *IEEE ICC*, pp. 21.1.1–21.1.5, IEEE, July 1985.

[41] M. Alard and R. Lassalle, "Principles of modulation and channel coding for digital broadcasting for mobile receivers," Technical Report, EBU Technical review, no 224, EBU, Aug. 1987.

[42] B. L. Floch, R. Halbert-Lassalle, and D. Castelain, "Digital sound broadcasting to mobile receivers," *IEEE Trans. Consumer Electron.*, vol. 35, pp. 493–503, Aug. 1989.

[43] J. C. Rault, D. castelain, and B. L. Floch, "The coded orthogonal frequency division multiplexing (COFDM) technique, and its application to digital radio broadcasting towards mobile receivers," in *IEEE GLOBECOM*, (New York, NY, USA), pp. 428–432, IEEE, 1989.

[44] P. Hoeher, J. Hagenauer, E. Offer, C. Rapp, and H. Schulze, "Performance of an RCPC-coded OFDM-based digital audio broadcasting (DAB) system," in *IEEE GLOBECOM*, (New York, NY, USA), pp. 40–46, IEEE, 1991.

[45] J. S. Chow, J. C. Tu, and J. M. Coiffi, "A discrete multi-tone transceiver system for HDSL applications," *IEEE J. Select. Areas. Commun.*, vol. 9, pp. 895–908, Aug. 1991.

[46] S. Moriyama, K. Tsuchida, M. Sasaki, and S. Yamazaki, "Digital outside-broadcasting-link using OFDM modulation scheme," *IEEE Trans. Broadcast.*, vol. 42, pp. 266–277, Sept. 1996.

[47] S. B. Slimane, "MC-CDMA with quadrature spreading over frquency slective fading channels," in *IEEE GLOBECOM*, (New York, NY, USA), pp. 315–319, IEEE, 1997.

[48] Q. Chen, E. S. Sousa, and S. Pasupathy, "Multicarrier CDMA with adaptive frequency hopping for mobile radio systems," *IEEE J. Select. Areas. Commun.*, vol. 14, pp. 1852–1858, Dec. 1996.

[49] A. C. Caswell, "Multicarrier transmission in a mobile radio channel," *IEE Elect. Lett.*, vol. 32, pp. 1962–1963, Oct. 1996.

[50] D. Dardari, "MCM systems with waveform shaping in multi-user environments: Effects of fading, interference and timing errors," in *IEEE GLOBECOM*, (New York, NY, USA), pp. 21–26, IEEE, 1997.

[51] H. Rohling and R. Gruneid, "Performance comparison of different multiple access schemes for the downlink of an OFDM communication system," in *IEEE Vehicular Technology Conference*, vol. 3, (New York, NY, USA), pp. 1365–1369, IEEE, 1997.

[52] W. A. C. Fernando and R. M. A. P. Rajatheva, "Performance of turbo and trellis coded OFDM for LEO satellite channels in global mobile communications," in *IEEE ICC*, (Atlanta, USA), pp. 56–60, IEEE, June 1998.

[53] L. Wei and C. Schlegel, "Synchronization requirements for multi-user OFDM on satellite mobile and two-path Rayleigh fading channels," *IEEE Trans. Commun.*, vol. 43, pp. 887–895, Feb/Mar/Apr. 1995.

[54] S. O'Leary, "Hierarchical transmission and COFDM systems," *IEEE Trans. Broadcast.*, vol. 43, pp. 166–174, June 1997.

[55] M. Schilpp, W. Sauer-Greff, W. Rupprecht, and E. Bogenfeld, "Infleunce of oscillator phase noise and clipping on OFDM for terrestrial broadcasting of digital HDTV," in *IEEE ICC*, (New York, NY, USA), pp. 1678–1682, IEEE, 1995.

[56] ETSI, "Digital video broadcasting (DVB); framing structure, channel coding and modulation for digital terrestrial television (DVB-T)," Technical Report, ETSI EN 300 744, European Telecommunication Standard Institute, Nov. 1999.

[57] IEEE Std 802.11a-1999 (supplement to IEEE Std 802.11-1999), "Part II: Wireless LAN medium access control (MAC) and physical layer PHY specifications: High speed physical layer in 5 GHz band," tech. rep., IEEE, Sept. 1999.

[58] J. Chuang and N. Sollenberger, "Beyond 3G: wideband wireless data access based on OFDM and dynamic packet assignment," *IEEE Commun. Mag.*, vol. 38, pp. 78–87, July 2000.

[59] C. Chuang, "High-speed wireless data access based on combining EDGE with wideband OFDM," *IEEE Commun. Mag.*, vol. 37, pp. 92–98, Nov. 1999.

[60] A. Bria, F. Gessler, O. Queseth, R. Stridh, M. Unbehaun, J. Wu, J. Zander, and M. Flament, "4th-generation wireless infrastructures: scenarios and research challenges," *IEEE Personal Communications*, vol. 8, pp. 25–31, Dec. 2001.

[61] M. Dinis and J. Fernandes, "Provision of sufficient transmission capacity for broadband mobile multimedia: a step towrds 4G," *IEEE Commun. Mag.*, vol. 39, pp. 46–54, Aug. 2001.

[62] J. G. Proakis, *Digital communications.* McGraw-Hill series in electrical engineering. Communications and signal processing, New York: McGraw-Hill, 3rd ed., 1995.

[63] H. Rohling, T. May, K. Bruninghaus, and R. Grunheid, "Broad-band OFDM radio transmission for mutimedia applications," *IEEE Proc.*, vol. 87, pp. 1778–1788, Oct. 1999.

[64] C. Röbing and V. Tarokh, "A construction of OFDM 16-QAM sequences having low peak powers," *IEEE Trans. Inform. Theory.*, vol. 47, pp. 2091–4, July 2001. Publisher: IEEE, USA. Journal Paper.

[65] C. V. Chong and V. Tarokh, "A simple encodable/decodable OFDM QPSK code with low peak-to-mean envelope power ratio," *IEEE Trans. Inform. Theory.*, vol. 47, pp. 3025–3029, Nov. 2001. Nov.

[66] T. Ginige, N. Rajatheva, and K. M. Ahmed, "Dynamic spreading code selection method for PAPR reduction in OFDM-CDMA systems with 4-QAM modulation," *IEEE Commun. Lett.*, vol. 5, pp. 39–43, Oct. 2001. Conference Paper.

[67] M. Park, H. Jun, J. Cho, N. Cho, D. Hong, and C. Kang, "PAPR reduction in OFDM transmission using Hadamard transform," in *IEEE Vehicular Technology Conference*, (Piscataway, NJ, USA), pp. 430–433, IEEE, 2000.

[68] L. J. Cimini and N. R. Sollenberger, "Peak-to-average power ratio reduction of an OFDM signal using partial transmit sequences," in *IEEE ICC*, (Vancouver, British Colombia, Canada), pp. 511–515, IEEE, 1999.

[69] S. Boyd, "Multitone signals with low crest factors," *IEEE Trans. Circuits Syst.*, vol. CAS-33, pp. 1018–1022, Oct. 1986.

[70] B.-J. Choi, E.-L. Kuan, and L. Hanzo, "Crest factor study of MC-CDMA and OFDM," in *IEEE Vehicular Technology Conference*, (Piscataway, NJ, USA), pp. 233–237, IEEE, 1999.

[71] L. Freiberg, A. Annamalai, and K. Bhargaava, "Crest factor reduction using orthogonal spreading codes in multi-carrier CDMA systems," in *IEEE PIMRC*, (New York, NY, USA), pp. 120–1224, IEEE, 1997.

[72] M. Friese, "Multitone signals with low crest factor," *IEEE Trans. Commun.*, vol. 45, pp. 1338–1344, Oct. 1997.

[73] E. van der Ouderaa, J. Schoukens and J. Renneboog, "Comments on multitone signals with low crest factor," *IEEE Trans. Circuits Syst.*, vol. 34, pp. 1125–1127, Sept. 1987.

[74] R. Enright and M. Darnell, "OFDM modem with peak-to-mean envelope power ratio reduction using adaptive clipping," in *IEE Seventh International Conference on HF Radio Systems and Techniques*, (London, UK.), pp. 44–49, IEE, 1997. Conference Paper.

[75] B. Sharif, M. Khalaj, "Peak to mean envelope power ratio of oversampled OFDM signals: An analytical approach," in *IEEE ICC*, pp. 1476 –1480, IEEE, 2001.

[76] M. Yoshida, E. Ishizu, Y. Asano, and T. Saito, "High-rate OFDM codes for peak envelope power reduction and error correction in MQAM systems," in *IEEE Vehicular Technology Conference*, vol. 3, (Piscataway, NJ, USA.), pp. 1148–53, IEEE, 2000. Conference Paper.

[77] H. Ochiai, *Analysis and Reduction of Peak-to-avarage power ratio in OFDM systems.* PhD thesis, The graduate school of engineering, The university of Tokyo, Mar. 2001.

[78] C. Tellambura, "Phase optimization criterion for reducing peak-to-average power ratio in OFDM," *IEE Elect. Lett.*, vol. 34, pp. 169–170, Jan. 1998.

[79] D. Wulich, "Comments on the peak factor of sampled and continous signals," *IEEE Commun. Lett.*, vol. 4, pp. 213–214, July 2000.

[80] H. Minn, C. Tellambura, and V. K. Bhargava, "On the peak factors of sampled and continuous signals," *IEEE Commun. Lett.*, vol. 5, pp. 129–131, Apr. 2001.

[81] M. Friese, "On the achievable information rate with peak-power limited orthogonal frequencey-division multiplexing," *IEEE Trans. Commun.*, vol. 46, pp. 2579–2587, Nov. 2000.

[82] R. van Nee, *OFDM wireless multimedia communications.* Boston, London: Artech House, 2000.

[83] H. Ochiai and H. Imai, "On the distribution of the peak-to-average power ratio in OFDM signals," *IEEE Trans. Commun.*, vol. 49, no. 2, pp. 282–289, 2001.

[84] K. G. Paterson and V. Tarokh, "On the existence and construction of good codes with low peak-to-average power ratio," *IEEE Trans. Inform. Theory.*, vol. 46, pp. 1974–1987, Sept. 2000.

[85] N. Dinur and D. Wulich, "Peak-to-average power ratio in high order OFDM," *IEEE Trans. Commun.*, vol. 49, pp. 1063–1072, June 2001.

[86] C. Tellambura, "Upper bound on peak factor of N-multiple carriers," *IEE Elect. Lett.*, vol. 33, pp. 1608–1609, Sept. 1997.

[87] P. W. J. Van Eetvelt, S. J. Shepherd, and S. K. Barton, "The distribution of peak factor in QPSK multi-carrier modulation," *Wireless Personal Communications, Kluwer Academic Publishers, Netherlands.*, vol. 2, no. 1-2, pp. 87–96, 1995.

[88] C. Tellambura, "Computation of the continuous-time PAR of an OFDM signal with BPSK subcarriers," *IEEE Commun. Lett.*, vol. 5, pp. 185–187, May 2001.

[89] C. Tellambura, "Upper bound on the peak factor of N-multiple carriers," *IEE Elect. Lett.*, vol. 33, pp. 1608–1609, Sept. 1997.

[90] I. S. Gradshteyn and I. M. Ryzhik, *Table of integrals, series, and products.* Academic Press, Inc., 5th ed., 1994.

[91] M. J. E. Golay, "A new search for skewsymmetric binary sequences with optimal merit factors," *IEEE Trans. Inform. Theory.*, vol. 36, pp. 1163–1166, sep 1990.

[92] M. R. Schroeder, *Number theory in science and communication.* Berlin: Springer, 2nd ed., 1984.

[93] D. R. Gimlin and C. R. Patisaul, "On minimizing the peak-to-average power ratio for the sum of N sinusoids," *IEEE Trans. Commun.*, vol. 41, pp. 631–635, Apr. 1993.

[94] S. Shlien, "Minimization of the peak amplitude of a waveform," *Signal Processing*, vol. 14, pp. 91–93, Jan. 1988.

[95] S. Narahashi and T. Nojima, "New phasing scheme of N-multiple carriers for reducing peak-to-avaerage power ratio," *IEE Elect. Lett.*, vol. 30, pp. 1382–1383, Aug. 1994.

[96] B. Popovic, "Synthesis of power efficient multitone signals with flat amplitude spectrum," *IEEE Trans. Commun.*, vol. 39, pp. 1031–1033, July 1991.

[97] S. Narahashi, K. Kumagai, and T. Nojima, "Minimising peak-to-average power ratio of multitone signals using steepest descent method," *IEE Elect. Lett.*, vol. 31, pp. 1552–1554, Aug. 1995.

[98] T. Høholdt, *Difference Sets, Sequences and their Correlation Properties*, vol. 542 of *Series C: Mathematical and Physical Sciences*. Kluwer Academic Publishers, 1999.

[99] H. Ochiai and H. Imai, "On the clipping for peak power reduction of OFDM signals," in *IEEE GLOBECOM*, (San Francisco, USA), pp. 731–735, IEEE, 2000.

[100] H. E. Rowe, "Memoryless nonlinearities with gaussian inouts: elentary results," Tech. Rep. 7, Bell sys. Tecj. J., 1982.

[101] X. Li and L. J. Cimini, "Effects of clipping and filtering on the performance of OFDM," *IEEE Commun. Lett.*, vol. 2, pp. 131–133, May 1998.

[102] R. Dinis and A. Gusmao, "On the performance evaluation of OFDM transmission using clipping techniques," in *IEEE Vehicular Technology Conference*, (Piscataway, NJ, USA), pp. 2923–2928, IEEE, 1999.

[103] R. O'Neill and L. N. Lopes, "Envelope variation and spectral splatter in clipped multicarrier signals," in *IEEE PIMRC*, pp. 71–75, IEEE, Sept. 1995.

[104] M. Faulkner, "The effect of filtering on the performance of OFDM systems," *IEEE Trans. Veh. Technol.*, vol. 49, pp. 1877–1884, Sept. 2000.

[105] D. Kim and G. L. Stuber, "Clipping noise mitigation for OFDM by decision-aided reconstruction," *IEEE Commun. Lett.*, vol. 3, pp. 4–6, Jan. 1999.

[106] N. Dinur and D. Wulich, "Peak to average power ratio in amplitude clipped higher oder OFDM," in *IEEE MILCOM*, vol. 2, pp. 684–687, IEEE, 1998.

[107] D. Wulich, N. Dinur, and A. Glinowiecki, "Level clipped high-order OFDM," *IEEE Trans. Commun.*, vol. 48, pp. 928–930, June 2000.

[108] R. O'Neill and L. B. Lopes, "Performance of amplitude limited multitone signals," in *IEEE Vehicular Technology Conference*, (New York, NY, USA), pp. 1675–1679, IEEE, 1994.

[109] D. J. G. Mestdagh, P. Spruyt, and B. U. Brain, "Analysis of clipping effect in DMT-based ADSL systems," in *IEEE ICC*, (New York, NY, USA), pp. 293–300, IEEE, 1994.

[110] J. Tellado, L. M. C. Hoo, and J. M. Coiffi, "Maximum likelihood detection of nonlinearly distorted multicarrier symbols by iterative decoding," in *IEEE GLOBECOM*, (Piscataway, NJ, USA), pp. 2493–2498, IEEE, 1999.

[111] M. Pauli and H.-P. Kuchenbebecker, "Minimization of the intermodulation distortion of a nonlinearly amplified OFDM signal," *Wireless Personal Communications*, vol. 4, pp. 93–101, Jan. 1997.

[112] J. Armstrong, "New OFDM peak-to-average power reduction scheme," in *IEEE Vehicular Technology Conference*, vol. 2, pp. 756–760, IEEE, 2001.

[113] E. Bogenfeld, R. Valentin, K. Metzger, and W. Sauer-Greff, "Influence of nonlinear HPA on trellsi-coded OFDM for terrestrial broadcasting of digital HDTV," in *IEEE GLOBECOM*, (New York, NY, USA), pp. 1433–1438, IEEE, 1993.

[114] G. Santella and F. Mazzenga, "A hybrid analytical simulation procedure for performance evaluation in M-QAM-OFDM schemes in presence of nonlinear distortions," *IEEE Trans. Veh. Technol.*, vol. 47, pp. 142–151, Feb. 1998.

[115] M. T. Le and L. Thibault, "Performance evaluation of COFDM for digital audio broadcasting part II: Effects of HPA nonlinearities," *IEEE Trans. Broadcast.*, vol. 44, pp. 165–171, June 1998.

[116] W. G. Jeon, K. H. Chang, and Y. S. Cho., "An adaptive data predistorter for compensation of nonlinear distortion in OFDM systems.," *IEEE Trans. Commun.*, vol. 45, pp. 1167–1171, Oct. 1997.

[117] M. Okada, H. Nishijima, and S. Komaki, "A new nonlinear distortiion compensator for OFDM signals in a multipath fading channel," in *IEEE PIMRC*, (New York, NY, USA), pp. 1100–1104, IEEE, 1997.

[118] X. Wang, T. T. Tjhung, and C. S. Ng, "Reduction of peak-to-average power ratio of OFDM system using a companding technique," *IEEE Trans. Broadcast.*, vol. 45, pp. 303–307, Sept. 1999.

[119] H. W. Kang, Y. S. Cho, and D. H. Youn, "On compensating nonlinear distortions of an OFDM system using an efficient adaptive predistorter," *IEEE Trans. Commun.*, vol. 47, pp. 522–526, Apr. 1999.

[120] G. Redaelli, M. Corvino, V. Paderni, A. Spalvieri, A. Leva, and D. Colonna, "Analysis of two digital adaptive pre-correctors for nonlinearity in OFDM systems," in *IEEE ICC*, (Piscataway, NJ, USA), pp. 172–177, IEEE, 1999.

[121] I. S. Park and E. J. Powers, "Compensation of nonlinear distortion in OFDM systems using a new predistorter," in *IEEE PIMRC*, pp. 811–815, IEEE, 1998.

[122] M.-G. D. Benedetto and P. Mandarini, "A new analog predistortion criterion with application to high efficiency digital radio links," *IEEE Trans. Commun.*, vol. 43, pp. 2966–2974, Nov. 1995.

[123] M.-G. D. Benedetto and P. Mandarini, "An application of MMSE predistortion to OFDM systems.," *IEEE Trans. Commun.*, vol. 44, pp. 1417–1420, Nov. 1996.

[124] A. Mattsson, G. Mendenhall, and T. Dittmer, "Comments on : Reduction of peak-to-average power ratio of OFDM system using a companding technique, IEEE Transactions on Broadcasting, vol. 45, no. 3, September 1999.," *IEEE Trans. Broadcast.*, vol. 45, pp. 418–419, Dec. 1999.

[125] X. Wang, T. T. Tjhung, and C. S. Ng, "Reply to the comments on: Reduction of peak-to-average power ratio of OFDM system using a companding technique, IEEE Transactions on Bbroadcasting vol. 45, no.3, September 1999," *IEEE Trans. Broadcast.*, vol. 45, pp. 420–422, Dec. 1999.

[126] L. Xiao, Huang Jianhua, C. Justin, and Z. Junli, "Companding transform for the reduction of peak-to-average power ratio of OFDM signals," in *IEEE Vehicular Technology Conference*, pp. 835 –839, IEEE, 2001.

[127] A. N. D'Andrea, V. Lottici, and R. Reggiannini, "An amplitude and phase predistortion to OFDM systems," in *IEEE GLOBECOM*, (San Francisco, CA, USA), pp. 1417 –1421, IEEE, 2000.

[128] A. N. D'Andrea, V. Lottici, and R. Reggiannini, "RF amplifier linearization through amplitude and phase predistortion," *IEEE Trans. Commun.*, vol. 44, pp. 1477 –1484, Nov. 1996.

[129] J. A. Davis and J. Jedwab, "Peak-to-mean power control in OFDM, Golay complementary sequences, and Reed-Muller codes," *IEEE Trans. Inform. Theory.*, vol. 45, pp. 2397–2417, Nov. 1999.

[130] S. Fragiacomo, C. Matrakidis, and J. J. O'Reilly, "Multicarrier transmission peak-to-average power reduction using simple block code," *IEE Elect. Lett.*, vol. 34, pp. 953–954, May 1998.

[131] Y. Zhang, Y. A., and C. J. Y., "Reducing multicarrier transmission peak power with a modified simple block code," in *ICCT*, pp. 578–580, IEEE, 2000.

[132] C. Tellambura, "Multicarrier transmission peak-to-average power reduction using simple block code," *IEE Elect. Lett.*, vol. 34, p. 1646, Aug. 1998.

[133] Y. Zhang, A. Yongacoglu, J.-Y. Chouinard, and L. Zhang, "OFDM peak power reduction by sub-block coding and its extended versions," in *IEEE Vehicular Technology Conference*, (Tokyo, Japan), pp. 695–699, IEEE, 1999.

[134] T. Wilkinson and E. A. Jones, "Minimization fo the peak to mean envelope power ratio of multicarrier transmission schemes by bloack coding," in *IEEE Vehicular Technology Conference*, (Chicago, IL, USA), pp. 825–829, IEEE, 1995.

[135] A. E. Jones and T. A. Wilkinson, "Combined coding for error control and increased robustness to system nonlinearities in OFDM," in *IEEE Vehicular Technology Conference*, (Atlanta, GA, USA), pp. 904–907, IEEE, 1996.

[136] V. Tarokh and H. Jafarkhani, "An algorithm for reducing the peak to average power ratio in a multicarrier communications systems," in *IEEE Vehicular Technology Conference*, (Piscataway, NJ, USA), pp. 680–684, IEEE, 1999.

[137] P. Fan and X.-G. Xia, "Block coded modulation for the reduction of the peak to average power ratio in OFDM systems," *IEEE Trans. Consumer Electron.*, pp. 1025–1029, 1999.

[138] D. Wulich, "Peak factor in orthogonal multicarrier modulation with variable levels," *IEE Elect. Lett.*, vol. 32, pp. 1859–1860, Sept. 1996.

[139] T. M. J. C. Y. Bar-Ness, "OFDM peak power reduction by a novel coding scheme with threshold control," in *IEEE Vehicular Technology Conference*, vol. 2, (Atlantic City, NJ, USA), pp. 669 –672, IEEE, 2001.

[140] S. Shepherd, J. Orriss, and S. Barton, "Asymptotic limits in peak envelope power reduction by redundant coding in orthogonal frequency-division multiplex modulation," *IEEE Trans. Commun.*, vol. 46, pp. 5–10, Jan. 1998.

[141] D. Wulich and L. Goldfeld, "Reduction of peak factor in orthogonal multicarrier modulation by amplitude limitting and coding," *IEEE Trans. Commun.*, vol. 47, pp. 18–21, Jan. 1999.

[142] J. A. Davis and J. Jedwab, "Peak-to-mean power control and error correction for OFDM transmission using Golay sequences and Reed-Muller codes," *IEE Elect. Lett.*, vol. 33, pp. 267–268, Feb. 1997.

[143] X. Li and J. A. Ritcey, "M-sequences for OFDM peak-to-average power ratio reduction and error correction," *IEE Elect. Lett.*, vol. 33, pp. 554–555, Mar. 1997.

[144] C. Tellambura, "Use of m-sequences for OFDM peak-to-average power ratio reduction," *IEE Elect. Lett.*, vol. 33, pp. 1300–1301, July 1997.

[145] J. Jedwab, "M-Sequences for OFDM peak-to-average power ratio reduction and error correction," *IEE Elect. Lett.*, vol. 33, pp. 1293–1294, July 1997.

[146] V. Tarokh and H. Jafarkhani, "On the computation and reduction of the peak-to average power ratio in multicarrier communications," *IEEE Trans. Commun.*, vol. 48, pp. 37–44, Jan. 2000.

[147] W. Henkel, "Analog codes for peak-to-average power ratio reduction," in *VDE-Verlag. Itg-Fachbericht*, pp. 151–155, VDE-Verlag, 2000.

[148] J. A. Davis and J. Jedwab, "Peak-to-mean power control in OFDM, Gloay complementary sequences and Reed-Muller codes," in *Proc. of International Symposium on Information Theory'98*, p. 190, IEEE, 1998.

[149] A. E. Jones and T. A. Wilkinson, "Performance of Reed-Muller codes and a maximum-likelihood decoding algorithm for OFDM," *IEEE Trans. Commun.*, vol. 47, pp. 949–952, July 1999.

[150] T. Høholdt, H. E. Jensen and J. Justesen, "Aperiodic correlations and the merit factor of a class of binary sequences," *IEEE Trans. Inform. Theory.*, vol. 31, pp. 549–552, July 1985.

[151] R. L. Frank, "Polyphase complementary codes," *IEEE Trans. Inform. Theory.*, vol. IT-26, no. 6, pp. 641–647, 1980.

[152] R. D. J. van Nee, "OFDM codes for peak-to-average power reduction and error correction," in *IEEE GLOBECOM*, (New York, NY, USA), pp. 740–744, IEEE, 1996.

[153] T. Hunziker and U. P. Bernhard, "Evaluation of coding and modulation schemes based on golay complementary sequences for efficient OFDM transmission," in *IEEE Vehicular Technology Conference*, pp. 1631–1635, IEEE, 1998.

[154] H. Ochiai and H. Imai, "Performance of the deliberate clipping with adaptive symbol selection for strictly band-limited OFDM systems," *IEEE J. Select. Areas. Commun.*, vol. 18, pp. 2270–2277, Nov. 2000.

[155] R. W. Bauml, R. F. H. Fischer, and J. B. Huber, "Reducing the peak-to-average power ratio of multicarrier modulation by selected mapping," *IEE Elect. Lett.*, vol. 32, pp. 2056–2057, Oct. 1996.

[156] A. D. S. Jayalath and C. Tellambura, "Use of data permutation to reduce the peak-to-average power ratio of an OFDM signal," *Wireless Communications and Mobile Computing Journal*, vol. 2, pp. 187–203, Mar. 2002.

[157] A. D. S. Jayalath and C. Tellambura, "Reducing the peak-to-average power ratio of an OFDM signal through bit or symbol interleaving," *IEE Elect. Lett.*, vol. 36, pp. 1161–1163, June 2000.

[158] A. D. S. Jayalath and C. Tellambura, "The use of interleaving to reduce the peak-to-average power ratio of an OFDM signal," in *IEEE GLOBECOM*, (San Francisco, California, USA), pp. 82 –86, IEEE, 2000.

[159] A. D. S. Jayalath and C. Tellambura, "Reducing the peak-to-average power ratio of an OFDM signal by interleaving," in *International Symposium on Wireless Personal Multimedia Communications*, (Bangkok, Thailand), pp. 698–703, IEEE, 2000.

[160] A. D. S. Jayalath and C. Tellambura, "Peak-to-average power ratio reduction of an OFDM signal using data randomization with embedded side information," in *IEEE International Symposium on Circuits and Systems*, (Sydney, Australia), IEEE, 2001.

[161] A. D. S. Jayalath and C. Tellambura, "Peak-to-average power ratio of a Zipper signal," in *IEEE Vehicular Technology Conference*, vol. 2, (Atlantic City, NJ, USA), pp. 1111–1114, IEEE, 2001.

[162] A. D. S. Jayalath and C. Tellambura, "Interleaved PC-OFDM to reduce the peak-to-average power ratio," in *DSPCS 02*, (Sydney, Asutralia), pp. 224–228, TITR, 2002.

[163] M. Breiling, S. H. Muller, and J. B. Hubber, "Distortionless reduction of peak power without explicit side information," in *IEEE GLOBECOM*, (San Francisco, CA, USA), pp. 1494 –1498, IEEE, 2000.

[164] M. Breiling, S. Müller–Weinfurtner, and J. Huber, "SLM peak–power reduction without explicit side information," *IEEE Commun. Lett.*, vol. 5, no. 6, pp. 239–241, 2001.

[165] G. Ungerboeck, "Channel coding with multilevel/phase signals," *IEEE Trans. Inform. Theory.*, vol. IT-28, pp. 55–67, Jan. 1982.

[166] C. Tellambura, "A coding technique for reducing peak-to-average power ratio in OFDM," in *IEEE GLOBECOM*, (Piscataway, NJ, USA), pp. 2783–2787, IEEE, 1998.

[167] C. Tellambura, "Improved phase factor computation for the PAR reduction of an OFDM signal using PTS," *IEEE Commun. Lett.*, vol. 5, pp. 135–137, Apr. 2001.

[168] S. G. Kang, J. G. Kim, and E. K. Joo, "A novel subblock partition scheme for partial transmit sequence OFDM," *IEEE Trans. Broadcast.*, vol. 45, pp. 333–338, Sept. 1999.

[169] G. Hill, M. Faulkner, and J. Singh, "Cyclic shifting and time inversion of partial transmit sequences to reduce the peak-to-average power ratio in OFDM," in *IEEE PIMRC*, vol. 2, (Piscataway, NJ, USA.), pp. 1256–1259, IEEE, 2000. Conference Paper.

[170] L. J. Cimini and N. R. Sollenberger, "Peak-to-average power ratio reduction of an OFDM signal using partial transmit sequences," *IEEE Commun. Lett.*, vol. 4, pp. 511–515, Mar. 1999.

[171] G. R. Hill, M. Faulkner, and J. Singh, "Reducing the peak-to-average power ratio in OFDM by cyclically shifting partial transmit sequences," *IEE Elect. Lett.*, vol. 36, pp. 560–561, Mar. 2000.

[172] L. J. Cimini and N. R. Sollenberger, "Peak-to-average power ratio reduction of an OFDM signal using partial transmit sequences with embedded side information," in *IEEE GLOBECOM*, (San Francisco, CA, USA), IEEE, Mar. 2000.

[173] C. Tellambura and A. D. S. Jayalath, "PAR reduction of an OFDM signal using partial transmit sequences," in *IEEE Vehicular Technology Conference*, vol. 1, (Atlantic City, NJ, USA), pp. 465 –469, IEEE, 2001.

[174] C. Tellambura, "Improved phase factor computation for the PAR reduction of an OFDM signal using PTS," *IEEE Commun. Lett.*, vol. 5, no. 4, 2001.

[175] L. J. Cimini, Jr. and N. R. Sollenberger, "Peak-to-average power ratio reduction of an OFDM signal using partial transmit sequences," *IEEE Commun. Lett.*, vol. 4, pp. 86–88, Mar. 2000.

[176] P. V. Eetvelt, G. Wade, and M. Thompson, "Peak to average power reduction for OFDM schemes by selected scrambling," *IEE Elect. Lett.*, vol. 32, pp. 1963–1964, Oct. 1996.

[177] P. K. Frenger and N. A. B. Sevensson, "Parallel combinatory OFDM signalling," in *IEEE PIMRC*, pp. 1069–1073, IEEE, 1996.

[178] P. K. Frenger and N. A. B. Sevensson, "Parallel combinatory OFDM signalling," *IEEE Trans. Commun.*, vol. 47, pp. 558–567, Apr. 1999.

[179] A. Sumasu, T. Ue, M. Usesugi, O. Kato, and K. Homma, "A method to reduce the peak power with signal space expansion (ESPAR) for OFDM system," in *IEEE Vehicular Technology Conference*, (Piscataway, NJ, USA), pp. 405–409, IEEE, 2000.

[180] J. Tellado and J. M. Coiffi, "Peak power reduction for multicarrier transmission," in *IEEE GLOBECOM*, (Piscataway, NJ, USA), pp. 219–224, IEEE, 1998.

[181] H. Chan-Soo, "Peak power reduction method for multicarrier transmission," *IEE Elect. Lett.*, vol. 37, pp. 1075–1077, Aug. 2001. Publisher: IEE, UK. Journal Paper.

[182] H. Kwok and D. Jones, "Par reduction via constellation shaping," in *International Symposium on Information Theory*, p. 166, IEEE, 2000.

[183] M. Harada, T. Yamazato, H. Okada, M. Katayama, and A. Ogawa, "An OFDM system with reduced non-linear effect," in *IEEE Vehicular Technology Conference*, pp. 1794–1798, IEEE, 2000.

[184] S. L. Miller and R. J. O'Dea, "Peak power and bandwidth efficient linear modulation," *IEEE Trans. Commun.*, vol. 46, pp. 1639–1648, Dec. 1998.

[185] J. Tellado and J. M. coiffi, "PAR reduction in multicarrier transmission systems," Technical Report, Stanford University, 1998.

[186] J. Tellado, *Peak to Average Power Reduction for Multicarrier Modulation.* PhD Dissertation, Stanford University, Sept. 1999.

[187] J. Tellado and J. M. Coiffi, "Efficient algorithms for reducing PAR in muticarrier systems," in *IEEE ISIT*, (Cambridge, MA, USA), p. 191, IEEE, 1998.

[188] M. J. F.-G. Garcia, J. M. Paez-Borrallo, and O. Edfors, "Orthogonal pilot sequences for peak-to-average power reduction in OFDM," in *IEEE Vehicular Technology Conference*, vol. 2, (Atlantic City, NJ, USA), pp. 650–654, IEEE, 2001.

[189] T. Takada, O. Muta, and Y. Akaiwa, "Peak power suppression with parity carrier for multi-carrier transmission," in *IEEE Vehicular Technology Conference*, (Piscataway, NJ, USA), pp. 2903–2907, IEEE, 1999.

[190] E. Lawrey and J. Kikkert, "Peak to average power ratio reduction of OFDM signals using peak reduction carriers," in *ISSPA*, (Brisbane, Australia), pp. 737–740, IEEE, 1999.

[191] H. Schmidt and K. D. Kammeyer, "Reducing the peak to average power ratio of multicarrier signals by adaptive subcarrier slection," in *IEEE ICUPC*, (New York, NY,USA), pp. 933–937, IEEE, 1998.

[192] J. A. Smith, J. R. Cruz, and D. Pinckley, "Method for reducing peak-to-average of a multicarrier waveform," in *IEEE Vehicular Technology Conference*, (Tokyo, Japan), pp. 542–546, IEEE, 2000.

[193] A. Verma and M. T. Arvind, "Peak to average power ratio reduction in multicarrier communication systems," in *IEEE ICPWC*, (Piscataway, NJ, USA), pp. 204–206, IEEE, 1999.

[194] J. E. M. Nelson, "Spectrum and waveform relations of multicarrier communications," in *IEEE MILCOM*, (McLean, Virginia, USA), pp. 255–259, IEEE, 1996.

[195] S. Attallah and J. E. M. Nilsson, "Sequences leading to minimum peak-to-average power ratios for DCT-based multicarrier modulation," *IEE Elect. Lett.*, vol. 34, pp. 1469–1470, July 1998.

[196] O. Muta and Y. Akaiwa, "A peak power reduction scheme with adaptive transmit power control for multicarrier transmission," in *IEEE Vehicular Technology Conference*, (Piscataway, NJ, USA), pp. 2144–2148, IEEE, 1999.

[197] O. Muta and Y. Akaiwa, "A peak power reduction scheme with adaptive transmit power control for multicarrier transmission," *Transactions of the Institute of Electronics & Communication Engineers of Japan*, vol. J83-B, pp. 289–296, Mar 200.

[198] S. B. Slimane, "Peak-to-average power ratio reduction of OFDM signals using pulse shaping," in *IEEE GLOBECOM*, (San Francisco, CA, USA), pp. 1412 –1416, IEEE, 2000.

[199] W. Henkel and B. Wagner, "Another application for trellis shaping: PAR reduction for DMT (OFDM)," *IEEE Trans. Commun.*, vol. 48, pp. 1471–1475, Sept. 2000.

[200] B. Daneshrad, L. J. Cimini Jr. and M. Carloni, "Clustered-OFDM transmitter implementation," in *IEEE PIMRC*, pp. 1064–1068, IEEE, 1996.

[201] L. J. J. Cimini, B. Daneshrad, and N. R. Sollenberger, "Clustered OFDM with transmitter diversity and coding," in *IEEE GLOBECOM*, pp. 703–707, IEEE, 1996.

[202] R. Gross and D. Veeneman, "SNR and spectral properties for a clipped DMT ADSL signal," in *IEEE ICC*, (New York, NY, USA), pp. 843–847, IEEE, 1994.

[203] D. A. Wiegandt, C. R. Nassar, and W. Zhiqiang, "Overcoming peak-to-average power ratio issues in OFDM via carrier-interferometry codes," in *IEEE Vehicular Technology Conference*, vol. 2, (Atlantic City, NJ, USA), pp. 660–663, IEEE, 2001.

[204] D. A. Wiegandt, C. R. Nassar, and W. Zhiqiang, "Peak-to-average power reduction in high-performance, high-throughput OFDM via pseudo-orthogonal carrier-interferometry coding," in *IEEE Pacific Rim Conference on Communications, Computers and signal Processing*, vol. 2, (Atlantic City, NJ, USA), pp. 453 –456, IEEE, 2001.

[205] M. Zekri, P. Boets, and L. V. Biesen, "DMT signals with low peak-to-average power ratio," in *IEEE International Symposium on Computers and Communications*, (Los Alamitos, CA, USA.), pp. 362–368, IEEE, 1999. Conference Paper.

[206] P. Young-Seo and S. L. Miller, "Peak-to-average power ratio suppression schemes in DFT based OFDM," in *IEEE Vehicular Technology Conference*, vol. 1, (Piscataway, NJ, USA.), pp. 292–297, IEEE, 2000. Conference Paper.

[207] M. Friese, "OFDM signals with low crest-factor," in *IEEE GLOBECOM*, pp. 290–294, IEEE, 1997.

[208] R. W. Bäuml, R. F. H. Fischer and J. B. Huber, "Reducing the peak-to-average power ratio of multicarrier modulation by selected mapping," *IEE Elect. Lett.*, vol. 32, pp. 2056–2057, Oct. 1996.

[209] J. Tellado, *Multicarrier modulation with low PAR*. Kluwer Academic Publishers, 2000.

[210] J. Park, J. Kim, and S. Choi, "Performance of MC-CDMA systems in non-independant Rayleigh fading," in *IEEE ICC*, (Piscataway, NJ, USA), pp. 506–510, IEEE, 1999.

[211] H. Ochiai and H. Imai, "OFDM-CDMA with peak power reduction based on the spreading sequences," in *IEEE ICC*, (New York, NY, USA), pp. 1299–1303, IEEE, 1998.

[212] M. Friese, "Multicarrier modulation with low peak-to-average power ratio," *IEE Elect. Lett.*, vol. 32, pp. 713–712, Apr. 1996.

[213] K. Laird, N. Whinnett, and S. Buljore, "A peak-to-average power reduction method for third generation CDMA reverse links," in *IEEE Vehicular Technology Conference*, (Piscataway, NJ, USA), pp. 551 –555, IEEE, 1999.

[214] C.-L. I and R. D. Gitlin, "Multi-code CDMA wireless personal communications networks," in *IEEE ICC*, pp. 1060–1064, IEEE, 1995.

[215] T. Wada, "Charatecristic of bit sequence applicable to constant amplitude orthogonal multicode systems," *IEICE Trans. Fundamentals*, vol. E83-A, pp. 2160–2164, Nov. 2000.

[216] T. Wada, T. Yamazato, M. Katayama, and A. Ogawa, "A constant amplitude coding for orthogonal multi-code CDMA systems," *IEICE Trans. Fundamentals*, vol. E80-A, pp. 2477–2484, Dec. 1997.

[217] T. Wada, T. Yamazato, M. Katayama, and A. Ogawa, "Error correcting capability of constant amplitude coding for orthogonal multi-code CDMA systems," *IEICE Trans. Fundamentals*, vol. E81-A, pp. 2166–2169, Oct. 1998.

[218] N. Guo and L. B. Milstein, "Uplink performance evaluation of multicode DS-CDMA systems in the presence of nonlinear distortions," *IEEE J. Select. Areas. Commun.*, vol. 18, pp. 1418–1428, Aug. 2000.

[219] K. Paterson, "On codes with low peak-to-average power ratio for multi-code CDMA." Submitted 2001.